

**Hallux Valgus: A Kinematic Study**

A DISSERTATION  
SUBMITTED TO THE FACULTY OF THE GRADUATE SCHOOL  
OF THE UNIVERSITY OF MINNESOTA  
BY

**Ward Mylo Glasoe**

IN PARTIAL FULFILLMENT OF THE REQUIREMENTS  
FOR THE DEGREE OF  
DOCTOR OF PHILOSOPHY

Michael Wade, PhD and Paula Ludewig, PT, PhD, Advisors

November, 2011

© Ward Mylo Glasoe 2011

## Acknowledgements

Many people contributed to this work.

Foremost, I acknowledge Dr. Paula Ludewig for her leadership in directing the research. The study of foot kinematics is technically demanding and working together, Paula and I overcame an assortment of unforeseen challenges. All along, Paula demonstrated the highest level of problem solving capabilities. She truly is a gifted researcher and teacher. Paula shared in the development of the methods and ultimately, in the success of the entire project. I stand forever grateful for the investment she made in teaching me kinematics, statistics, and the business aspects of research. Paula is a special friend.

Dr. Vandana Phadke wrote the computer code that output the kinematic calculations. Vandana made other contributions to this project - too many to list. We studied as graduate students in Dr. Ludewig's biomechanics research laboratory. Together we survived the rigors of graduate school and through it all, we forged a lasting kinship.

I acknowledge Dr. Fernando Pena who assisted in the cadaver experiment, and in securing funding for this work. Funding was received by Minnesota Medical Foundation, University of Minnesota in 2006 and 2009, by the American Physical Therapy Association (APTA) Foundation in 2007 and 2008, and by the Arthritis Foundation North Central Chapter in 2008.

I thank my co-advisor Dr. Michael Wade for taking me on as a Kinesiology student. Thank you as well to the other members of the committee, Drs. Jurgen Konczak, David Nuckley, and Deborah Nawoczinski. I also extend my thank you to Drs. Hitesh Mehta and Kristen Pickett for helping me collect and analyze the foot-to-ground loading data.

In closing, I acknowledge the students of the University of Minnesota, Program in Physical Therapy, Musculoskeletal Biomechanics Research Laboratory (MBRL). I am deeply indebted to Linda Kohler, Sanjay Sarkar, Kristin Zhao, Hitesh Mehta, and Arin Ellingson for their help and constant encouragement. You guys made the journey fun.

## **Dedication**

To Jan – my lifetime partner, you were a constant source of love and encouragement.

To Luke and Lisa – my children, they were always supportive of my work and career.

To Doran and Arlene – my parents, they taught the value of individual responsibility.

## Abstract

**Background and significance:** This study measured the change in tarsal kinematics associated with hallux valgus deformity. The condition is a progressive foot deformity characterized by abduction of the hallux and corresponding adduction of the first metatarsal (ray). The theory advanced for testing was that collapse of the arch initiates deformity. **Research Methods:** Data was collected on cadaver feet (N = 9) and human subjects (N = 20). The study culminated in using weightbearing imaging methods. Subjects stood to simulate gait midstance (MS), heel off (HO), and terminal stance (TS) in an open-upright MR scanner. From the imaged data, selected bones were reconstructed and foot posture and joint motion were measured. **Analysis:** A mixed effect ANOVA model compared the variables tested between group (hallux valgus vs. controls) and across conditions (MS, HO, TS). In addition, correlation techniques assessed the relationship in arch angle (height) to the change in first ray adduction evaluated across gait events. **Results:** The calcaneus everted 7° more ( $P < 0.05$ ) in subjects with hallux valgus as compared to controls. The first ray adducted 10° more ( $F = 44.17, P < 0.001$ ) in subjects having deformity, with orientation of the first ray axis inclined 23° during middle stance as compared to 6° in controls. Arch angle did not differ between groups ( $P = 0.46$ ). Additionally, no significant relationship ( $R^2 \leq 0.04$ ) was found in kinematic variables *in vivo* but when testing cadavers, a negative relationship ( $r = -0.73$ ) was identified between arch height and vertical tilt of the first ray axis. **Discussion and conclusion:** Results, in part, support theory and complement research. Inclination of the first ray axis may contribute to adduction of the first ray.

| <b>Table of Contents</b>                                 | <b>Page</b> |
|--|-------------|
| Acknowledgements.....                                    | i           |
| Dedication .....   | ii          |
| Abstract .....   | iii         |
| List of Tables .....                                     | ix          |
| List of Figures.....                                     | x           |
| List of Appendices .....                                 | xi          |
| <br>   |             |
| CHAPTER I.   |             |
| INTRODUCTION .....                                       | 1           |
| Background of the Study .....                            | 1           |
| Thesis Organization .....                                | 3           |
| Aims and Hypotheses .....                                | 4           |
| Statistical Analyses .....                               | 7           |
| Figure Legend (Chapter I.) .....                         | 9           |
| References (Chapter I.) .....                            | 10          |
| <br>   |             |
| CHAPTER II.  |             |
| HALLUX VALGUS AND THE FIRST METATARSAL ARCH SEGMENT..... | 12          |
| Introductory Summary .....                               | 12          |
| Introduction.....  | 12          |
| Part 1: Anatomy, Pathomechanics, and Etiology.....       | 14          |
|  | iv          |

|  |    |
|--|----|
| Functional anatomy and associated kinematics .....                           | 14 |
| Pathomechanics of hallux valgus.....   | 15 |
| Etiology.....  | 17 |
| Part 2: A Theoretical Perspective on Hallux Valgus .....                     | 20 |
| Theory introduced.....   | 20 |
| First metatarsal axis .....  | 21 |
| Collapse of the arch orients the first metatarsal axis toward vertical ..... | 23 |
| Instability of the first metatarsal arch segment .....                       | 25 |
| Theory derived evidence for orthoses treatment.....                          | 28 |
| Summary .....  | 30 |
| Figure Legend (Chapter II.) .....  | 32 |
| References (Chapter II.).....  | 35 |

### CHAPTER III.

|   |    |
|---|----|
| ARCH HEIGHT AND FIRST METATARSAL JOINT AXIS ORIENTATION.... | 41 |
| Introductory Summary .....                                  | 41 |
| Introduction.....   | 42 |
| Methods.....  | 44 |
| Specimen preparation.....                                   | 44 |
| Kinematic modeling.....                                     | 45 |
| Procedures .....  | 47 |
| Analysis.....   | 48 |

|                                   |    |
|-----------------------------------|----|
| Results.....                      | 49 |
| Discussion.....                   | 50 |
| Summary.....                      | 55 |
| Figure Legend (Chapter III.)..... | 59 |
| References (Chapter III.) .....   | 62 |

CHAPTER IV.

|   |    |
|---|----|
| CALCANEUS AND NAVICULAR KINEMATICS.....   | 65 |
| Introductory Summary .....                | 65 |
| Introduction.....                         | 66 |
| Methods.....                              | 72 |
| Subjects .....                            | 72 |
| Image and reconstruction procedures ..... | 74 |
| Kinematic measurement procedures .....    | 77 |
| Data analysis .....                       | 79 |
| Results.....                              | 80 |
| Discussion.....                           | 82 |
| Bone angle alignment .....                | 82 |
| Angle – gait event comparisons .....      | 83 |
| Calcaneus-to-fibula angles.....           | 87 |
| Navicular-to-calcaneus angles .....       | 90 |
| Limitations of the study .....            | 92 |



|                                  |     |
|----------------------------------|-----|
| Summary .....                    | 93  |
| Figure Legend (Chapter IV.)..... | 97  |
| References (Chapter IV.) .....   | 100 |

CHAPTER V.

|   |     |
|---|-----|
| FIRST RAY KINEMATICS IN SUBJECTS WITH HALLUX VALGUS ..... | 105 |
| Introductory Summary .....                                | 105 |
| Introduction.....   | 106 |
| Methods.....  | 110 |
| Subjects .....  | 110 |
| Scanning and image reconstruction procedures.....         | 111 |
| Kinematic measurement procedures .....                    | 115 |
| Data analysis .....                                       | 117 |
| Results.....  | 118 |
| Discussion.....   | 120 |
| Rationale for data interpretation .....                   | 120 |
| First ray-navicular angles and rotations.....             | 121 |
| First ray axis orientation .....                          | 124 |
| Regression analysis measurements .....                    | 126 |
| Limitations of the study .....                            | 128 |
| Summary .....   | 129 |
| Figure Legend (Chapter V.).....                           | 132 |

|  |     |
|--|-----|
| References (Chapter V.).....                           | 136 |
| CHAPTER VI.  |     |
| OVERALL SUMMARY AND DISCUSSION.....                    | 140 |
| Introduction.....                                      | 140 |
| Part 1. Imaging Measurement of Tarsal Kinematics ..... | 142 |
| Part 2. Results Synthesized.....                       | 145 |
| Hypothesis testing results .....                       | 145 |
| Key findings.....                                      | 148 |
| Clinical implications .....                            | 152 |
| Summary.....   | 155 |
| References (Chapter VI.) .....                         | 157 |
| REFERENCES .....                                       | 161 |
| APPENDICES .....                                       | 176 |

| <b>List of Tables</b>   | <b>Page</b> |
|---|-------------|
| Table 3.1. Specimen Characteristics .....   | 56          |
| Table 3.2. Segments, Digitized Points, and Coordinate Definitions.....            | 57          |
| Table 3.3. Helical axis parameters, and first ray rotation .....                  | 58          |
| Table 3.4. Correlation Results.....   | 58          |
| Table 4.1. Group mean $\pm$ SD (range) demographic and foot structure angle ..... | 95          |
| Table 4.2. Group angles recorded across gait events .....                         | 96          |
| Table 5.1. Group mean $\pm$ SD (range) for the measurement of bone angles.....    | 130         |
| Table 5.2. Group angles recorded in the body planes .....                         | 130         |
| Table 5.3. First ray rotations (Phi) and helical axis components .....            | 131         |
| Table 5.4. Multiple regression analysis results .....                             | 131         |

| <b>List of Figures</b>   | <b>Page</b> |
|--|-------------|
| Figure 1.1. Diagram showing a sagittal view of the medial arch.....                  | 9           |
| Figure 1.2. Sagittal view of a subject's midstance (MS) bone dataset.....            | 9           |
| Figure 2.1. Hallux valgus disrupts normal alignment of the joint.....                | 33          |
| Figure 2.2. The first metatarsal axis represented in 3 different foot postures ..... | 33          |
| Figure 2.3. Estimates of helical axis vectors .....                                  | 34          |
| Figure 2.4. A pendulum glued to the nail of the hallux demonstrates .....            | 34          |
| Figure 3.1. Intracortical pins were used to attach the motion sensors to bone.....   | 60          |
| Figure 3.2. Estimates of the helical axis vectors .....                              | 60          |
| Figure 3.3. First metatarsal mean static angular positions displayed.....            | 61          |
| Figure 3.4. Shows the process used to compute the HA vertical projection angle ..... | 61          |
| Figure 4.1. A. Weightbearing MR test conditions .....                                | 98          |
| Figure 4.2. Bone angle alignment was measured on the midstance bone datasets .....   | 98          |
| Figure 4.3. Group angles measured in the anatomical body planes .....                | 99          |
| Figure 4.4. Hindfoot frontal view of a subject's bone dataset .....                  | 99          |
| Figure 5.1. A. Gait (MS, HO, TS) was simulated with the subject standing .....       | 133         |
| Figure 5.2. Bone angles measured on the midstance (MS) bone datasets.....            | 133         |
| Figure 5.3. Sagittal view of a single subject bone dataset.....                      | 134         |
| Figure 5.4. Group angles plotted in the body planes across gait midstance (MS) ..... | 134         |
| Figure 5.5. Significant* group-by-condition interaction ( $P = 0.037$ ).....         | 135         |

| <b>List of Appendices</b>  | <b>Page</b> |
|--|-------------|
| 1. Introduction.....   | 176         |
| 2. Measurement Error Experiments .....                                   | 177         |
| 2.1. Image Processing Basic Error .....                                  | 177         |
| 2.2. Image Processing Bone-on-Bone Angle Error .....                     | 178         |
| 2.3. Error: Foot or Wedge Deformation.....                               | 180         |
| 3. Foot Loading Experiment .....   | 181         |
| 4. Individual subject data: display of helical axis vectors .....        | 186         |
| 5. Data analysis: influence of body weight on first ray kinematics ..... | 187         |
| 6. IRB Approval Document .....   | 188         |
| 7. Appendix Citations .....  | 189         |

CHAPTER I.  
INTRODUCTION

**Background of the Study**

Hallux valgus is a foot deformity characterized by the abduction displacement of the hallux with corresponding adduction of the first metatarsal arch segment.<sup>1</sup> The condition is often referred to as a bunion. Greater than 90% of patients receiving treatment for hallux valgus are female.<sup>2-4</sup> Prevalence is highest in the elderly. One study<sup>5</sup> identified hallux valgus in 36% of community-based adults age 55 and older. Despite its common occurrence,<sup>5</sup> there is little quantitative evidence on which conservative treatment is based.<sup>3,6</sup> Deformity does progress until corrected by surgery.

This study of hallux valgus measured the kinematics of the foot and arch (Fig. 1). The medial arch is composed of the calcaneus, talus, navicular, cuneiforms, and the first three metatarsals.<sup>7</sup> Distal to the metatarsals are the proximal phalanges of the toes. Spanning the length of the foot is a thick band of tissue called the plantar fascia. It runs from the undersurface of the calcaneus making attachment to the toes (Fig. 1).<sup>7</sup> Weight applied tightens the plantar fascia to support the arch, especially into late stance when the heel lifts from the ground and the toes dorsiflex.<sup>8</sup>

Joint motion is defined in terms of the body planes, with rotation of a body segment described as occurring about X, Y, and Z axes. The International Society of Biomechanics<sup>9</sup> recommends foot kinematics be defined with X pointing forward, Y vertically upwards, and Z right. Rotation in the frontal plane (X-axis) is inversion and eversion. Transverse plane (Y-axis) rotation is adduction and abduction. Sagittal plane (Z-axis) rotation is dorsiflexion and plantar flexion.

In this study of foot kinematics, tarsal angles computed about X, Y, and Z axes were described as rotations in the frontal, transverse, and sagittal planes in 3D kinematics descriptions. This description is not strictly correct, as sequential rotations are occurring about axes which have already rotated out of their original plane. However, this descriptive simplification is consistent with how kinematics are presented in clinical journals as it eases data presentation.<sup>10, 11</sup>

This three-part investigation<sup>12-14</sup> tested whether eversion of the calcaneus and collapse of the arch are factors of hallux valgus deformity.<sup>15</sup> Kinetic modeling<sup>16, 17</sup> has shown that walking in excess pronation shifts the ground reaction force to the medial side of the first metatarsophalangeal (1-MTP) joint, pushing the hallux into deformity.<sup>15</sup> Kinematic studies<sup>10, 11</sup> conducted on subjects having hallux valgus have not shown this directly.

Based on information gained from my past study of first ray biomechanics<sup>18-21</sup> and hallux valgus foot deformity,<sup>22</sup> and upon review of the relevant clinical literature, I published (in

collaboration with mentors) theory<sup>23</sup> to propose a mechanism by which collapse of the arch may initiate deformity. The word “theory” is used throughout the document in a colloquial sense. Theory discussed means a “doctrine of speculation”, as opposed to how the word may be used in science to make a statement of fact. Theory tested was premised on collapse of the arch tilting the first ray (first metatarsal and cuneiform) axis towards vertical, allowing the first ray arch segment to adduct into deformity. To investigate, the study culminated in measuring tarsal kinematics from reconstructed MR-imaged bone datasets.<sup>12, 13</sup> Arch angle,<sup>24</sup> for example, is shown in Figure 2.

### **Thesis Organization**

This was a three part investigation. Each study tested some aspect of theory related to onset and progression of hallux valgus.<sup>23</sup> The theory paper, which included an extensive review of the literature, is presented as Chapter II.

The three separate research reports are written as Chapters III, IV, and V for thesis distribution. Each report was formatted for journal submission. The title, abstract and key words, the manuscript text with subheadings, the tables, figures, figure legend, and references have been prepared to meet journal guidelines. Due to University Graduate School thesis formatting standards, the section written to open the chapter (manuscript) as a structured abstract could not be titled “Abstract”. Therefore, the chapters open under the subheading “Introductory Summary” (as suggested by the Graduate School). An



extra paragraph added to the introductory summary begins Chapter IV and V. This opening paragraph serves to bridge the research together between chapters. Finally, to meet Graduate School formatting standards, the thesis concludes by listing, in alphabetical order, all cited references.

Study 1 (Chapter III) reported angular kinematics measured on cadaver feet ( $n = 9$ ). The study tested our methods.<sup>14</sup> How we loaded the foot to simulate gait, and our use of a finite helical axis (FHA) to quantify the first ray axis were original to this work. Study 1 has been published.<sup>14</sup> The paper is presented as Chapter III.

Research continued by collecting image-based data on subjects grouped with ( $N = 10$ ) and without ( $N = 10$ ) hallux valgus. Subjects were placed standing in a MR scanner to simulate gait midstance (MS), heel off (HO), and terminal stance (TS). From the scanned images, selected foot and leg bones were reconstructed as 3D objects (Fig. 2) using computer software. Tarsal kinematics were then measured and compared between groups and across gait events, with the hindfoot and forefoot kinematics parsed into two separate studies. Study 2 (Chapter IV) reports the calcaneus and navicular kinematics.<sup>12</sup> Study 3 (Chapter V) reports the measurement of first ray kinematics.<sup>13</sup>

### **Aims and Hypotheses (H.)**

Listed by Chapter, Study, and Abridged Title.

Chapter III. Study 1. (1) *Arch Height and First Ray Joint Axis Orientation.*<sup>14</sup>

Aim 1. (1.1) To determine a method to measure first ray-to-navicular axis of joint rotation across simulated static gait foot postures.

H.1.1) A decomposition of helical axis parameters can be used to quantify the orientation of the first ray axis between gait events.

Aim 2. (1.2) To determine the relationship between arch height and first ray-navicular axis orientation to changes in foot kinematics common to hallux valgus deformity.

H.1.2) The combined variables of arch height and first ray axis orientation are related to the increased intermetatarsal (IM) angle and increased adduction of the first ray measured while the foot was placed to simulate gait loading.

Chapter IV. Study 2. (2) *Calcaneus Kinematics in Subjects with Hallux Valgus*.<sup>12</sup>

Aim 1 (2.1) To determine the extent to which hallux valgus deformity altered the alignment of the intermetatarsal (IM) angle, and the arch angle (Fig. 2) in the foot.

H.2.1) Subjects having hallux valgus would demonstrate a larger IM angle, and would demonstrate larger arch angle as compared to controls.

Aim 2. (2.2) To determine calcaneus angular positioning relative to the fibula at each tested gait event (MS, HO, TS) in subjects having hallux valgus as compared to controls.

H.2.2) The calcaneus would evert more in relation to the fibula at each gait event (MS, HO, TS) in subjects having hallux valgus as compared to controls.

Aim 3. (2.3) To determine whether navicular angular positioning relative to the calcaneus and relative to a MR laboratory frame (MR reference) differs in subjects having hallux valgus as compared to controls when measured across gait events (MS, HO, TS).

H.2.3) The navicular would evert more at HO with respect to the calcaneus and the MR reference in subjects having hallux valgus as compared to controls.

Aim 4. (2.4) To determine frontal plane angular positioning of the navicular in relation to the calcaneus across the progression of gait events.

H.2.4) For both groups, the navicular would evert more in relation to the calcaneus at HO as compared to MS, and it would invert more with respect to the calcaneus at TS as compared to HO.

Chapter V. Study 3.(3) *First Ray Kinematics in Subjects with Hallux Valgus.*<sup>13</sup>

- Aim 1. (3.1) To determine adduction angular orientation of the first ray and its axis in subjects with hallux valgus as compared to controls across gait events.
- H.3.1) The first ray would adduct more in relation to the navicular in subjects having hallux valgus and accordingly, the first ray axis would orient more vertical between the progression of gait events as compared to controls.
- Aim 2. (3.2) To determine frontal plane angular positioning of the first ray in subjects having hallux valgus as compared to controls across gait events.
- H.3.2) Subjects with hallux valgus would have greater eversion of the first ray relative to the navicular at HO as compared to controls.
- Aim 3. (3.3) To determine the relationship between arch angle and first ray-navicular axis orientation between gait events in the subjects sampled.
- H.3.3) Arch angle considered in combination with the change in navicular-to-world eversion angle measured between MS and HO (middle stance), and between HO and TS (late stance) as variables in a regression model would relate at a level of  $R^2 \geq 0.30$  to vertical orientation of the first ray axis measured between the same gait events.

### **Statistical Analyses**

The statistical testing performed in this three part investigation of hallux valgus foot deformity included descriptive as well as parametric analyses. The data collected was

screened for non-normality by examining each variable for skewness and kurtosis.

Significant results were recorded at  $P \leq 0.05$ . The exact types of statistical analyses

performed are identified in the separate research reports.

## Figure Legend (Chapter I.)

**Fig. 1.1.** Diagram showing a sagittal view of the medial arch. The plantar fascia runs from the calcaneus forward to the toes, and tightens under body weight to support the arch.

**Fig. 1.2.** Sagittal view of a subject's midstance (MS) bone dataset. The bones represented are the proximal phalanx of the hallux, first metatarsal, navicular, and calcaneus. The measure of arch angle is shown, defined by lines connecting the dorsal shaft of the first metatarsal and the inferior aspect of the calcaneus.

**Figure 1.1.**

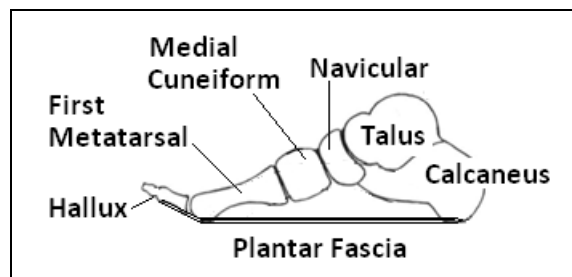
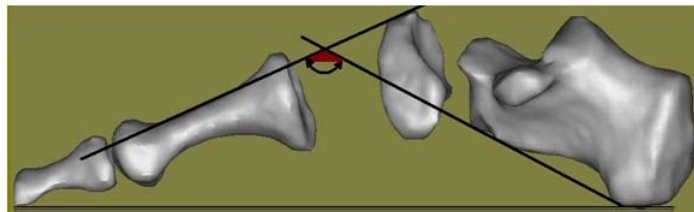


**Figure 1.2.**



## References (Chapter I.)

1. Ferrari J, Higgins J, Prior T. Interventions for treating hallux valgus (abductovalgus) and bunions. *Cochrane Database of Systematic Reviews*. 2004;Issue 1. Art. No.:CD000964.DOI:10.1002/14651858.CD000964.pub2.
2. Coughlin M, Jones C. Hallux valgus: demographics, etiology, and radiographic assessment. *Foot Ankle Int*. 2007;28:759-777.
3. Torkki M, Malmivaara A, Scitsalo S, Hoikka V, Laippala P, Paavolainen P. Surgery vs orthosis vs watchful waiting for hallux valgus. *J Am Med Assoc*. 2001(285):2474-2480.
4. Torkki M, Malmivaara A, Seitsalo S, Hoikka V, Laippala P, Paavolainen P. Hallux valgus: immediate operation versus 1 year of waiting with and without orthoses. *Acta Orthop Scand*. 2003;74(2):209-215.
5. Menz H, Roddy E, Thomas E, Croft P. Impact of hallux valgus severity on general and foot-specific health-related quality of life. *Arthritis Care & Res*. 2011;63(3):396-404.
6. Easley M, Trnka H. Current concepts review: hallux valgus Part 1: pathomechanics, clinical assessment, and nonoperative management. *Foot Ankle Int*. 2007;28(5):654-659.
7. Thordarson DB, Schmotzer H, Chon J, Peters J. Dynamic support of the human longitudinal arch. *Clinical Orthopaedics and Related Research*. 1995;316:165-172.
8. Hamel A, Donahue S, Sharkey N. Contributions of active and passive toe flexion to forefoot loading. *Clin Orthop*. 2001;393:326-334.
9. Wu G, Siegler S, Allard P, et al. ISB recommendation on definitions of joint coordinate system of various joints for the reporting of human joint motion--part I: Ankle, hip, and spine. *J Biomech*. 2002;35:543-548.
10. Canseco K, Rankine L, Long L, Smedberg T, Marks R, Harris G. Motion of the multisegmental foot in hallux valgus. *Foot Ankle Int*. 2010;31:146-152.
11. Deschamps K, Birch I, Desloovere K, Matricali G. The impact of hallux valgus on foot kinematics: A cross-sectional. *Gait Posture*. 2010;32:102-106.
12. Glasoe W, et al. Calcaneus and navicular kinematics in hallux valgus: a weightbearing imaging study. *TBD*. 2011:Ready for Journal Submission.
13. Glasoe W, et al. First ray kinematics in hallux valgus: a weightbearing imaging study. *TBD*. 2011:Ready for Journal Submission.
14. Glasoe W, Pena F, Phadke V, Ludewig P. Arch height and first metatarsal joint axis orientation as related variables in foot structure and function: theory related to bunion. *Foot Ankle Int*. 2008;29(6):647-655.
15. Inman V. Hallux valgus: a review of etiologic factors. *Orthop Clin N Amer*. 1974;5(1):59-66.

16. Eustace S, Byrne J, Beausang O, Codd M, Stack J, Stephens M. Hallux valgus, first metatarsal pronation and collapse of the medial longitudinal arch - a radiological correlation. *Skeletal Radiol.* 1994;23:191-194.
17. Talbot K, Saltzman C. Hallucal rotation: a method of measurement and relationship to bunion deformity. *Foot Ankle Int.* 1997;18(9):550-556.
18. Allen M, Cuddeford T, Glasoe W, et al. Relationship between static mobility of the first ray and first ray, midfoot, and hindfoot motion during gait. *Foot Ankle Int.* 2004;25(6):391-396.
19. Brown K, Bursey D, Arneson L, Andrews C, Ludewig P, Glasoe W. Consideration of digitization precision when building local coordinate axes for a foot model. *J Biomech.* 2009;42:1263-1239.
20. Glasoe W, Coughlin M. A critical analysis of Dudley Morton's concept of disordered foot function. *J Foot Ankle Surg.* 2006;45:147-155.
21. Glasoe W, Yack H, Saltzman C. Anatomy and biomechanics of the first ray. *Phys Ther.* 1999;79(9):854-859.
22. Glasoe W, Allen M, Saltzman C. First ray dorsal mobility in relation to hallux valgus deformity and first intermetatarsal angle. *Foot Ankle Int.* 2001;22(2):98-101.
23. Glasoe W, Nuckley D, Ludewig P. Hallux valgus and the first metatarsal arch segment: a theoretical biomechanical perspective. *Phys Ther.* 2010;90:110-120.
24. Wilken J, Rao S, Saltzman C, Yack H. The effect of arch height on kinematic coupling during walking. *Clin Biomech.* 2011;26(3):318-323.



## CHAPTER II.

### HALLUX VALGUS AND THE FIRST METATARSAL ARCH SEGMENT

#### **Introductory Summary**

Hallux valgus is a progressive foot deformity characterized by a lateral deviation of the hallux with corresponding medial deviation of the first metatarsal. Late stage changes may render the hallux painful and without functional utility leading to impaired gait. Various environmental, genetic, and anatomical predispositions have been suggested but the exact cause of hallux valgus is unknown. Evidence indicates that conservative intervention for hallux valgus provides relief from symptoms but does not reverse deformity. Part 1 of this perspective reviews the literature describing the anatomy, pathomechanics, and etiology of hallux valgus. Part 2 expands on the biomechanical initiators of hallux valgus attributed to the first metatarsal. Theory advanced is that collapse of the arch with vertical orientation (tilt) of the first metatarsal axis initiates deformity. To counteract the progression of hallux valgus, we use theory to discuss a possible mechanism by which foot orthoses can bolster the arch and re-orient the first metatarsal axis horizontally. **Key Words:** Foot deformity, Bunion, Orthoses, First ray

#### **Introduction**

Hallux valgus (Fig. 1) is an irreversible foot deformity.<sup>1-3</sup> The condition, which in lay terminology is called bunion, is characterized by a lateral deviation (abduction) of the hallux with a corresponding medial deviation (adduction) of the first metatarsal.

Deformity disrupts the normal straight alignment of the first metatarsophalangeal (MTP) joint. When hallux valgus is severe, the first MTP joint may dislocate leading to impaired gait.<sup>3</sup>

Bunion is a Latin word meaning enlargement which refers to the chronic swollen appearance of the medial projected eminence that develops as the hallux deviates laterally into deformity.<sup>1,4</sup> Pain when experienced is usually localized to the swelling (bunion) or in the first MTP joint itself.<sup>3</sup> Shoes may aggravate the condition. To reduce discomfort, individuals having hallux valgus are advised to avoid wearing high-heeled pointed-toed shoes. Shoes made from soft leather that are flat in style work best and if necessary, the toe box can be stretched to accommodate for bunion enlargement.<sup>5,6</sup>

Therapy for hallux valgus aims to correct the forces acting on the first MTP joint.

Suggestions for care include foot exercise to rebalance muscle strength (force-generating capacity),<sup>7</sup> and the use of toe spacers and splinting worn by the patient to stretch tissue tightness.<sup>5,6</sup> Foot orthoses may also be incorporated into treatment.<sup>8</sup> Regardless of the treatment applied, current available evidence indicates that deformity will progress until fixed by surgery.<sup>1</sup> Indications for surgery include pain or dysfunction that prevents activity or lifestyle choices, the inability to find shoes that fit, and to address cosmetic

concerns.<sup>4</sup> More than 100 surgical techniques are used to correct for variation in hallux valgus deformity,<sup>4</sup> with an estimated 210,000 surgeries performed each year in the United States.<sup>9, 10</sup>

Part 1 of this perspective reviews the anatomy, pathomechanics, and the etiology of hallux valgus. This review suggests a characteristic or behavior of the first metatarsal may initiate hallux valgus or contribute to its recurrence following surgery. The kinetic and kinematic behaviors of the first metatarsal arch segment are further evaluated in Part 2 wherein a theoretical perspective on the genesis of hallux valgus is presented. The purpose of the manuscript is to develop a biomechanically derived perspective on hallux valgus and suggest indications for conservative orthoses treatment strategies.

## **Part 1: Anatomy, Pathomechanics, and Etiology**

### **Functional anatomy and associated kinematics**

The hallux has a distal and proximal phalanx (Fig. 1). The proximal phalanx articulates with the first metatarsal. The metatarsophalangeal (MTP) joint is a biaxial condylar articulation that relies on a synovial capsule, collateral ligaments, and a fibrous plantar plate to maintain joint stability.<sup>11</sup> A medial and lateral sesamoid bone, encased in the tendons of the intrinsic muscles lie beneath the head of the first metatarsal.<sup>12</sup> The first metatarsal articulates proximally with the medial cuneiform and the base of the second metatarsal.<sup>11, 13</sup> The metatarsocuneiform (MC) joint is a stable union having a dense plantar ligament that works to fortify the medial longitudinal arch.<sup>13</sup> The base of the first

metatarsal makes neighboring contact with the second metatarsal (Fig. 1). The Lisfranc ligament connects the first and second metatarsals.<sup>11</sup> Severe hallux valgus deformity may disrupt each of these bony contacts and joint structures.

The first metatarsal in connection with the medial cuneiform is called the first ray. The first metatarsal and cuneiform bones move together as a single unified arch segment but separate from the second metatarsal.<sup>11-13</sup> As is commonly done in the literature,<sup>11-13</sup> the word first metatarsal is used generically in this perspective to describe the combined kinematics of the first metatarsal-cuneiform arch segment.

Bone segments rotate around joint axis systems. A joint axis can be thought of as a line that varies in 3-d position and orientation by which a segment rotates in a perpendicular plane.<sup>14</sup> In its simplest form, a joint axis may be likened to a pin about which a hinge rotates. In the foot, sagittal plane dorsi- plantar flexion occurs about a medial-lateral directed joint axis, transverse plane add- abduction occurs about a vertical axis, and frontal plane in- eversion occurs about a longitudinal axis. Because joints do not truly align perpendicular to the cardinal planes,<sup>15, 16</sup> rotations of the hallux and first metatarsal segments occur in some proportion across each of the cardinal planes. Besides describing motion, the terms abduction of the hallux and adduction of the first metatarsal describe the direction of hallux valgus foot deformity (Fig. 1).

### **Pathomechanics of hallux valgus**

The progression of hallux valgus, although not well understood, is predictable.<sup>3, 17</sup> The tensile strength of the medial collateral ligament of the first MTP joint weakens and the hallux abducts laterally into valgus.<sup>3, 17</sup> Coincident with abduction of the hallux, the metatarsal shifts medially into adduction potentially subluxating the sesamometatarsal articulation.<sup>18, 19</sup> Hallux Valgus Angle (Fig. 1.A) refers to the offset in first MTP joint positioning.<sup>20</sup> The related separation between the first and second metatarsals which increases as deformity becomes worse is called the Intermetatarsal 1-2 Angle (Fig. 1.B).<sup>11</sup> Deformity is judged severe when Hallux Valgus Angle is greater than 40 degrees and the Intermetatarsal Angle is greater than 16 degrees.<sup>20, 21</sup> Severe deformity leaves the medial aspect of the metatarsal articular surface uncovered and exposed to trauma. This gives rise to hypertrophy resulting in the cosmetic feature most associated with hallux valgus.<sup>3</sup>

Hallux valgus alters bony contact pressures across the first MTP joint members.<sup>3, 17</sup> As a result of incongruity in contact pressures, lesions develop in the articular cartilage. Eventually the cartilage erodes and changes the shape of the first metatarsal head (Fig. 1). Scranton and Rutkowski<sup>22</sup> qualitatively evaluated the extent of cartilage and subchondral bone damage in 35 cadavers having hallux valgus. Erosion of the plantar surface of the metatarsal head was present in every specimen having completely dislocated sesamoids. In a different study, Roukis et al<sup>23</sup> mapped articular wear patterns in 166 feet undergoing hallux valgus surgery. All patients older than 50 showed erosive damage involving nearly half of the combined MTP joint surface area. Such late stage changes in joint structure may render the hallux painful and without functional utility.<sup>3, 4, 17</sup>

Deformity remains and worsens due to the unbalance of moments acting on the hallux during gait. Plantar pressure measurements are highest near the end of stance when loads carried by the hallux approach 40 percent of body weight.<sup>24</sup> Walking with a laterally rotated foot angle and/or walking in excess foot pronation are gait compensations known to redirect the distribution of weight to the medial side of the hallux.<sup>3, 18, 25</sup> Moment generated mostly by the flexor hallucis longus (FHL) counters the ground force moment reacting to dorsiflex the hallux.<sup>26-28</sup> These action-reaction moments have been modeled to explain the progression of deformity.<sup>27, 28</sup> As the hallux abducts, the ground reaction force (GRF) acting on the hallux has a medial component which increasingly works to displace the first metatarsal into adduction. The magnitude of this medial force component equals the GRF acting on the hallux multiplied by the tangent of the angle approximating the hallux valgus angle.<sup>28</sup> For example, should the angle of hallux deformity be 45° (shown in Fig 1) the medial component of force pushing the first metatarsal into adduction would be equal to the load carried by the hallux. Added to this is the misdirected moment action of FHL muscle. In response to developing deformity, the resultant pull of the FHL shifts from a plantar to a lateral direction changing the joint moment action from the sagittal to the transverse plane.<sup>26, 27</sup>

## **Etiology**

The cause of hallux valgus is unknown.<sup>1</sup> Many theories have been put forth, and perhaps most common is that ill-fitting footwear may contribute.<sup>29-31</sup> The prevalence of hallux

valgus is highest in the female populations living in western societies that wear fashionable shoes.<sup>32</sup> Shoes worn by females typically have a high-heel and narrow toe box.<sup>33</sup> Heeled shoes increase pressure borne by the forefoot and when worn over prolonged time periods, may lead to adaptive shortening of the ankle plantar flexor muscles.<sup>3,33</sup> Decreased ankle dorsiflexion is, by itself considered a factor in hallux valgus.<sup>3</sup>

Epidemiologic data demonstrate the highest incidence of hallux valgus in the elderly<sup>34</sup> with females representing ninety percent of all cases.<sup>21</sup> Specifically, Gould et al<sup>35</sup> estimated the deformity to affect 1 in every 45 individuals over the age of 50. Deformity may also develop in childhood. The term juvenile hallux valgus is used when the condition presents prior to skeletal maturity.<sup>36,37</sup>

Greater than 60 percent of patients having hallux valgus show family history of the deformity.<sup>38,39</sup> Congenital neurological pathology like ankle equinus associated with cerebral palsy, as well as chronic inflammatory conditions have been found related with hallux valgus.<sup>3,4,40</sup> Damage of the first MTP joint occurs in nearly 25 percent of patients having rheumatoid arthritis (RA).<sup>41</sup> Arthritis weakens the articular tissues leaving the weightbearing joints at risk of dislocation; collapse of the arch is common.<sup>42-44</sup> Coughlin<sup>17,20,38</sup> reported that 10 percent of surgeries performed in his practice to correct hallux valgus are for inflammatory arthritic conditions, predominantly RA.<sup>21</sup>

Premised on the belief that structure influences function, research has investigated length of the first metatarsal as a separate factor in hallux valgus. Both the relative long<sup>2, 45, 46</sup> and short<sup>47-49</sup> first metatarsal have been reported associated with deformity progression. These opposing results suggest that length of the first metatarsal may be incidental to the development of deformity, or that length affects are significant only when combined with other precursor traits.

Shape of the first metatarsal head has also been explored as a potential predisposition of hallux valgus.<sup>3, 46, 50, 51</sup> A flattened head is considered to be resistive to deforming forces, whereas a round head is thought more prone to allow the hallux to drift into deformity.<sup>3</sup> A retrospective review of 110 foot radiographs of patients having hallux valgus identified the head of the first metatarsal to be shaped “round” in 100 percent of those having a long first metatarsal in comparison to their second metatarsal.<sup>46</sup> When discussing this no-exception finding, the authors postulated that a long first metatarsal impedes MTP joint dorsiflexion and redirects the hallux into valgus. The finding,<sup>46</sup> however, may be questioned because the contribution of joint erosion was not considered in the visual analysis used in classifying shape of the metatarsal head. Other studies<sup>3, 50, 51</sup> having also reviewed radiographs in patients with hallux valgus report no trends in data to support the notion that roundness of the metatarsal head leads to deformity.

Even though the shape and geometry of the first metatarsal head exhibit little correlation with the development of hallux valgus, variation in first metatarsocuneiform joint



osteology is thought to precipitate first MTP joint malalignment.<sup>13, 40, 52, 53</sup> Ferrari et al<sup>52</sup> reconstructed the bones of the medial arch from image data in the feet of 107 skeletons. Measurements made on the bone images showed the connecting facets of the metatarsal-cuneiform joint in females were shaped to permit the first metatarsal to translate medially into adduction. Ferrari<sup>52</sup> discussed this difference in joint structure between genders to explain why hallux valgus develops most often in females. These results, although interesting, cannot be easily incorporated into treatment.

The predisposition most identified with hallux valgus is collapse of the medial arch, especially as it relates to instability of the first metatarsal.<sup>36, 54-59</sup> Because the first metatarsal and the neighboring bones of the medial longitudinal arch can be held supported with foot orthoses, this area of biomechanical study holds promise for treatment. Part 2 of this perspective explores the co-dependent kinetic and kinematic behaviors of the arch and first metatarsal. The theory advanced is that collapse of the arch with vertical orientation of the first metatarsal axis initiates hallux valgus. Consistent with the research reviewed, a novel mechanism is discussed by which orthoses used to bolster the arch might counteract deformity progression.

## **Part 2: A Theoretical Perspective on Hallux Valgus**

### **Theory introduced**

Over 40 years ago John Ebisui<sup>60</sup> suggested the first metatarsal axis could precipitate hallux valgus and issued the following challenge to understanding and treatment:

*“Whether the first ray axis is intimately related to hallux valgus is a matter of conjecture. Further investigation will be necessary before any definitive conclusion can be made. It is hoped that this study will stimulate others to investigate the fundamental mechanics of hallux valgus. It is our contention that more emphasis should be placed upon the cause and prevention of deformity rather than on the many variations of surgical procedures for its correction”.*

Part 2 of the perspective gives a response to this challenge wherein the first metatarsal axis and its predisposition to hallux valgus are described. The literature and theory is predicated upon 3 major tenets: (1) The first metatarsal rotates about its own axis; (2) Collapse of the arch orients (tilts) of the first metatarsal axis toward vertical which allows the first metatarsal to adduct with less anatomical resistance; and (3) Instability of the first metatarsal arch segment is a related factor of hallux valgus.

These tenets of first metatarsal biomechanics support our theory for hallux valgus that collapse of the arch with vertical orientation of the first metatarsal axis initiates deformity. Part 2 concludes with a discussion utilizing this theoretical perspective to advocate for orthoses based treatment strategies.

### **First metatarsal axis**

Studies on cadavers provide the only primary sourced research describing the first metatarsal axis.<sup>15, 60-65</sup> Hicks<sup>15</sup> was the first researcher to describe the position and

orientation of the first metatarsal axis. He located the axis by observing the trajectory of an external jig fastened to bone while imposing an external load to move the first metatarsal. With the foot (N = 15) positioned non-weightbearing, the metatarsal arch segment rotated about an axis estimated to orient almost horizontal and passing between the navicular and the base of the third metatarsal (Fig. 2). The observed motion of the first metatarsal in relation to the navicular coupled dorsiflexion with inversion (DF-IN), and plantar flexion with eversion (PF-EV).<sup>15</sup> Kelso and coworkers<sup>64</sup> also conducted a non-weightbearing experiment (N = 24) using similar methods except that first metatarsal motions were measured by a gravity sensitive device. Data confirmed the metatarsal moved independent of the foot in a pattern of motion as Hicks had described.<sup>15</sup> Kelso<sup>64</sup> expressed reservations that non-weightbearing measurements may not capture the kinematics of foot function. Studies<sup>66, 67</sup> support this concern noting that weightbearing vs. non-weightbearing measurements differ. This explains why the patterns of motions (DF-IN; PF-EV) reported by Hicks<sup>15</sup> and by Kelso<sup>64</sup> have been measured opposite (DF-EV; PF-IN) in cadaveric weightbearing experiments<sup>61, 62, 65, 68</sup> and in gait.<sup>67, 69, 70</sup> Collectively, this research demonstrates two key findings: 1) the first metatarsal has the capacity to move as an independent foot segment; 2) the parameters defining the first metatarsal axis can be quantified.

Position and orientation are physical traits of a joint axis. Recall that an axis defines a location in 3-d space about which neighboring segments displace. Figure 2.B shows a visual representation of the first metatarsal axis. The axis is drawn passing between

navicular and the base of the third metatarsal.<sup>14</sup> The position of these two bones in relation to the first metatarsal provides an estimate of how the axis orients in space. One would anticipate that axis orientation would be unique between individuals but similar across foot types.

Joint axis orientation can influence the direction of segment rotations. This characteristic of directed joint motion may play a role in the genesis of hallux valgus. If the first metatarsal axis runs medial-lateral across the foot and orients horizontal in the transverse plane,<sup>15</sup> resulting segment rotations would occur in the sagittal plane. But change the orientation of the first metatarsal axis and the direction of segment rotation must change accordingly.

### **Collapse of the arch orients the first metatarsal axis toward vertical**

Building on the previous biomechanical perspective, we evaluate the collapse for the arch under weightbearing load and its potential to orient the first metatarsal axis vertically creating first metatarsal adduction known to precipitate hallux valgus deformity.

A recent study did link orientation of the first metatarsal axis to arch height. Glasoe and colleagues<sup>62</sup> quantified orientation of the first metatarsal axis in cadaver specimens during a sequence of static gait events. Staged gait events included foot flat, heel off, and terminal stance. Orientation of the first metatarsal axis was extracted as helical parameters.<sup>71</sup> The helical axis (Fig. 3) represented the location about which the first

metatarsal and midfoot segments rotated in relation to each other. Orientation of the axis varied between specimens, and was found inversely related to arch height with  $r = -0.73$ .<sup>62</sup> The metatarsal axis oriented more towards vertical (Fig. 3 see vectors colored red, blue, green) as the arch dropped in height. When considered as conjoined variables, vertical axis orientation and arch height accounted for 69 percent of the variance in Intermetatarsal 1-2 Angle and change in metatarsal adduction positioning. The experiment<sup>62</sup> had several limitations in helping clinicians and researchers understand if the axis of the first metatarsal may contribute to hallux valgus. The specimens tested did not have obvious deformity, foot type was not defined, the sample was small, the load imposed was below physiologic levels (100 N), only selected foot postures were studied, and arch height was measured while the foot was static. Nevertheless, results did show the first metatarsal axis to orient more vertical in the low arched foot and by action, directed the metatarsal into adduction.<sup>62</sup>

Flattening of the foot under body weight may alter the orientation of the first metatarsal axis. Should the medial arch flatten completely under imposed load, the navicular could drop to the ground. The navicular would then rest in a relative position below the more stable and centrally located tarsometatarsal midfoot joints (Fig. 2.A). Such a precipitous drop in navicular position would lower the most medial point of the first metatarsal axis while the lateral point of the axis is raised. The just described collapse of the medial arch could orient the axis towards vertical and by effect, transfer partial angular rotation about the axis from the sagittal to the transverse anatomical plane.<sup>62</sup> Dorsiflexion of the first

metatarsal as should occur in early stance as the arch lowers under advancing weight would then become dorsiflexion/adduction (directed rotation about an axis oriented vertical). And adduction of the first metatarsal occurring under full weightbearing load could progressively enlarge the Intermetatarsal Angle (Fig. 1). Thus, the condition of hallux valgus may develop secondary to changes in the orientation of the first metatarsal axis.<sup>62</sup>

Orientation of the first MTP joint axis (different from the first metatarsal axis) is known to be altered in late stage hallux valgus.<sup>18, 22</sup> The axis about which the hallux rotates is located in the first metatarsal head. In the non-deformed well aligned foot structure, the joint axis of hallux rotation runs horizontal passing medial-lateral through the metatarsal head.<sup>16</sup> When deformity is severe the distal arch segments pronate (evert) tilting the first MTP joint axis towards vertical,<sup>25</sup> which by result changes the direction of available hallux joint motion from the sagittal to the transverse plane.<sup>18, 22</sup>

### **Instability of the first metatarsal arch segment**

Instability of the first metatarsal arch segment is a related factor of hallux valgus.<sup>72-74</sup>

Stability of the first metatarsal is assessed as a static clinical measurement using a variety of methods to include manual, mechanical, and radiographic stress testing.<sup>55,57,73</sup>

Common across testing methods is that a displacement force is imposed to the first metatarsal head while the relative position of the lesser metatarsals is held stable.<sup>55</sup> The condition, called first metatarsal hypermobility,<sup>12</sup> is defined clinically as demonstrable

laxity of the distal arch segment with related widening of the Intermetatarsal 1-2 Angle.<sup>72-</sup>

74

Hypermobility of the first metatarsal is a frequent predisposition listed for hallux valgus.<sup>72-74</sup> Faber and coworkers<sup>72</sup> identified the first metatarsal to be hypermobile in 60 of 94 (64 %) patients undergoing corrective hallux valgus surgeries. Lee and Young<sup>73</sup> reported the metatarsal to be hypermobile in 38 percent of patients having hallux valgus. Roukis and Landsman<sup>74</sup> agreed that a relationship does exist but estimated the incidence of hallux valgus and associated metatarsal hypermobility to be no higher than 10 percent. The presence of hypermobility was judged in each of these studies<sup>72-74</sup> by manual test methods. Manual assessment of first metatarsal hypermobility has uncertain reliability and measured results may be influenced by examiner bias.<sup>75, 76</sup> This weakness in the testing procedure may account for the wide discrepancy in reported incidence across studies.<sup>72-74</sup> Nevertheless, sufficient evidence exists to show that first metatarsal mobility is increased in individuals having hallux valgus, and that a large Intermetatarsal Angle is an indicator of first metatarsal hypermobility.<sup>72-74</sup>

Results from other studies<sup>77-79</sup> have revealed the first metatarsal may become hypermobile as deformity progresses. Coughlin and colleagues<sup>77, 78</sup> demonstrated nearly a 50 percent reduction in dorsal excursion of the first metatarsal in cadavers (from 11.0 to 5.2mm) and in patients (from 7.2 to 4.5mm) after the deformity into hallux valgus was corrected with surgery. Deformity was corrected using a proximal osteotomy

realignment technique of the first metatarsal that did not incorporate arthrodesis of the first metatarsocuneiform (MC) joint. Kim et al<sup>79</sup> reported a similar mean drop (6.8 to 3.2 mm) in metatarsal mobility in a consecutive series of 67 patients who underwent corrective hallux valgus surgery. Realignment was again made without arthrodesis of the first MC joint. Coughlin<sup>77, 78</sup> reasoned that realignment by itself reduced mobility of the first metatarsal to levels considered normal because the plantar fascia could better stabilize the metatarsal when the arch and hallux were aligned. However, since Coughlin's method of making mechanical measurement of first metatarsal mobility did not tighten the plantar fascia,<sup>77, 78</sup> other medial arch joint structures must act to limit motion of the first metatarsal in the correctly aligned foot. Two critical points can be taken from these studies<sup>77-79</sup> First, passive mobility of the first metatarsal is dependent on its alignment in the foot. Second, adduction of the first metatarsal as occurs with hallux valgus can make the first metatarsal unstable.

Lapidus<sup>57</sup> labeled adduction of the first metatarsal leading to first metatarsal hypermobility to be a non-evolved primate trait when he introduced surgical arthrodesis of the first MC joint to correct severe hallux valgus deformity. Presently, there is no consensus on whether fusion of the first MC joint is routinely necessary when correcting for hallux valgus.<sup>57-59, 77, 78</sup> The surgery is technically demanding,<sup>21</sup> and the rate of patient satisfaction ranges between 75 - 90 percent with nonunion and other long-term complications approaching 10 percent.<sup>58, 59, 80</sup> There is agreement across studies,<sup>57-59, 77, 78</sup> however, that adduction of the first metatarsal disrupts the capacity of the medial arch to



carry weight, and that gait impairments will become worse if deformity is left uncorrected.<sup>19, 63</sup>

Generalized joint laxity is a significant predictor of first metatarsal hypermobility.<sup>81, 82</sup> Patients having hallux valgus demonstrate high incidence of multijoint laxity.<sup>36, 83</sup> Harris and Beeson<sup>36</sup> identified generalized joint laxity in 42 percent of girls (age 10 to 21 years) having symptomatic hallux valgus. The hallux drifts into deformity because the collateral ligaments lack sufficient stiffness to stabilize the first MTP joint.<sup>84</sup> But what precipitates malpositioning of the first MTP joint members may stem from laxity of the Lisfranc (tarsometatarsal) or the other plantar arch ligaments which permit the first metatarsal to deviate away from the stable second metatarsal, collapsing the truss mechanics of the medial arch.<sup>11, 12</sup> The exact mechanism that precipitates deformity in the hyper-lax foot is unknown.

### **Theory derived evidence for orthoses treatment**

A pendulum attached to the hallux (Fig. 4) demonstrates how standing in extreme pronation orients the first MTP joint obliquely.<sup>85</sup> Biomechanical modeling<sup>18, 86</sup> suggests the ground reaction force vector shifts to the medial side of the hallux during late stance in the gait cycle, imposing a net valgus moment to the MTP joint, thus predisposing the development of deformity. Extreme pronation of the foot joints as quantified by radiographic methods is commonly seen in patients having hallux valgus.<sup>22, 25, 40, 55</sup> The incidence has been reported as high as 50 percent.<sup>87</sup> This relationship has not been

confirmed with measurements taken from footprints.<sup>38, 51, 77</sup> Footprints, however, do not predict arch height,<sup>88</sup> nor do footprints identify the behavior or motion of the arch under weightbearing load.<sup>88, 89</sup>

The pendulum demonstration (Fig 4.) was first published by Verne T Inman MD, PhD.<sup>25</sup> He concluded that a hyper-lax arch with corresponding extreme pronation of the medial arch joints was a certain predisposition of hallux valgus. Treatment of early stage hallux valgus, Inman urged, should involve “a heel cup, shoe insert, or arch support to rectify the pronation, rather than by an attempt to make surgical correction”.<sup>25</sup>

A randomized control trial conducted by Kilmartin et al<sup>37</sup> found orthoses made deformity worse in children aged 9 and 10 years old having juvenile hallux valgus. The study assessed the use of rigid-partial-contact custom made orthoses designed to limit hindfoot pronation versus no treatment. Those receiving treatment were judged compliant if orthoses were worn to follow-up appointments. Follow-up radiographic evaluations were performed 3 years after enrollment. Hallux valgus angle had “deteriorated” in both groups, and the angle of deformity had become largest in children treated with orthoses. Concern has been voiced regarding the suitability of the orthoses prescribed.<sup>1</sup> Besides this very relevant concern as well as the issue of non-verifiable compliance, the orthoses custom fit by Kilmartin et al<sup>37</sup> were never re-made in response to the child’s growth or change in footwear. The perspective weighs these cumulative

limitations when drawing conclusions on whether orthoses have value in the treatment of hallux valgus.

More current randomized control trial evidence has recognized the benefits of treating hallux valgus with foot orthoses. Torkki and coworkers published one year<sup>10</sup> and two year<sup>8</sup> follow-up trials comparing orthoses, surgery, and no treatment. A consecutive series of 211 adult patients (mean age 49 years) seeking care for mild or moderate hallux valgus deformity participated. The orthoses were custom-made using a negative cast technique with individual prescription written according to the presenting deformity. Patients treated with orthoses described themselves improved on a global assessment scale at one year follow-up.<sup>10</sup> At year two,<sup>8</sup> patients treated with orthoses were as satisfied as those having surgery, and more satisfied than controls. Torkki and colleagues<sup>10</sup> did not speculate on why early intervention with orthoses might forestall the need for corrective surgery.<sup>8</sup> But consistent with theory advanced in this perspective, it could be that orthoses fit to the arch may orient the first metatarsal axis horizontal. This ultimately changed the associated joint interactions. We contend, therefore, that orthoses constructed to bolster the arch and orient the first metatarsal horizontal may work to contain the kinetics and kinematics of the first metatarsal to the sagittal plane.<sup>18, 22, 62</sup>

### **Summary**

Multiple factors have been implicated in the etiology of hallux valgus. This perspective suggests that collapse of the arch under weightbearing load orients the first metatarsal

axis towards vertical and predisposes adduction of the first metatarsal which initiates deformity. This grounded theory was built upon the following points:

- The first metatarsal rotates about its own axis.
- Orientation of this axis is variable and dependent on the shape of the medial arch.
- The arch is best able to carry weight and keep its shape when the first metatarsal is properly aligned.
- Collapse of the arch tends to orient the first metatarsal axis towards vertical.
- Adduction of the first metatarsal occurs about a vertical axis.
- Adduction of the first metatarsal predisposes hallux valgus.

Orthoses designed to keep the medial arch from collapsing under load may orient the first metatarsal axis towards the horizontal which may in theory, help contain physiological rotation of the first metatarsal to the sagittal plane and optimize the internal properties of the medial arch to carry weight. For this reasoning to be applied in practice, research needs to identify specific foot types and patient populations who would benefit from wearing orthoses constructed to support the arch with intent to orient the first metatarsal axis horizontal. Clinical trials could then be pursued to investigate if orthoses used early in the treatment of hallux valgus may reduce or even reverse the progression of deformity.

## Figure Legend (Chapter II.)

**Fig. 2.1.** Hallux valgus disrupts normal alignment of the metatarsophalangeal joint.

Arrows indicate the direction of joint member deformity displacements. The hallux abducts while the first metatarsocuneiform segments adducts. The severity of the hallux-metatarsal deformity is measured by: A) Hallux Valgus Angle. B) Intermetatarsal 1-2 Angle.

**Fig. 2.2.** The first metatarsal axis represented in 3 different foot postures. A) Pronation.

B) Neutral. C) Supination. Orientation of the axis changes as a function of arch height.

**Fig. 2.3.** Estimates of helical axis vectors about which the first metatarsal rotated (N = 9).

The reference coordinate frame is embedded in the midfoot, as shown in the superimposed image of the foot.

**Fig. 2.4.** A pendulum glued to the nail of the hallux demonstrates how foot posture impacts the alignment of the first MTP joint. A) Supination. B) Pronation.

Reprinted with permission from *Surgery of the Foot and Ankle*, 8ed. MJ Coughlin, RA Mann, CL Saltzman. pp 200, Copyright Mosby Elsevier; 2007.

Figure 2.1.

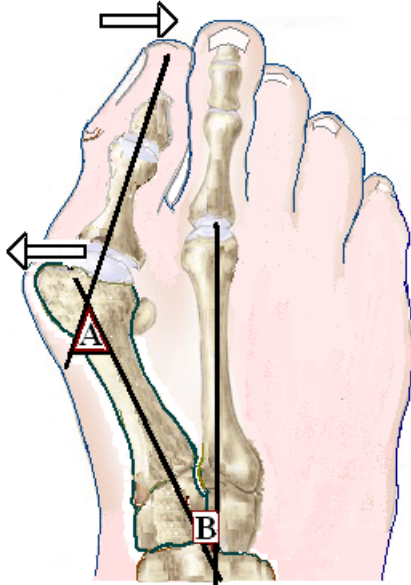


Figure 2.2.

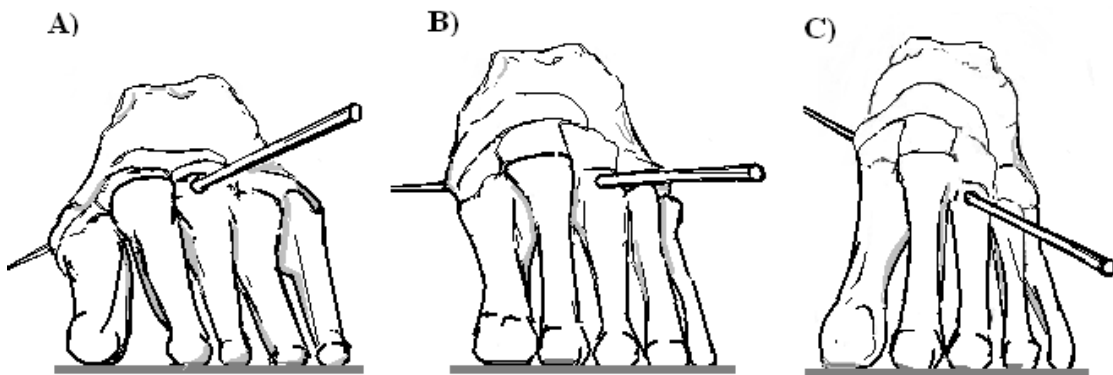


Figure 2.3.

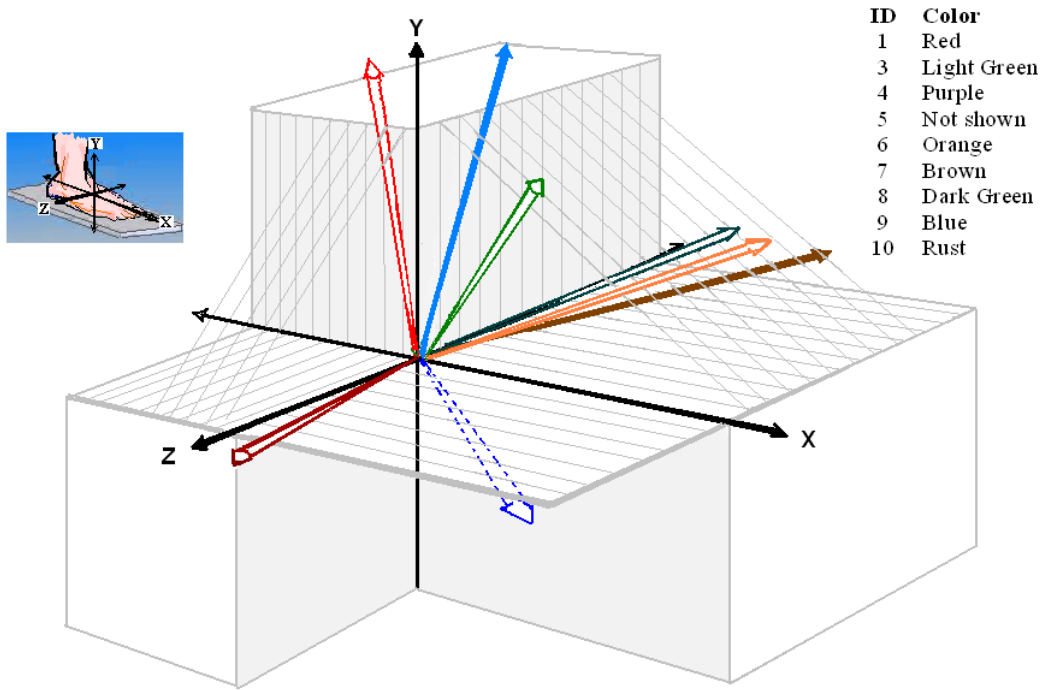
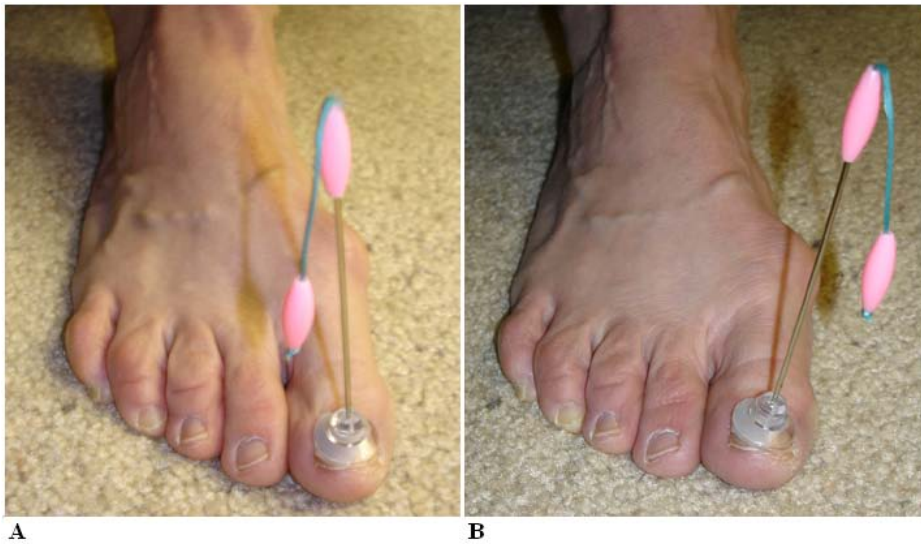


Figure 2.4.



## References (Chapter II.)

1. Ferrari J, Higgins J, Prior T. Interventions for treating hallux valgus (abductovalgus) and bunions. *Cochrane Database of Systematic Reviews*. 2004;Issue 1. Art. No.:CD000964.DOI:10.1002/14651858.CD000964.pub2.
2. Hardy R, Clapham J. Observations on hallux valgus: based on a controlled series. *J Bone Joint Surg*. 1951;33-B:376-391.
3. Mann R, Coughlin M. Hallux valgus - etiology, anatomy, treatment, and surgical considerations. *Clin Orthop Rel Res*. 1981;157:31-41.
4. Easley M, Trnka H. Current concepts review: hallux valgus Part 1: pathomechanics, clinical assessment, and nonoperative management. *Foot Ankle Int*. 2007;28(5):654-659.
5. Caselli M, George D. Foot deformities: biomechanical and pathomechanical changes associated with aging, part 1. *Clin Podiatr Med Surg*. 2003;20:487-509.
6. Hart E, deAsla R, Grottkau B. Current concepts in the treatment of hallux valgus. *Orthopaedic Nursing*. 2008;27(5):274-280.
7. Groiso J. Juvenile hallux valgus. A conservative approach to treatment. *J Bone Joint Surg*. 1992;74-A:1367-1374.
8. Torkki M, Malmivaara A, Seitsalo S, Hoikka V, Laippala P, Paavolainen P. Hallux valgus: immediate operation versus 1 year of waiting with and without orthoses. *Acta Orthop Scand*. 2003;74(2):209-215.
9. Thompson F, Coughlin M. The high price of high-fashion footwear. *J Bone Joint Surg Am*. 1994;10:1586-1593.
10. Torkki M, Malmivaara A, Scitsalo S, Hoikka V, Laippala P, Paavolainen P. Surgery vs orthosis vs watchful waiting for hallux valgus. *J Am Med Assoc*. 2001;285:2474-2480.
11. Romash M, Fugate D, Yanklowit B. Passive motion of the first metatarsal cuneiform joint: preoperative assessment. *Foot Ankle*. 1990;10(6):293-298.
12. Glasoe W, Yack H, Saltzman C. Anatomy and biomechanics of the first ray. *Phys Ther*. 1999;79(9):854-859.
13. Wanivenhaus A, Pretterklieber M. First tarsometatarsal joint: anatomical biomechanical study. *Foot Ankle Int*. 1989;9(4):153-157.
14. Woltring H. Representation and calculation of 3-D joint movement. *Human Movement Science*. 1991;10:603-616.
15. Hicks J. The mechanics of the foot. I. The joints. *J Anat*. 1953;87:345-357.
16. Shereff M. Pathology, anatomy and biomechanics of hallux valgus. *Orthopaedics*. 1990;13(9):939-945.
17. Coughlin M. Hallux valgus. *J Bone Joint Surg*. 1996;78A:932-966.



18. Talbot K, Saltzman C. Hallucal rotation: a method of measurement and relationship to bunion deformity. *Foot Ankle Int.* 1997;18(9):550-556.
19. Tanaka Y, Takakura Y, Sugimoto K, Kumai T, Sakamoto T, Kadono K. Precise anatomic configuration changes in the first ray of the hallux valgus. *Foot Ankle Int.* 2000;21:651-656.
20. Coughlin M, Saltzman C, Nunley J. Angular measurements in the evaluation of hallux valgus deformities: a report of the ad hoc committee of the American Orthopaedic Foot and Ankle Society on Angular Measurements. *Foot Ankle Int.* 2002;23:68-74.
21. Coughlin M. Hallux valgus in men: effect of the distal metatarsal articular angle on hallux valgus correction. *Foot Ankle Int.* 1997;18(8):463-470.
22. Scranton P, Rutkowski R. Anatomic variations in the first ray: Part I. Anatomic aspects related to bunion surgery. *Clin Orthop Rel Res.* 1980;151:244-255.
23. Roukis T, Weil LJ, Weil LS, Landsman A. Predicting articular erosion in hallux valgus: clinical, radiographic, and intraoperative analysis. *J Foot Ankle Surg.* 2005;44(1):13-21.
24. Kernozek T, Elfessi A, Sterriker S. Clinical and biomechanical risk factors of patients diagnosed with hallux valgus. *J Am Podiatr Med Assoc.* 2003;93(2):97-103.
25. Inman V. Hallux valgus: a review of etiologic factors. *Orthop Clin N Amer.* 1974;5(1):59-66.
26. Saltzman C, Aper R, Brown T. Anatomic determinants of first metatarsophalangeal flexion moments in hallux valgus. *Clin Orthop.* 1997;339(6):261-269.
27. Sanders A, Snijders C, Linge B. Medial deviation of the first metatarsal head as a result of flexion forces in hallux valgus. *Foot Ankle Int.* 1992;13(9):515-522.
28. Snijder C, Snijder J, Philippens M. Biomechanics of hallux valgus and spread foot. *Foot Ankle.* 1986;7:26-39.
29. Barnicott N, Hardy R. The position of hallux in Western Africans. *J Anat.* 1952;89:355-361.
30. MacLennan R. Prevalence of hallux valgus in neolithic New Guinea population. *Lancet.* 1966;1:1398-1400.
31. Sim-Fook. A comparison of foot forms among the non-shoe and shoe-wearing Chinese people. *J Bone Joint Surg AM.* 1958;40:1058-1062.
32. Kato S, Watanabe S. The etiology of hallux valgus in Japan. *Clin Orthop.* 1981;157:188-191.
33. Menz H, Morris M. Determinants of disabling foot pain in retirement village residents. *J Am Podiatr Med Assoc.* 2005;95:573-579.
34. Dunn J, Link C, Felson D, Crincoli M, Keysor J, McKinley J. Prevalence of foot and ankle conditions in a multiethnic community sample of older adults. *Am J Epidemiol.* 2004;159:491-498.
35. Gould N, Schneider W, Ashikaga T. Epidemiological survey of foot problems in the continental United States. *Foot Ankle.* 1980;1:8-10.

36. Harris M-C, Beeson P. Generalized hypermobility: Is it a predisposing factor towards the development of juvenile hallux abducto-valgus? Part 2. *The Foot*. 1998;8(4):203-209.
37. Kilmartin T, Barrington R, Wallace W. A controlled prospective trial of a foot orthosis for juvenile hallux valgus. *J Bone Joint Surg*. 1994;76-B:210-214.
38. Coughlin M. Juvenile hallux valgus: etiology and treatment. *Foot Ankle Int*. 1995;16(11):682-697.
39. Hardy R, Clapham J. Hallux valgus, predisposing anatomical causes. *Lancet*. 1952;1180-1183.
40. Scranton P, McDermott J. Prognostic factors in bunion surgery. *Foot Ankle Int*. 1995;16(11):698-704.
41. Belt E, Kaarela K, Lehto M. Destruction and arthroplasties of the metatarsophalangeal joints in seropositive rheumatoids arthritis. *Scand H Rheumatol*. 1998;27:194-196.
42. Turner D, Woodburn J, Helliwell P, Cornwall M, Emery P. Pes planovalgus in rheumatoid arthritis: a descriptive and analytical study of foot function determined by gait analysis. *Musculoskeletal Care*. 2003;1:21-33.
43. Turner D, Helliwell P, Lohmann Siegel K, Woodburn J. Biomechanics of the foot in rheumatoid arthritis: identifying abnormal function and the factors associated with localized disease 'impact'. *Clin Biomech*. 2008;23:93-100.
44. Woodburn J, Nelson K, Siegel K, Kepple T, Gerber L. Multisegment foot motion during gait: proof of concept in rheumatoid arthritis. *J Rheumatol*. 2004;31(10):1918-1927.
45. Bryant A, Tinley P, Singer K. A comparison of radiographic measurements in normal, hallux valgus, and hallux limitus feet. *J Foot Ankle Surg*. 2000;39:39-43.
46. Mancuso J, Abramow S, Landsman M, Waldman M, Carioscia M. The zero-plus first metatarsal and its relationship to bunion deformity. *J Foot Ankle Surg*. 2003;42(6):319-326.
47. Ross-Smith N. Hallux valgus and rigidus treated by arthrodesis of the metatarsophalangeal joint. *Br Med J*. 1952;2:1385-1387.
48. Truslow W. Metatarsus primus varus or hallux valgus? *J Bone Joint Surg*. 1925;7:98-108.
49. Viladot A. Metatarsalgia due to biomechanical alterations of the forefoot. *Orthop Clin N Am*. 1973;4:165-178.
50. Ferrari J, Malone-Lee J. The shape of the metatarsal head as a cause of hallux abductovalgus. *Foot Ankle Int*. 2002;23:236-242.
51. Kilmartin T, Wallace W. First metatarsal head shape in juvenile hallux abducto valgus. *J Foot Surg*. 1991;30:506-508.
52. Ferrari J, Hopkinson D, Linney A. Size and shape differences between male and female foot bone. Is the female foot predisposed to hallux abducto valgus deformity? *J Am Podiatr Med Assoc*. 2004;94(5):434-452.

53. Johnson K, Kile T. Hallux valgus due to cuneiform-metatarsal instability. *J South Orthop Assoc.* 1994;3(4):273-282.
54. Glasoe W, Allen M, Saltzman C. First ray dorsal mobility in relation to hallux valgus deformity and first intermetatarsal angle. *Foot Ankle Int.* 2001;22(2):98-101.
55. Kalen V, Breecher A. Relationship between adolescent bunions and flatfeet. *Foot Ankle.* 1988;8(6):331-336.
56. Klaue K, Hansen S, Masquelet A. Clinical, quantitative assessment of first tarsometatarsal mobility in the sagittal plane and its relation to hallux valgus deformity. *Foot Ankle Int.* 1994;15(1):9-13.
57. Lapidus P. The operative correction of the metatarsus varus primus in hallux valgus. *Surg Gynecol Obstet.* 1934;58:183-191.
58. Myerson M. Metatarsocuneiform arthrodesis for treatment of hallux valgus and metatarsus primus varus. *Orthopedics.* 1990;13(9):1025-1031.
59. Sangeorzan B, Hansen S. Modified Lapidus procedures for hallux valgus. *Foot Ankle Int.* 1989;9(6):262-266.
60. Ebisui J. The first ray axis and first metatarsophalangeal joint. *J Am Podiatr Assoc.* 1968;58(4):160-168.
61. D'Amico J, Schuster R. Motion of the first ray. *J Am Podiatr Assoc.* 1979;69:17-23.
62. Glasoe W, Pena F, Phadke V, Ludewig P. Arch height and first metatarsal joint axis orientation as related variables in foot structure and function: theory related to bunion. *Foot Ankle Int.* 2008;29(6):647-655.
63. Johnson C, Christensen J. Biomechanics of the first ray part 1. The effects of peroneus longus function: a three-dimensional kinematic study on a cadaver model. *J Foot Ankle Surg.* 1999;38(5):313-321.
64. Kelso S, Richie D, Cohen I, Weed J, Root M. Direction and range of the first ray. *J Am Podiatr Med Assoc.* 1982;72:600-605.
65. Oldenbrook L, Smith C. Metatarsal head motion secondary to rearfoot pronation and supination. *J Am Podiatr Assoc.* 1979;69(1):24-28.
66. Khaw F, Mak P, Johnson G, Briggs P. Distal ligamentous restraints of the first metatarsal. An in vitro biomechanical study. *Clin Biomech.* 2005;20:653-658.
67. Wolf P, Stacoff A, Liu A, et al. Functional units of the human foot. *Gait Posture.* 2008;28:434-431.
68. Nester C, Liu A, Ward E, et al. In vitro study of foot kinematics using a dynamic walking cadaver model. *J Biomech.* 2007;40:1927-1937.
69. Allen M, Cuddeford T, Glasoe W, et al. Relationship between static mobility of the first ray and first ray, midfoot, and hindfoot motion during gait. *Foot Ankle Int.* 2004;25(6):391-396.

70. Cornwall M, McPoil T. Motion of the calcaneus, navicular, and first metatarsal during the stance phase of walking. *J Am Podiatr Med Assoc.* 2002;92(2):67-76.
71. Engsborg J, Andrews J. Kinematic analysis of the talocalcaneal/talocrural joint during running support. *Med Sci Sports Exerc.* 1987;19(3):275-284.
72. Faber F, Kleinrensink G, Mulder P, Verhaar J. Mobility of the first tarsometatarsal joint in hallux valgus patients: a radiographic analysis. *Foot Ankle Int.* 2001;22(12):965-969.
73. Lee K, Young K. Measurement of first-ray mobility vs. hallux valgus patients. *Foot Ankle Int.* 2001;22(12):960-964.
74. Roukis T, Landsman A. Hypermobility of the first ray: a critical review of the literature. *J Foot Ankle Surg.* 2003;42(6):377-390.
75. Cornwall M, Fishco W, McPoil T, Lane C, O'Donnell D, Hunt L. Reliability and validity of the clinically assessing first-ray mobility of the foot. *J Am Podiatr Med Assoc.* 2004;94(5):470-476.
76. Glasoe W, Allen M, Saltzman C, Ludewig P, Sublett S. Comparison of two methods used to assess first ray mobility. *Foot Ankle Int.* 2002;23(3):248-252.
77. Coughlin M, Jones C. Hallux valgus and first ray mobility. *J Bone Joint Surg.* 2007;89A(9):1887-1898.
78. Coughlin M, Jones C, Viladot R, et al. Hallux valgus and first ray mobility: a cadaveric study. *Foot Ankle Int.* 2004;25(8):537-544.
79. Kim J, Park J, Hwang S, Young K, Sung I. Mobility changes of the first ray after hallux valgus surgery: clinical results after proximal metatarsal chevron osteotomy and distal soft tissue procedure. *Foot Ankle Int.* 2008;29(5):468-472.
80. Coetzee J, Wickum D. The Lapidus procedure: a prospective cohort outcome study. *Foot Ankle Int.* 2004;25:526-531.
81. Glasoe W, Allen M, Kepros T, Stonewall L, Ludewig P. Dorsal first ray mobility in women athletes with a history of stress fracture of the second or third metatarsal. *J Orthop Sports Phys Ther.* 2002;32(11):560-567.
82. Glasoe W, Allen M, Ludewig P, Saltzman C. Dorsal mobility and first ray stiffness in patients with diabetes mellitus. *Foot Ankle Int.* 2004;25(8):250-555.
83. Carl A, Ross S, Evanski P, Waugh T. Hypermobility in hallux valgus. *Foot Ankle Int.* 1988;8(5):264-270.
84. Uchiyama E, Kitaoka H, Luo Z, Grande J, Kura H, An K. Pathomechanics of hallux valgus: biomechanical and immunohistochemical study. *Foot Ankle Int.* 2005;26:732-738.
85. Coughlin M. *Adult Hallux Valgus.* In: Coughlin MJ, Mann RA, Saltzman CL, eds. *Surgery of the Foot and Ankle. Vol 1. 8th ed.* Philadelphia: Mosby; 2007.

86. Eustace S, Byrne J, Beausang O, Codd M, Stack J, Stephens M. Hallux valgus, first metatarsal pronation and collapse of the medial longitudinal arch - a radiological correlation. *Skeletal Radiol.* 1994;23:191-194.
87. Scranton P. Adolescent bunions: diagnosis and management. *Pediatr Ann.* 1982;11:518-520.
88. Hawes M, Nachbauer W, Sovak D, Nigg B. Footprint parameters as a measure of arch height. *Foot Ankle.* 1992;13(1):22-26.
89. Mathieson I, Upton D, Prior T. Examining the validity of selected measures of foot type. *J Am Podiatr Med Assoc.* 2004;94(3):275-281.

## CHAPTER III.

### ARCH HEIGHT AND FIRST METATARSAL JOINT AXIS ORIENTATION

#### **Introductory Summary**

This study investigated the association of arch height combined with first metatarsal joint axis vertical (V) - orientation to the size of the 1-2 intermetatarsal angle (IMA) and first metatarsal adduction/abduction position in gait event foot postures, kinematics commonly affected by bunions. *Methods:* Nine cadaver specimens were mounted in a loading frame. Measures of arch height ratio and IMA were made. Next, with the foot placed in gait event posture an electromagnetic device tracked 3D displacement of the bone segments from which the relative angle of rotations between the first metatarsal and navicular, and helical axis (HA) parameters were obtained. Canonical correlation method of analysis assessed the relationship among the variables. *Results:* A negative relationship ( $r = -0.73$ ) was found between arch height and first metatarsal HA V-orientation. When considered as combined variables, arch height and metatarsal HA V-orientation accounted for 69% of the variance of IMA and change in first metatarsal adduction/abduction position. *Conclusion:* Orientation of the first metatarsal joint axis was highly variable between specimens and related to arch height. The conjoined factors of arch height and first metatarsal HA V-orientation accounted for most of the variance of IMA and change in first metatarsal adduction/abduction position during the sequence of gait event postures. This could suggest that orthosis arch support has potential to reorient

the metatarsal joint axis out-of-vertical and in effect, contain the first metatarsal from displacing into adduction and towards bunion deformity. Theory introduced in this study may help to explain the genesis of bunion and considers the mechanism by which orthosis may prevent bunion from worsening into late stage deformity. **Key Words:** Biomechanics, First Ray, Helical Axis, Orthoses.

## 1. Introduction

The first metatarsal moves independently about its own axis but with considerable individual variability.<sup>1-3</sup> The influence of the first metatarsal joint axis on its directional motion has been considered in several quasi-static cadaveric experiments.<sup>2, 4-8</sup> The study by Hicks<sup>2</sup> directly investigated the location and orientation of the first metatarsal joint axis of rotation. He<sup>2</sup> fastened a mechanical jig to specimens positioned non-weightbearing with the ankle in neutral. By maneuvering the jig in a manner so the external wire assembly did not bind during forced motion, Hicks<sup>2</sup> estimated that the axis of the first metatarsal runs nearly horizontal between the navicular and the base of the third metatarsal at an angle 45° to the frontal and sagittal planes.

The instantaneous axis of rotation for any particular arc-of-motion is an imagined line about which a joint rotates in a plane perpendicular. Dorsi- and plantar flexion motions of the forefoot occur about a mediolateral joint axis, adduction and abduction motions occur about a vertical axis, inversion and eversion about a longitudinal axis. This description of motion is understood clinically. Rotation of the first metatarsal about its

axis, as was described by Hicks,<sup>2</sup> should couple simultaneous and equal amounts of undeterred dorsiflexion with inversion and plantar flexion with eversion. Foot postures change during gait. Accordingly, the orientation of the first metatarsal axis must change as a function of arch height. Research has not considered how foot posture might influence the orientation of the first metatarsal joint axis or impact the predisposition to the development of bunion.

The incidence of bunion is highest in older people, and develops with familiar tendency predominantly in women.<sup>9</sup> Other etiologic factors may include a congenital predisposition, disease related impairments, and structural malalignments of the foot.<sup>9-13</sup> Bunion is made worse when pronation of the foot is extreme.<sup>11, 12</sup> This related occurrence may in part be explained by malalignment in the orientation of the first metatarsal joint axis. The second metatarsal serves as the central strut of forefoot stability.<sup>2</sup> Pronation lowers the medial arch in relation to the fixed more centrally located second metatarsal, dropping the navicular closer to the ground while the proximal base of the third metatarsal is raised. Tipping an axis vertically tends to transfer motion away from the sagittal and towards the transverse plane. Altered profiles of first metatarsal structure and function are the pathomechanics most associated with bunion<sup>10, 14</sup> and other first metatarsophalangeal joint pathologies.<sup>9, 15</sup> It seems reasonable, therefore to conclude that some acquired first metatarsal problems may result from malalignment in orientation of the metatarsal joint axis.



This in vitro study provides a comprehensive helical axis (HA) description of the relative change in first metatarsal positions collected during a sequence of controlled gait event static foot postures. The experiment investigated the strength of association of arch height combined with the vertical orientation of the first metatarsal joint axis to the structural 1-2 intermetatarsal angle (IMA) and change in first metatarsal adduction/abduction position.<sup>5,13</sup> The null hypothesis tested was that the combined variables of arch height and metatarsal axis orientation are unrelated to IMA and change in first metatarsal adduction/abduction position measured in gait event postures.

## **2. Methods**

### **2.1 Specimen preparation**

Ten fresh frozen cadaver foot specimens were tested. An error made when testing specimen #02 caused its data to be uninterpretable; analysis was performed on 9 specimens (Table 1). Use of cadavers permitted the rigid fixation of pins into bone.<sup>16,17</sup> Specimens had no history of foot surgery. All had joint dorsiflexion of at least 5° at the ankle and 60° at the hallux. The University of Minnesota Anatomy Bequest Program approved the study and provided the specimens.

Specimens were thawed and sectioned mid-tibia. The cut was made proximal to the medial malleolus at a length equal to the straight-line distance measured between the medial malleolus and the first metatarsal head. The most proximal 6 cm bony end was

stripped of all soft tissues and potted in polymethylmethacrylate. Potting fixed the fibula to the tibia, and provided a surface by which the specimen was loaded for testing.<sup>18</sup>

Preparation of the specimen included fixation of the subtalar joint, and placement of 2.5 mm intracortical pins into selected bones. An orthopaedic surgeon (F.A.P.) performed both procedures. The calcaneus was held fixed to talus in the neutral frontal plane with two partially threaded 6.5 mm screws to remove subtalar joint motion during loading. The pins drilled into the tibia, calcaneus, navicular, medial cuneiform, first metatarsal, the proximal phalanx of the hallux, and the second metatarsal allowed direct motion tracking of the bone by attached sensors (Fig. 1). The advantage in measuring kinematic motion from sensors pinned directly to bone is that recorded data is unaffected by skin movement artifact.

## **2.2 Kinematic modeling**

Kinematic data was recorded with a Flock of Birds<sup>TM</sup> (FoB) electromagnetic motion analysis system (Ascension Technology, Burlington, VT, USA).<sup>16, 19</sup> This system monitored the relative motion of receiving sensors in relation to a transmitter. The magnetic fields transmitter-to-sensor spatial location of each segment was collected and analyzed by computer algorithms in a global system expressed as orthogonal coordinates. The FoB system is highly accurate having errors of less than 2% over its operating range, and sensitive enough to read rotational changes of 0.1°.<sup>20</sup>

A 6-segment foot model plus leg was used (Table 2). The embedded coordinates were constructed from digitized skeletal points. Once constructed, the embedded anatomical axes identified by the attached segment sensor recorded the spatial relationship between segments.<sup>21</sup>

Data were processed as 3 sequential euler angle rotations, and helical parameters to provide HA vertical (V) -orientation of the first metatarsal relative to the midfoot embedded coordinate system. A helical axis is a direction cosine vector (DCV) having unit length which defines the 3D axis of rotation between two sequential positions (Fig. 2). Vertical orientation of the HA was calculated [ $\theta = \tan^{-1} (\cos Y/\cos Z)$ ] as the projection of the overall vector in the y-direction of the midfoot reference frame.<sup>22</sup>

Anticipating the axis of the first metatarsal to be located near the midfoot is consistent with what Hicks reported.<sup>22</sup> Because the contour of the arch lowers early in stance until heel off and raises following,<sup>23, 24</sup> helical axis V-orientations were computed from kinematic data collected at foot flat and heel off, and again at heel off and terminal stance.

Digitization of the landmarks was performed by a single examiner (W.M.G.) using a stylus with measured tip offsets. Table 2 lists the points digitized and fixed coordinate definitions. Definitions conformed to the right hand rule. Left sided data were converted to right sided equivalency. The positive Z axis projected lateralward, positive X forward, and positive Y upward. For example, the leg coordinate originated midway between the

malleoli so the *Z* axis pointed laterally along the transmalleolar line, the *X* axis pointed anteriorly and perpendicular to a plane made by the points of the leg and malleoli, the *Y* axis pointed superiorly.<sup>21</sup> All coordinate definitions followed this general pattern of direction.

### **2.3 Procedures**

The potted end of the specimen was placed in an assembly mounted directly to an Instron (Instron Corp, Norwood, MA, USA) loading frame. The assembly had a pivot adjustment making it possible to position the foot under the imposed load in a way that simulated gait (Fig. 1). A 100 N axial load was imposed at each position. Data collected in neutral stance provided base line comparisons.

Digitization of the skeletal points, and the measures of arch height and IMA were made with the foot positioned in neutral posture while under load. Arch height measured by standard rule was computed as a ratio of navicular height divided by length of the truncated foot. This normalized ratio closely reflects the radiographic indices of the medial longitudinal arch structure.<sup>25</sup> Arch ratios average 0.18 in older people aged 62 to 94.<sup>26</sup> The IMA was calculated as a cosine dot product function from the vectors of first and second metatarsal digitized long axis points. An IMA of 9° is the upper limit of normal alignment in the adult foot.<sup>27, 28</sup>

Data were collected at the gait event postures of foot flat (FF), midstance (MS), late stance (LS), heel off (HO), and terminal stance (TS). Each event was assumed to represent a time instance of continuous foot motion during a gait cycle (Fig. 3). Ankle and hallux joint positions served as the reference for replicating the gait events.<sup>29-32</sup> The ankle was placed in a position of plantar flexion ( $5^{\circ}$ ) at FF, neutral at MS, dorsiflexed  $5^{\circ}$  at LS and at HO, and plantar flexed  $10^{\circ}$  at TS. The hallux was dorsiflexed  $35^{\circ}$  at HO (Fig. 1B) and  $60^{\circ}$  (Fig. 1C) at TS. One second (100 Hz) of static “no-motion” data was sampled. The gait event foot postures were collected in random order and repeated to assess the reliability of the measurements.

The tibia was fixed to the talus with two screws when loading at HO and TS (Fig. 1). This method of temporarily fixating the ankle joint allowed the imposed 100 N axial load to be transmitted forward onto the forefoot. The force beneath the first metatarsal was measured with a load cell. Force carried by the first metatarsal was greatest when loading the foot into terminal stance, averaging 25 N. This proportion of load carried by the first metatarsal is comparable to weight distribution values during gait.<sup>33</sup>

## **2.4 Analysis**

The controlled static foot postures served as the independent test variable. Arch height and HA V-orientation were intervening variables. The IMA 1-2 along with the change in relative adduction/abduction angle between the first metatarsal and the navicular recorded during the sequence of gait event postures were the response variables.

Statistical analysis was performed using SPSS 15.0 for Windows (SPSS Inc, Chicago, IL). Descriptive statistics were calculated for all variables. Analysis included the computation of intraclass correlation coefficients (ICC) and standard error of measurements (SEM) to assess trial-to-trial consistency of the Cardan angle ordered rotations. Canonical correlation analysis assessed the linear relationship between grouped data sets. The canonical coefficients interpret like the Pearson's  $r^{34}$  and were used to explain the relationship of the combined arch height and HA V-orientation variables as compared for association to the response variables of IMA and the first metatarsal adduction/abduction position.

### **3. Results**

The mean arch height ratio was  $0.21 \pm .03$ . Mean IMA 1-2 was  $8.0^\circ \pm 4.2$  (Table 1).

Mean angular first metatarsal positions measured with respect to the navicular across the simulated gait events are displayed in Figure 3. Trial-to-trial reliability was excellent ( $ICC_{3,1} = 0.99$ ) with SEM values ranging from 1.6 to 1.9°. Table 3 shows the relative adduction (+) or abduction (-) angles between the navicular and first metatarsal measured at the specified simulated gait events. The column labeled rotation in Table 3 reports the total rotation of the first metatarsal measured about its oblique axis without regard to the anatomical planes.

The Z, X, Y helical axis component parameters are in Table 3. The first metatarsal HA vectors graphically represented in Figure 2 are approximations of these values. The HA vertical projection angles displayed in Figure 4.B were calculated for each specimen. A maximum value of 90° was assigned to the Y positive component vertical reference coordinate; the Z axis was 0°. Hypothetically, a helical axis having a Y component length of 1 and angle of 0° would project nearly vertical, with adduction or abduction the motions observed.

Canonical correlation solutions computed between early stance (FF and HO) and late stance (HO and TS) gait event data are in Table 4. The first composite variate explains the shared variance and indicates the relative direction and strength of the correlation.<sup>34</sup> The early stance canonical variates were 0.83 and 0.25. The late stance coefficients were 0.74 and 0.12. Canonical solutions are meaningful in explaining the relation of the two sets of variables if the correlation is 0.30 (9% of variance) or higher.<sup>34</sup> For completeness, univariate correlations for all tested variables are reported (Table 4).

#### **4. Discussion**

We used a helical axis approach to investigate the orientation of the first metatarsal joint axis. The cosines of 3 directional angles specify HA orientation with respect to an embedded reference anatomical coordinate systems.<sup>35</sup> Figure 2 shows the approximations of HA vectors computed from the early stance data. Vectors for each specimen are displayed except #05. The HA parameters of specimen #05 were negative

(Table 3); this vector would project down and behind the reference coordinate. Showing HA vectors projecting from reference coordinate in this manner (Fig 2) helps convey the importance of considering alignment of the midfoot anatomical coordinate system as a key factor when defining the orientation of the first metatarsal joint axis.

Arch height and first metatarsal HA V-orientation were found related to the response measurements of IMA and change in first metatarsal adduction/abduction position during the sequence of the static gait foot postures. The canonical correlation method of analysis identified the shared variance in the set of response variables explained by the set of intervening variables.<sup>36</sup> The first canonical correlation 0.83 computed from the early stance gait event data accounted for 69% of the shared variance (Table 4). This composite loaded with equal parts arch height and HA V-orientation, suggesting the two intervening variables contributed equally to the structure and assessed essentially the same phenomenon. The first canonical correlation 0.74 for the late stance gait event data sets explained a comparably smaller percentage (55%) of the shared variance. This composite loaded 3-times heavier with HA V-orientation than with arch height.

Evidence of this uneven loadings in structure can be seen in the late stance univariate  $r$  values (Table 4), where HA V-orientation was the predominant intervening variable related to IMA ( $r = -0.31$ ) and change in metatarsal position ( $r = 0.67$ ). Based on these findings, we speculate that arch height and HA V-orientation are conjoined factors that influence the weightbearing kinematics of the first metatarsal mostly when weight is distributed across the full span of the medial arch.



The relationship ( $r = -0.73$ ) between arch height and HA V-orientation for early stance was strongly negative indicating that the metatarsal joint axis had increased vertical orientation in the lower arched foot (Table 4).<sup>13</sup> This finding has clinical importance because collapse of the medial arch is believed a comorbid consequence of bunion.<sup>11-13</sup> Although evidence is limited,<sup>11-13, 37</sup> intervention with orthosis during the early stages of bunion seems to reduce pain and improve gait. We speculate that support of the arch may mechanically reorient the metatarsal joint axis out-of-vertical and in effect, contain the first metatarsal from displacing into adduction and towards bunion deformity. This mechanism by which orthosis may prevent the progression of bunion is testable. This research team is presently preparing to test patients having severe bunion to assess the influence of metatarsal axis orientation and/or arch height as factors related to bunion. Future clinical trials should investigate if bolstering the arch in manner comfortable for a patient can functionally reorient the joint axis during gait.

We found little available motion at the first metatarsocuneiform and cuneonavicular joints. Comparable results have been reported in other in vitro foot studies. Johnson, 1999 #263; Nester, 2007 #467; Wanivenhaus, 1989 #68} Relative angles between the first ray (metatarsal and cuneiform) and the navicular averaged less than  $3^\circ$  in any anatomical plane of motion (Fig 3.). The first ray angular position dorsiflexed from FF to HO, and plantar flexed from HO to TS. This pattern in metatarsal positioning has been observed in vivo<sup>21, 38, 39</sup> where the first metatarsal dorsiflexed in early stance under weight

acceptance, and plantar flexed into late stance due to tightening of the plantar fascia which shortens the foot. Such comparable results support the construct validity of this present work.

The points digitized and the corresponding axis coordinate definitions (Table 2) were refined from versions described by Leardini<sup>21, 40</sup> and others.<sup>16, 19, 30</sup> Points digitized were not always contained in the segment defined. The hindfoot local coordinate, for example, was constructed from points located on both the calcaneus and the leg. Leardini<sup>21, 40</sup> advocated building the hindfoot segment exclusively with calcaneus points, to include the sustentaculum tali. The sustentaculum tali cannot easily be palpated when the foot is bearing weight. Low precision in identifying the digitized points creates errors in axis alignment which reduces the reliability of joint angle measurements.<sup>41</sup> The downside to digitizing points located outside of the defined segment is that a component of the “true” intersegmental joint position may be lost. Our model forced the Y axis coordinates of the calcaneus and leg segments to be coincidental. As a consequence, we did not capture the actual leg-to-calcaneus frontal plane relationship presenting in neutral stance. Research interested in describing hindfoot kinematics may want to explore other options to model the hindfoot.

Points digitized to build the segment coordinates were not validated to assure accuracy. Our computer animated the newly constructed coordinates while points were digitized. This animation provided visual confirmation that the embedded coordinates systems

realistically portrayed the foot. The hallux coordinate, made from all points located on the proximal phalanx,<sup>16,19</sup> did not always capture the observed hallux-to-first metatarsal joint position, especially in the frontal plane. Because the selected digitized hallux points were located close to each other (< 2 cm), even small error associated with palpation exaggerated the problem of coordinate misalignment.<sup>42</sup> Dorsiflexion was the only component of hallux-to-first metatarsal rotation used in this study, and this measure was used only for the purpose of standardizing the static foot postures. Future research may want to explore other options for building the hallux local coordinate from digitized points.

The load imposed in this study was well below physiological levels. Valderrabano et al<sup>17</sup> have used similar methods of axial loading to measure ankle kinematics in cadaver specimens. They advocate for keeping the load at 200N or less because higher loads tend to alter the natural occurring joint kinematics of the foot. In our study, this risk of overload contamination was greatest while testing the foot in late stance postures when the heel lifted (Fig. 1). We found testing at 100 N allowed the first metatarsal to carry load in percentage values similar to gait,<sup>33</sup> but that this percentage-in-magnitude of load carried by the first metatarsal dropped when testing at 200 N. For this reason, all data was collected under an imposed load of 100 N.

We acknowledge additional limitations. The sample was small (N = 9). Specimens tested did not have obvious bunion deformity but instead were thought to represent the

older adult population. Neither dynamic motion nor the contribution of muscles was considered so it is possible that the action of muscles which modulate the extremes of first metatarsal motion during gait<sup>38</sup> could create helical joint axis rotations different from what this study found. Therefore, inferences drawn from this study should be made with caution until further in vivo work can replicate these findings

## **6. Summary**

The development of bunion is complex. Understanding the weightbearing kinematics of the first metatarsal is critical for the advancement of care. In summary, this in vitro investigation found the HA orientation of the first metatarsal to be highly variable between specimens and related to arch height ( $r = -0.73$ ). Considered together, arch height ratio and first metatarsal helical axis V-orientation explained 69% of the variance of IMA and change in first metatarsal adduction/abduction position during gait event postures. Results suggest that a flat-arched foot, a structure frequently found in patients having bunion<sup>11</sup> may tip the metatarsal joint axis toward vertical and predispose medial malalignment of the first metatarsal into deformity common to bunion. This study provides theory for future studies to explore the genesis of bunion from a biomechanical perspective.

**Table 3.1.** Specimen Characteristics.

| ID – Side<br>(N = 9) | Sex | Age<br>(yrs) | Mass<br>(kg) | Arch Height<br>(ratio) | IMA 1-2<br>(degrees) |
|----------------------|-----|--------------|--------------|------------------------|----------------------|
| 01-R                 | F   | 82           | 59           | .19                    | 6.1                  |
| 03-L                 | F   | 68           | 75           | .20                    | 17.2                 |
| 04-R                 | F   | 81           | 48           | .21                    | 10.1                 |
| *05-L                | M   | 43           | 105          | .26                    | 5.6                  |
| 06-L                 | M   | 76           | 73           | .18                    | 7.3                  |
| 07-L                 | M   | 77           | 68           | .25                    | 8.8                  |
| 08-L                 | F   | 94           | 63           | .22                    | 2.5                  |
| 09-R                 | M   | 81           | 63           | .17                    | 4.7                  |
| *10-R                | --  | --           | --           | .27                    | 10.0                 |
| Mean ± SD            |     | 75 ± 15      | 69 ± 17      | .21 ± .03              | 8.0 ± 4.25           |

\* Single specimen, both right and left foot tested.

**Table 3.2.** Segments, Digitized Points, and Coordinate Definitions.

| <b>Segment: Digitized Points</b>  | <b>Axis</b> | <b>Definitions</b>   |
|---|-------------|--|
| Leg<br>Proximal medial & lateral leg<br>Medial malleolus<br>Lateral malleolus                             | Z<br>X<br>Y | <u>Origin</u> : midpoint between the malleoli.<br>Orthogonal to Y and X axes, positive lateral.<br>Orthogonal to the Y axis and a plane through the malleoli,<br>positive forward. Passing through the midpoints of the proximal leg and malleoli, positive upward.  |
| Calcaneus<br>Proximal medial & lateral leg<br>Medial & lateral malleolus<br>Calcaneus tubercle            | Z<br>X<br>Y | <u>Origin</u> : point marking the calcaneus tubercle.<br>Orthogonal to Y axis and a plane through the midpoints of the leg and calcaneus, positive direction lateral.<br>Orthogonal to Z and Y axes, positive direction forward.<br>Passing through the midpoints of the proximal leg and malleoli, positive upward.                     |
| Midfoot (navicular)<br>Navicular tubercle<br>Peroneal tubercle<br>2-Metatarsal head                       | Z<br>X<br>Y | <u>Origin</u> : midpoint between the navicular and cuboid tubercles. Orthogonal to X and Y axes, positive direction lateral. In line with the 2-met head passing the midpoint of navicular and peroneal tubercles, positive forward. Orthogonal to the X axis and a plane through midpoints of the tubercles and 2-met, positive upward. |
| Medial Cuneiform<br>Dorsal prominence cuneiform<br>Plantar ridge cuneiform<br>1-Met medial & lateral head | Z<br>X<br>Y | <u>Origin</u> : point marking dorsal prominence of the medial cuneiform. Orthogonal to Y axis and a plane through the digitized points, positive direction lateral. Orthogonal to Z and Y axes, positive forward. Passing through the cuneiform points, positive upward.   |
| First Metatarsal<br>1-Met medial & lateral base<br>1-Met medial & lateral head                            | Z<br>X<br>Y | <u>Origin</u> : midpoint of the distal first metatarsal head.<br>Orthogonal to X and Y axes, positive direction lateral.<br>Passing through midpoints of the metatarsal, positive forward. Orthogonal to the X axis and a plane through 1-metatarsal midpoints and mediodistal metatarsal head, positive upward.                         |
| Hallux<br>Proximal phalanx medial base<br>Proximal phalanx medial head<br>Proximal phalanx lateral head   | Z<br>X<br>Y | <u>Origin</u> : point marking the proximal medial base.<br>Orthogonal to X and Y axes, positive direction lateral.<br>Passing through the proximal and distal medial points of the proximal phalanx of the hallux, positive forward.<br>Orthogonal to the X axis and a plane through the digitized points, positive upward.              |
| Second Metatarsal<br>2-Met medial & lateral base<br>2-Met medial & lateral head                           | Z<br>X<br>Y | <u>Origin</u> : midpoint of the distal second metatarsal head.<br>Orthogonal to X and Y axes, positive direction lateral.<br>Passing through midpoints of the metatarsal, positive forward. Orthogonal to the X axis and a plane through 2-metatarsal midpoints and mediodistal metatarsal head, positive upward.                        |

**Table 3.3.** Helical axis parameters, and first ray rotation and change in position data.

| Early Stance Gait Events (FF and HO). |                |                |                |              | Late Stance Gait Events (HO and TS). |                |                |                |              |
|---------------------------------------|----------------|----------------|----------------|--------------|--------------------------------------|----------------|----------------|----------------|--------------|
| ID                                    | Z <sub>c</sub> | X <sub>c</sub> | Y <sub>c</sub> | Rotation (°) | ID                                   | Z <sub>c</sub> | X <sub>c</sub> | Y <sub>c</sub> | Rotation (°) |
| 1                                     | 0.17           | -0.45          | 0.88           | 5.84         | 1                                    | -0.51          | 0.27           | -0.82          | 3.81         |
| 3                                     | 0.57           | 0.65           | 0.50           | 2.36         | 3                                    | -0.58          | -0.61          | -0.54          | 4.98         |
| 4                                     | 0.71           | 0.71           | -0.00          | 8.02         | 4                                    | -0.36          | -0.82          | 0.44           | 9.43         |
| 5                                     | -0.78          | -0.29          | -0.56          | 0.68         | 5                                    | -0.69          | 0.57           | -0.45          | 1.24         |
| 6                                     | -0.10          | 0.90           | 0.42           | 2.25         | 6                                    | -0.10          | -0.93          | 0.35           | 2.85         |
| 7                                     | -0.82          | 0.50           | 0.28           | 1.91         | 7                                    | -0.60          | -0.69          | 0.41           | 4.62         |
| 8                                     | -0.10          | 0.87           | 0.48           | 3.81         | 8                                    | -0.25          | -0.90          | 0.35           | 4.01         |
| 9                                     | -0.59          | 0.29           | 0.76           | 5.89         | 9                                    | 0.46           | -0.89          | 0.07           | 5.88         |
| 10                                    | 0.93           | 0.37           | 0.03           | 3.17         | 10                                   | -0.65          | -0.62          | -0.43          | 3.59         |

A positive value indicates adduction, a negative value indicates abduction.

**Table 3.4.** Correlation Results.

**A. Early Stance Gait Events (FF to HO)**

**B. Late Stance Gait Events (HO to TS)**

| *Canonical Correlations |      |
|-------------------------|------|
| 1.                      | 0.83 |
| 2.                      | 0.25 |

| *Canonical Correlations |      |
|-------------------------|------|
| 1.                      | 0.74 |
| 2.                      | 0.12 |

**Early Stance Correlation Coefficients (r)**

|             | Arch Height | HA V-Orient | IMA 1-2 | 1-Met |
|-------------|-------------|-------------|---------|-------|
| Arch Height | 1.00        | -0.73       | -0.06   | -0.78 |
| HA V-Orient |             | 1.00        | -0.24   | 0.75  |
| IMA 1-2     |             |             | 1.00    | -0.07 |
| 1-Met       |             |             |         | 1.00  |

**Late Stance Correlation Coefficients (r)**

|             | Arch Height | HA V-Orient | IMA 1-2 | 1-Met |
|-------------|-------------|-------------|---------|-------|
| Arch Height | 1.00        | -0.23       | -0.06   | 0.09  |
| HA V-Orient |             | 1.00        | -0.31   | 0.67  |
| IMA 1-2     |             |             | 1.00    | -0.61 |
| 1-Met       |             |             |         | 1.00  |

\* The number of canonical correlations is equal to the number of variables in the smallest data set.

### Figure Legend (Chapter III.)

**Fig. 3.1.** Intracortical pins were used to attach the motion sensors to bone. Shown are the static gait event foot postures of: A. Foot Flat, B. Heel Off, C. Terminal Stance.

**Fig. 3.2.** Estimates of the helical axis vectors about which the first metatarsal rotated for each specimen. These vectors were drawn from data collected at the gait events of foot flat and heel off. The reference coordinate frame is embedded in the midfoot, as shown in the superimposed image of the foot.

**Fig. 3.3.** First metatarsal mean static angular positions displayed in the anatomical planes in gait cycle series. The scale is identical between graphs. First metatarsal joint angle values are in relation to the navicular and referenced to the neutral foot posture.

**Fig. 3.4.** Shows the process used to compute the HA vertical projection angle. A. Drawn in isolation is the HA vector of specimen #03, with  $41^\circ$  calculated as the magnitude of vertical orientation displayed on the ZY plane of the reference coordinate system. B. Shows the vertical projection angle for all nine specimens. The displayed vertical projections angles were calculated [ $\theta = \tan^{-1}(\cos Y/\cos Z)$ ] from foot flat and heel off gait event data.



Figure 3.1.

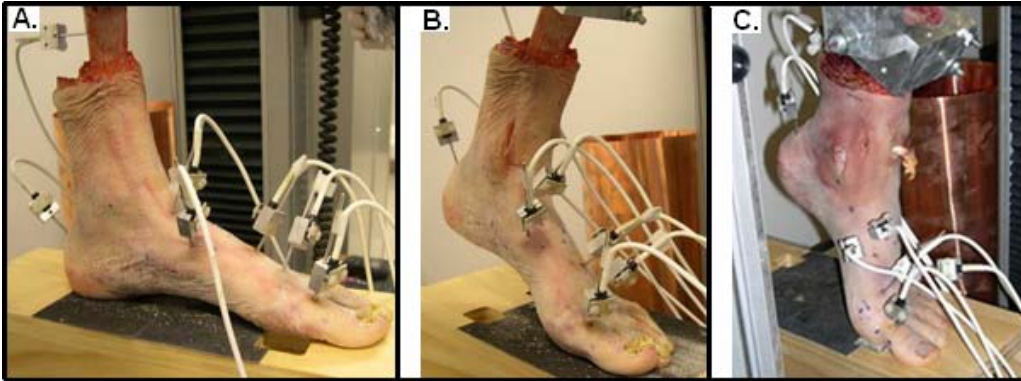


Figure 3.2.

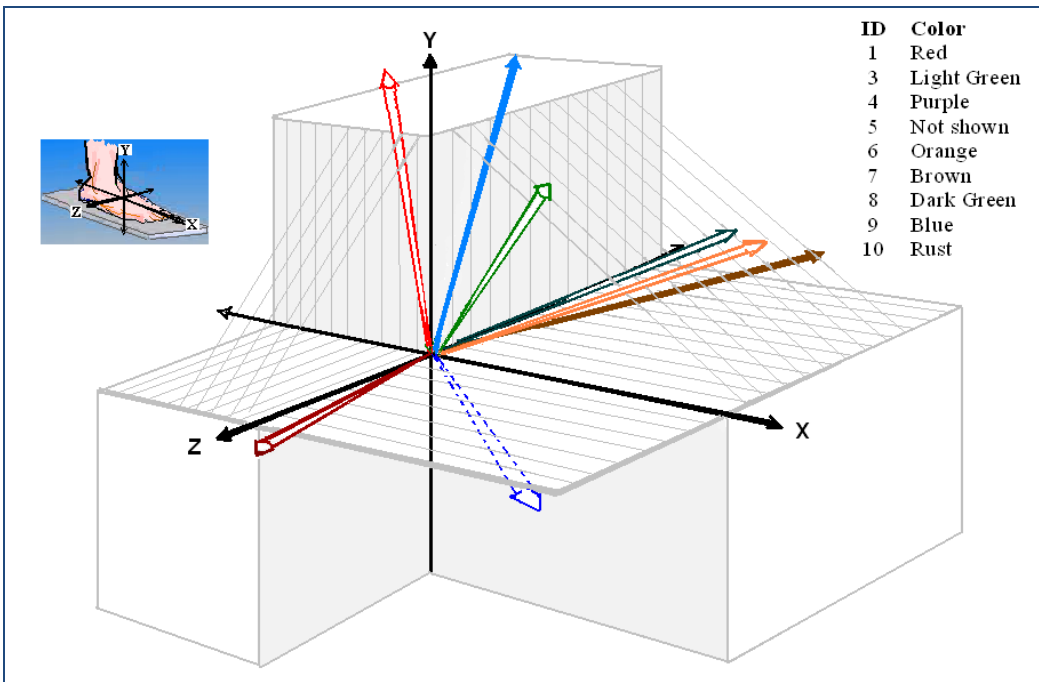


Figure 3.3.

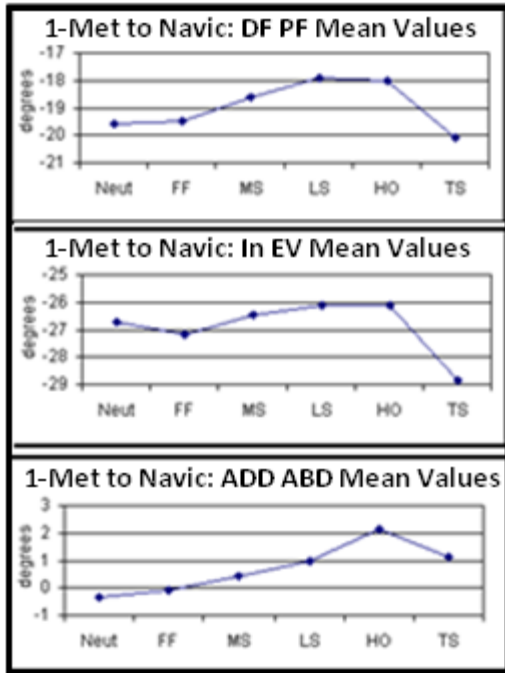
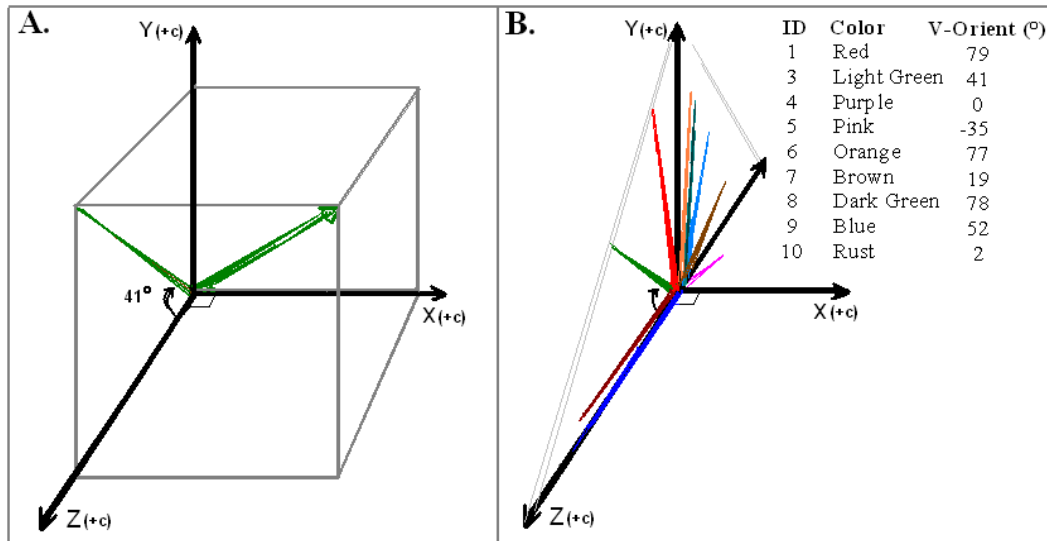


Figure 3.4.



### References (Chapter III.)

1. Coughlin M, Jones C, Viladot R, et al. Hallux valgus and first ray mobility: a cadaveric study. *Foot Ankle Int.* 2004;25(8):537-544.
2. Hicks J. The mechanics of the foot. I. The joints. *J Anat.* 1953;87:345-357.
3. Johnson C, Christensen J. Biomechanics of the first ray part 1. The effects of peroneus longus function: a three-dimensional kinematic study on a cadaver model. *J Foot Ankle Surg.* 1999;38(5):313-321.
4. D'Amico J, Schuster R. Motion of the first ray. *J Am Podiatr Assoc.* 1979;69:17-23.
5. Ebisui J. The first ray axis and first metatarsophalangeal joint. *J Am Podiatr Assoc.* 1968;58(4):160-168.
6. Kelso S, Richie D, Cohen I, Weed J, Root M. Direction and range of the first ray. *J Am Podiatr Med Assoc.* 1982;72:600-605.
7. Khaw F, Mak P, Johnson G, Briggs P. Distal ligamentous restraints of the first metatarsal. An in vitro biomechanical study. *Clin Biomech.* 2005;20:653-658.
8. Oldenbrook L, Smith C. Metatarsal head motion secondary to rearfoot pronation and supination. *J Am Podiatr Assoc.* 1979;69(1):24-28.
9. Coughlin M. Hallux valgus: an instructional course lecture. *J Bone Joint Surg.* 1996;78A:932-966.
10. Easley M, Trnka H. Current concepts review: hallux valgus Part 1: pathomechanics, clinical assessment, and nonoperative management. *Foot Ankle Int.* 2007;28(5):654-659.
11. Inman V. Hallux valgus: a review of etiologic factors. *Orthop Clin N Amer.* 1974;5(1):59-66.
12. Scranton P, McDermott J. Prognostic factors in bunion surgery. *Foot Ankle Int.* 1995;16(11):698-704.
13. Scranton P, Rutkowski R. Anatomic variations in the first ray: Part I. Anatomic aspects related to bunion surgery. *Clin Orthop Rel Res.* 1980;151:244-255.
14. Glasoe W, Allen M, Saltzman C. First ray dorsal mobility in relation to hallux valgus deformity and first intermetatarsal angle. *Foot Ankle Int.* 2001;22(2):98-101.
15. Mann R, Coughlin M. Hallux valgus - etiology, anatomy, treatment, and surgical considerations. *Clin Orthop Rel Res.* 1981;157:31-41.
16. Umberger B, Nawoczinski D, Baumhauer J. Reliability and validity of first metatarsophalangeal joint orientation measured with an electromagnetic tracking device. *Clin Biomech.* 1999;14:74-76.
17. Valderrabano V, Hintermann B, Nigg B, Stefanyshyn P. Kinematic changes after fusion and total replacement of the ankle part 1: range of motion. *Foot Ankle Int.* 2003;24:881-887.
18. LaPrade R, Bollom T, Wentorf F, Wills N, Meister K. Mechanical properties of posterolateral structures of the knee. *Am J Sports Med.* 2005;33:1386-1391.

19. Nawoczenski D, Ludewig P. The effect of forefoot and arch posting orthotic designs on first metatarsophalangeal joint kinematics during gait. *J Orthop Sports Phys Ther.* 2004;34(6):317-327.
20. Milne A, Chess D, Johnson J, King G. Accuracy of an electromagnetic tracking device: a study of optimal range and metal interference. *J Biomech.* 1996;29:791-793.
21. Leardini A, Benedetti M, Cantani F, Simoncini L, Giannini S. An anatomically based protocol for the description of foot segment kinematics during gait. *Clin Biomech.* 1999;14:528-536.
22. Zatsiorsky V. *Kinematics of Human Motion: Human Kinetics*; 1998.
23. Wearing S, Urry S, Pearlman P, Dubois P, Smeathers J. Serial measurement of calcaneal pitch during midstance. *J Am Podiatr Med Assoc.* 1999;89(4):188-193.
24. Wearing S, Urry S, Pearlman P, Smeathers J, Dubois P. Sagittal plane motion of the human arch during gait: a videofluoroscopic analysis. *Foot Ankle Int.* 1998;19(11):738-742.
25. Saltzman C, Nawoczenski D, Talbot K. Measurement of the medial longitudinal arch. *Arch Phys Med Rehabil.* 1995;76(1):45-49.
26. Menz H, Munteanu S. Validity of 3 clinical techniques for the measurement of static foot posture in older people. *J Orthop Sport Phys Ther.* 2005;35(8):479-486.
27. Fritz G, Prieskorn D. First metatarsocuneiform motion: a radiographic and statistical analysis. *Foot Ankle Int.* 1995;16(3):117-123.
28. Saltzman C, Brandser E, Berbaum K, et al. Reliability of standard foot radiographic measurements. *Foot Ankle Int.* 1994;15(12):661-665.
29. Hunt A, Smith R, Torode M, Keenan A. Inter-segment foot motion and ground reaction forces over stance phase of walking. *Clin Biomech.* 2001;16:592-600.
30. Kidder S, Abuzzahab F, Harris G, Johnson J. A system for the analysis of foot and ankle kinematics during gait. *IEEE Trans Rehabil Eng.* 1996;4(1):25-32.
31. Pohl M, Messenger N, Buckley J. Forefoot, rearfoot and shank coupling: effect of variations in speed and mode of gait. *Gait Posture.* 2006;25:1-8.
32. Rattanaprasert U, Smith R, Sullivan M, Gilleard W. Three-dimensional kinematics of the forefoot, rearfoot, and leg without function of tibialis posterior in comparison with normals during stance phase of walking. *Clin Biomech.* 1999;14:14-23.
33. Hayafune N, Hayafune Y, Jacob H. Pressure and force distribution characteristics under the normal foot during the push-off phase in gait. *The Foot.* 1999;9:88-92.
34. Tabachnick B, Fidell L. *Using Multivariate Statistics.* 5th ed. Boston: Pearson Education; 2007.
35. Engsborg J, Andrews J. Kinematic analysis of the talocalcaneal/talocrural joint during running support. *Med Sci Sports Exerc.* 1987;19(3):275-284.
36. Takane Y, Hwang H. Generalized constrained canonical correlation analysis. *Multivariate Behav Res.* 2002;37:163-195.

37. Torkki M, Malmivaara A, Scitsalo S, Hoikka V, Laippala P, Paavolainen P. Surgery vs orthosis vs watchful waiting for hallux valgus. *J Am Med Assoc.* 2001;285:2474-2480.
38. Allen M, Cuddeford T, Glasoe W, et al. Relationship between static mobility of the first ray and first ray, midfoot, and hindfoot motion during gait. *Foot Ankle Int.* 2004;25(6):391-396.
39. Cornwall M, McPoil T. Motion of the calcaneus, navicular, and first metatarsal during the stance phase of walking. *J Am Podiatr Med Assoc.* 2002;92(2):67-76.
40. Leardini A, Benedetti M, Berti L, Bettinelli D, Nativo R, Giannini S. Rear-foot, mid-foot and fore-foot motion during the stance phase of gait. *Gait Posture.* 2006;25:453-462.
41. Piazza S, Cavanagh P. Measurement of the screw-home motion of the knee is sensitive to errors in axis alignment. *J Biomech.* 2000;33:1029-1034.
42. Small C, Pichora D, Bryant J, Griffiths P. Precision and accuracy of bone landmarks in characterizing hand and wrist positions. *J Biomed Eng.* 1993;15:371-378.

## CHAPTER IV.

### CALCANEUS AND NAVICULAR KINEMATICS

#### **Introductory Summary**

In the previous cadaveric study (Chapter III), orientation of the first ray axis was found variable among specimens, with tilt of the axis inversely related to arch height ( $r = -0.73$ ). Simulations of gait provided a systematic way to measure and analyze kinematics. These methods are now applied *in vivo* (Chapter IV) to measure the change in tarsal kinematics associated with hallux valgus. Imaged-based data were acquired on subjects placed standing in an open-MR scanner. Subjects were grouped with ( $N = 10$ ) and without ( $N = 10$ ) hallux valgus. The angles measured were then compared between groups and across gait conditions.

Hallux valgus affects foot posture and gait kinematics. This study measured the intermetatarsal (IM) 1-2 angle and first metatarsal-to-calcaneus (arch) angle, and computed the calcaneus-fibular and navicular-calcaneus angles (rotations) across gait events. **Methods:** The data of 10 subjects with and without hallux valgus were compared. MR scans were taken with the subject placed weightbearing to simulate gait midstance (MS), heel off (HO), and terminal stance (TS). From the images, selected tarsals were reconstructed with an inertial coordinate frame embedded in each bone. Planar measurements of bone angle alignment were made on the MS bone datasets. The

calcaneus-fibular and navicular-calcaneus inter-tarsal rotations, expressed as Cardan angles, were determined across gait events. Independent *t-tests* assessed the difference in bone angle alignment. A mixed effect ANOVA model compared the inter-tarsal angles between groups and conditions. **Results:** The mean IM angle was statistically larger by 6° in the hallux valgus group; there was no group difference in the arch angle. Subjects grouped with hallux valgus had greater ( $P < 0.05$ ) calcaneal eversion by 6.6° at MS, 7.4° at HO, and 7.9° at TS. Their navicular-calcaneus angle was more inverted by 5.8° at HO ( $P < 0.05$ ). In both groups, the navicular angle became increasingly inverted relative to the calcaneus between successive gait events, with a mean difference of 5.1° ( $P < 0.05$ ) measured from HO to TS in the hallux valgus group. **Conclusion:** This study established a relationship between hallux valgus and eversion of the calcaneus. Clinicians may choose to consider this result when deciding how best to control hindfoot posture and motion in the treatment of hallux valgus deformity. **Key words:** Biomechanics, Hindfoot; Foot deformity; Bone datasets.

## 1. Introduction

Discovery is needed to improve the treatment of hallux valgus, the most common foot deformity in the elderly.<sup>1,2</sup> Hallux valgus is characterized by a lateral deviation (abduction) of the hallux with a corresponding medial deviation (adduction) of the first metatarsal. A 2004 Cochrane systematic review<sup>3</sup> concluded that conservative intervention does not prevent the progression of deformity. Current therapies include the modification of footwear and the use of orthoses,<sup>4-7</sup> exercise to rebalance muscle

strength,<sup>8,9</sup> and splinting to stretch tissue tightness.<sup>10,11</sup> Of these treatments, orthoses have been used successfully for the management of symptoms.<sup>3,12</sup>

To what extent foot kinematics are, or are not changed by hallux valgus is a topic of debate.<sup>1,12-15</sup> Studies published in 2010 by Deschamps et al.<sup>14</sup> and by Canseco et al.<sup>13</sup> used traditional surface marker and modeling techniques to measure kinematics in patients having hallux valgus. Both researchers modeled the foot as 3 rigid segments (hallux, forefoot, hindfoot) and computed distal-to-proximal inter-segment motion to quantify differences in kinematics across the gait cycle. Differences were found in hallux-on-forefoot rotations in the hallux valgus group as compared to controls.<sup>13,14</sup> The finding, however, is without anatomical or clinical construct. The hallux articulates with the first metatarsal - not the forefoot as a whole, and the modeled forefoot is not a rigid segment. The forefoot is comprised of 5 mobile metatarsals that move independent of each other.<sup>16,17</sup> Due to errors with rigid body assumptions, research published since 2007<sup>16,18</sup> has recommended against modeling the forefoot as a rigid segment.<sup>17,19,20</sup>

The foot models used by Deschamps et al.<sup>14</sup> and by Canseco et al.<sup>13</sup> to measure tarsal kinematics had additional limitations. Deschamps' model complicated the measure of hallux-on-forefoot angles by building the hallux coordinate frame from points located external to it.<sup>14</sup> In larger context, the models used in both of the studies<sup>13,14</sup> simplified the anatomy such that mid-to-hindfoot motions could not be tested. Despite the potential for error<sup>16,18</sup> and the limitations associated with measuring kinematics from foot models,



Deschamps and colleagues<sup>14</sup> concluded that changes associated with deformity are “small” and isolated to the hallux, and that “other segments are not affected in a major way”. This definitive statement may be questioned, given the modeling methods used<sup>13, 14</sup> and taking into account the progressive and debilitating nature of hallux valgus deformity.<sup>1, 21</sup>

Deschamps et al.<sup>14</sup> also analyzed tarsal kinematics in reference to a standard neutral standing position, where all inter-segment angles were defined as zero. Lost from the data was the measure of foot alignment, as standing posture was made the same among subjects. The chance of finding group difference was further diluted by measurement error. Foot kinematics measured from skin-mounted markers and modeled as aggregate rigid segments, introduce error that when summed together can approach 10°. This error exceeds the magnitude of most tarsal rotations during gait.<sup>16, 20</sup> The determination of error comes from an experiment that fixed motion sensors to bone-pins screwed into the tarsals in 6 healthy male subjects, and tracked their movement over repeated walking trials.<sup>17, 19, 20, 22</sup> Measures were then compared to data collected with surface markers, modeled as non-anatomic rigid segments.<sup>16</sup>

Foot kinematics have also been measured using computer tomography (CT)<sup>23</sup> and magnetic resonance (MR) imaging.<sup>24, 25</sup> The technique is called Kinematic Imaging (KI). Imaging quantifies bone morphology, and when a series of images are reconstructed to represent a sequence of joint movements, the change in bone position can be measured as

“motion”. The error in measuring tarsal rotations from imaging is less than  $3^\circ$ ;<sup>26-28</sup> about half the error of skin surface measurements of joint motion.<sup>28</sup>

Imaging does introduce other limitations to the measurement of kinematics.

Conventional scans are taken in a sequence of static poses while the subject lays supine, the foot loaded with a small percentage of body weight.<sup>23-25, 27</sup> Lying supine does not replicate gait, which has led some<sup>26-28</sup> to question the validity of the measurement. Wolf et al.<sup>28</sup> investigated the change in tarsal orientation measured from a sequence of images acquired while the subject lay supine, compared to measures taken from fixed bone pins while the subject stood on both feet. The angles computed from supine imaging did not correspond to the angles measured when the subject stood. Mean differences were as high as  $10^\circ$ , twice the error determined for image data processing ( $< 3^\circ$ ) or bone pin measurements ( $2-6^\circ$ ) of tarsal motion.<sup>28</sup> Results indicate posture dependency, and that imaging measures of kinematics should be acquired under vertical loading conditions. Open-MR technology now permits a subject to stand in the scanner. This creates new opportunity for researchers.

Discovery is needed to guide decision making in the treatment of hallux valgus.<sup>6, 7</sup>

Positional control of the calcaneus and navicular are most targeted in orthotic interventions,<sup>4, 6, 7, 29</sup> as both tarsals demonstrate measurable rotation during gait. Bone pin study results<sup>6, 7</sup> report the calcaneus-tibia total (SD) component rotations averaged  $17.0^\circ$  ( $2.1^\circ$ ) in the sagittal plane,  $7.3^\circ$  ( $2.4^\circ$ ) in the transverse plane, and  $11.3^\circ$  ( $3.5^\circ$ ) in the

frontal plane.<sup>19</sup> Navicular-calcaneus total (SD) component rotations averaged 6.1°(3.0°) in the sagittal plane, 11.3°(5.6°) in the transverse plane, and 9.5°(2.7°) in the frontal plane.<sup>16</sup> The relative magnitude of these inter-tarsal angles highlights the importance of the calcaneus and navicular joint motions in the transfer of load between the ground and foot during gait.

Excess eversion of the calcaneus is reported to be a predisposition for hallux valgus deformity.<sup>15, 30, 31</sup> As the calcaneus everts, the arch everts causing weight to be carried on the medial side of the first metatarsophalangeal (1-MTP) joint. Weight then presumably pushes the hallux lateral (into valgus). To quantify changes in the hallux valgus foot, this current study tested subjects having deformity believing they would demonstrate: 1) increased eversion of the calcaneus,<sup>15, 31</sup> 2) an enlarged intermetatarsal (IM) angle,<sup>12</sup> and 3) a lowered arch<sup>32</sup> as compared to controls. Height of the arch was quantified by the first metatarsal-and-calcaneus angle measured from a sagittal view of the foot.<sup>33</sup> The measure is called arch angle.<sup>34</sup>

Interdependency exists in the weightbearing behaviors of the arch and calcaneus. The arch is comprised of wedge shaped bones that lean against each other, held supported proximally by the calcaneus. The navicular is located at the center of the arch, making it the arch “keystone”. When positioned properly, load carried on the navicular acts to stabilize the arch. Should the navicular evert, the arch is destabilized and the calcaneus

may be pulled into excess eversion malaligning the foot.<sup>12, 15, 30, 32</sup> Related to this concept, we published theory<sup>12</sup> detailing how collapse of the arch may precipitate hallux valgus. Now to investigate, we hypothesize the navicular would evert more relative to the calcaneus at heel off in subjects with hallux valgus. At heel off, the foot is maximally pronated allowing the navicular freedom to move.<sup>34</sup>

Navicular rotations are related to the gait timing action of the arch.<sup>17</sup> When describing the inter-tarsal bone pin results<sup>16, 17, 19, 20, 22</sup> we need to consider the direction of the navicular relative to calcaneus angles. The directions can be gleaned from one graph that showed the navicular angle plotted over the gait cycle.<sup>16</sup> The navicular everted 5° during the majority of stance. It then abruptly reversed direction at heel off, inverting 4° during the remainder of stance. Because only healthy subjects were sampled,<sup>16</sup> and because the navicular and calcaneus were defined from coordinate frames built from shared landmarks, we are prevented from learning more.<sup>35</sup> Other studies<sup>36, 37</sup> have used traditional gait analysis methods to track motion of the navicular by mounting a triad of markers to the overlying skin. The navicular everts as the arch gradually lowers into heel off, and inverts as the arch rapidly raises into terminal stance.<sup>36, 37</sup> A secondary aim of our study tested the timing of navicular rotations across gait events. We hypothesized the navicular (relative to the calcaneus) would be more everted at heel off as compared to midstance, and more inverted at terminal stance as compared to heel off. In testing navicular-calcaneus rotations, we provide data by which the construct validity of the data reported in this imaging study may be judged.

To summarize, this study used imaging to measure kinematics in subjects having hallux valgus. The foot was scanned to simulate midstance (MS), heel off (HO), and terminal stance (TS). General Hypothesis 1. investigated the extent that deformity altered alignment of the arch, believing subjects with hallux valgus would demonstrate an enlarged intermetatarsal (IM) and arch angles. General Hypothesis 2. (*i, ii, iii*) tested the effects of group and condition on the relative position of the relationship of the calcaneus to fibula, the navicular to calcaneus, and the navicular to world laboratory (reference) frame angles during gait progression:

- i) The calcaneus would evert more in relation to the fibula at each tested gait event (MS, HO, TS) in subjects having hallux valgus as compared to controls.
- ii) The navicular would evert more with respect to the calcaneus and the MR reference in subjects having hallux valgus at HO as compared to controls.
- iii) For both groups, the navicular would evert more in relation to the calcaneus at HO as compared to MS, and would invert more with respect to the calcaneus at TS as compared to HO.

## **2. Methods**

### **2.1 Subjects**

Twenty-one adult females were recruited from the general University and larger metropolitan area population. Women comprise 90% of the patient cohort of interest, and are the focus of this research.<sup>38</sup> Informed consent was obtained in accordance with

University IRB (#0709M16823) guidelines. One subject became faint while being tested. She did not complete the study. Her data were not included for analysis.

The data of 20 subjects were studied (Table 1). Ten had hallux valgus angulation  $\geq 25^\circ$  (angle measured on the MS dataset).<sup>1</sup> For subjects having bilateral deformity, the foot with the largest hallux angle was scanned. Ten subjects group matched by age had no visible evidence of hallux valgus deformity. A power calculation based on pilot results indicated that a group difference of  $5^\circ$  in tarsal positioning, computed with a between subject SD of  $3.5^\circ$ , had 80% power to reach significance if 10 subjects were sampled per group. A group difference of  $5^\circ$  in calcaneal eversion is considered a clinically meaningful indicator of foot deformity.<sup>39</sup> Five degrees exceeds the error previous research has assigned to image data processing methods.<sup>26-28</sup>

All subjects were independent in their mobility and daily activities. Subjects unable to stand for one hour were excluded. Also excluded were those having a contraindication to MR imaging, and those having a foot deformity (other than hallux valgus) identified during a clinical screening such as a rigid flat foot, collapse of the hindfoot attributed to posterior tibialis tendon dysfunction, varus (adduction  $> 5^\circ$ ) of the hallux, Charcot midfoot deformity, and hammer toes. Excluded were subjects insensate to 5.07 Semmes Weinstein monofilament testing (a precursor of Charcot deformity);<sup>40</sup> as were those having history of rheumatoid arthritis based on the American College of Rheumatology criteria,<sup>41</sup> self-reported episodic gout, history or visible evidence of plantar foot

ulceration, history of toe or forefoot surgery or joint stiffness that limited dorsiflexion of the 1-MTP joint to  $50^{\circ}$  or less, or ankle dorsiflexion to  $10^{\circ}$  or less.

Subjects were grouped with or without deformity by the measure of hallux angle (Table 1). The angle defined the alignment of the proximal phalanx of the hallux and the first metatarsal. The angle is measured in clinical practice from lines drawn on a weightbearing radiograph.<sup>1</sup> The angle is positive when the hallux turns lateral (valgus) and negative when it turns medial (Table 1). The angle was measured by a single examiner (WG) using a computer tool from a transverse plane screen-shot of the MS bone datasets (Fig 2.A). The examiner also measured the intermetatarsal (IM),<sup>1, 42</sup> as well as the arch angle.<sup>43</sup> The IM angle (Fig 2.B) was formed by the intersection of lines that bisected the first and second metatarsal shafts. Arch angle (Fig 2.C) was defined by lines connecting the first metatarsal and the inferior calcaneus. Reliability of the measurements was assessed during a preliminary evaluation of the methods.<sup>44</sup> A second examiner, blinded from the first examiner's results, measured the same bone angles (Fig. 2) on 15 of the 20 subjects. Inter-rater reliability was excellent in all cases ( $ICC \geq 0.97$ ;  $SEM \leq 2^{\circ}$ ).

## **2.2 Image and reconstruction procedures**

Kinematic angles were calculated from a sequence of MR images.<sup>27</sup> The scanner used was a FONAR (Melville, NY, USA) Multi-Position Upright 0.6 Tesla magnet. Images were obtained in the sagittal plane, using a T1-weighted 3D gradient-recall-echo

sequence with fat suppression (flip angle = 60°, NEX = 1) scanning protocol. The scan field, composed of 128 sagittal slices centered on the midfoot, captured the foot/ankle in a 256 x 256 matrix. Image resolution was 1.0 mm x 1.0 mm, giving a precise 3D location of each voxel in the scanner field. Six minutes were required to complete each scan.

The subject stood in the scanner leaning against an upright back support (Fig. 1.A). The foot, placed in a receiver coil, was scanned to simulate gait midstance (MS), heel off (HO), and terminal stance (TS). Gait conditions (Fig. 1.B) were standardized by the ankle angle.<sup>45</sup> Joint positioning was determined *a priori* from the literature.<sup>46,47</sup> The ankle was dorsiflexed 5° at MS, dorsiflexed 10° at HO, and plantar flexed 10° at TS. To accomplish this, the subject stood level on the scanner platform at MS, on one 15° wedge at HO, and on two 15° wedges at TS. The wedges were made of hard rubber that did not compress when loaded. When standing at TS, an additional wedge angled at 10° was placed beneath the subject's toes. Wedging the toes tightened the plantar fascia<sup>45</sup> as should happen into terminal stance.<sup>34</sup> In each gait pose, the subject stood while partially kneeling into a padded bolster (Fig. 1.A), their weight distributed equally on both feet. This was necessary to prevent movement artifact on the MR scans.

Scanned images were exported in DICOM (Digital Imaging and Communications in Medicine) file format to Materialise's Interactive Medical Image Control System 14.1 (MIMICS, Materialise, Leuven, Belgium) computer software for processing.<sup>26,27</sup> The software combined the 128 image slices into a stack. A threshold color applied to the



uploaded image gave contrast to a bone. The bone's perimeter was then traced by an operator using a computerized hand-tool. The segmented area within the perimeter became a filled volume, referred to as a mask.<sup>25, 48, 49</sup> The volume represented the imaged bone with its location known in the MR scanner reference frame, hence forth called the MR reference.<sup>25-27, 48, 49</sup>

A total of six bone objects were reconstructed. These were the proximal phalanx of the hallux, first and second metatarsals, the navicular, calcaneus, and the distal end of the fibula. The bones once reconstructed displayed as a "bone dataset" in accordance to how the foot was positioned for each scan. Mattingly et al.<sup>27</sup> used a similar scanning protocol to reconstruct the navicular in a known 3D space, demonstrating accuracy to  $0.26^\circ$  for rotation.

Each bone mask was embedded with a principal axis coordinate frame. A computer algorithm calculated the least and greatest moments of inertia for the volume. From this calculation, the computer embedded an inertial coordinate frame at the volume's centroid.<sup>25, 48, 49</sup> The frame's primary axis aligned coincident to the bone's least moment of inertia. The secondary axis of the orthogonal coordinate frame aligned coincident to the greatest moment of inertia, and the tertiary axis was made from a cross-product of the primary and secondary axes that defined the bone.

Because bone reconstructions (Fig. 1.B) were segmented by an examiner using a hand-tool, the same bone rendered slightly differently between gait events. This introduced a potential for error, because any change in a bone's shape could reorient its coordinate frame. Subsequently, when calculating the angles, altered orientation of the frame would then misrepresent as a change in the orientation of that bone. To eliminate this potential for error, registration was performed to link together each subject's datasets (MS, HO, TS) in the MR world.<sup>26</sup> Registration is a multi-step computer procedure. The MS bone 3D object was exported in stereolithograph (.stl) file format. The files were next imported into the MIMIMCS projects at HO, and at TS.<sup>26</sup> The bone.stl displayed as it was originally positioned at MS. Registration then translated and rotated the bone.stl superimposing it upon the bone object reconstructed to represent that same bone. In the end, registration output a 4 X 4 transformation matrix which recorded the change in the orientation of the bone.stl files between gait events.

### **2.3 Kinematic measurement procedures**

Each bone with its coordinate frame was then displayed for viewing. Two observations were made. First, the coordinate frames embedded into the datasets were consistent and repeatable. This made it possible to calculate the bone rotations for all subjects from one custom written computer code. Second, in each bone except for the navicular, the embedded frame aligned close to the anatomical body planes. Whereas the navicular coordinate frame aligned out-of-plane. So that angles measured relative to the navicular could be described with clinical language, the navicular frame was mathematically

corrected to zero in the MR reference at midstance (MS). The correction factor was then applied to the subject's navicular segmented at HO and TS such that any change in its orientation from MS could be identified but as a consequence, subject differences in navicular position were "zeroed-out" at MS

To aid in data interpretation, Mimics coordinate frame axes were adapted to  $X$ ,  $Y$ ,  $Z$  (conformed to the right hand rule). The positive  $X$ -axis of the newly adapted frame pointed approximately forward, the positive  $Y$ -axis upward, and the positive  $Z$ -axis lateral.<sup>45, 50</sup> Inter-tarsal angles were computed using a  $Z$ ,  $Y'$ ,  $X''$  sequence of Cardan ordered rotations following ISB (International Society of Biomechanics) recommendations.<sup>51</sup> In the final analysis, left sided data was converted to right sided equivalency, and the angles calculated were reported in the body planes as directed rotations about the specified coordinate axes<sup>45, 50</sup>

Sagittal plane dorsiflexion (+) and plantar flexion (-) about the  $Z$ -axis.

Transverse plane adduction (+) and abduction (-) about the  $Y$ -axis.

Frontal plane inversion (+) and eversion (-) about the  $X$ -axis.

Inter-tarsal angles were computed as rotation of the distal bone coordinate frame relative to the proximal bone coordinate frame. The transformation matrices used to calculate the angular change in position of the bones across gait events were computed in Matlab Software Version 7.6 (Mathworks Inc., Natick, USA) from a custom-written code. To determine the collective image data processing error, a series of angles were measured for

a single subject (Appendix B.2). The difference in the angles measured for 3 trials across the succession of gait events was  $\leq 3^\circ$ ,<sup>52</sup> considered the estimate of error for the inter-tarsal angles measured in this study.<sup>52</sup>

## **2.4 Data analysis**

Analyses were performed using NCSS (Kaysville, Utah) Edition 2007. Data were screened for non-normality by examining for skewness and kurtosis of each variable using the cutoffs of -2 to 2 for skewness, and -4 to 4 for kurtosis. All variables fell within the cutoffs.

Independent *t*-tests were performed to assess for group differences in demographics, and to assess for group differences in the measurement of bone angle alignment (Table 1).

Group mean comparisons for the 3 segments (Table 2) were analyzed about the Z, Y, X axes in each body plane. The 9 angles were compared using a 2 x 3 mixed-model with the between subject factor of group (hallux valgus vs. control) and the within subject factor of condition (MS, HO, TS) to assess for difference in the computed angles.

Significance was set at an alpha level of  $P < 0.05$  for each analysis. If group-by-condition interaction effects were detected, Tukey follow-up analyses were performed.

When not finding interaction, pairwise comparisons of the angles were tested when significant condition effects were identified, or when the experimental hypothesis put

forth called for pairwise comparison testing. All pairwise comparisons were planned *a priori*.

### 3. Results

Table 1 reports subject demographics, and the measurements of bone angle alignment. There was no difference between groups in age, height, or body mass index. For the bone angles, both the hallux and IM angles were larger ( $P < 0.01$ ) in subjects having deformity. Group differences were  $28^\circ$  for the hallux angle, and  $6^\circ$  for the IM angle. There was no group difference ( $P = 0.46$ ) in the arch angles, with nearly the same mean, SD, and range observed (Table 1).

The ANOVA models assessed the calcaneus-fibula, navicular-calcaneus, and navicular-world angles in the body planes (sagittal, transverse, frontal) for group and condition main effects, and for group-by-condition interactions. Figure 3 plots group angle (mean with 95% confidence interval) against condition. Several significant ( $P < 0.05$ ) main effects were found (Table 2), whereas group-by-condition interactions were not statistically significant ( $F \leq 1.77$ ;  $P \geq 0.18$ ). The group and condition main effects, and the associated significant pairwise comparisons are presented in the following paragraphs.

Hypothesis 2.i called for making pairwise group comparisons in the frontal plane calcaneus-fibula angles at each gait event. The calcaneus was more everted ( $P < 0.05$ ) in

hallux valgus subjects. Group differences averaged 6.6° at MS, 7.4° at HO, and 7.9° at TS. Groups responded the same across conditions (no interaction).

Hypothesis 2.ii called for the comparison of the frontal plane navicular-calcaneus group angles, and navicular-world group angles. The navicular-calcaneus omnibus group effect approached significance ( $F = 1.57$ ;  $df = 1, 18$ ;  $P = 0.22$ ) with the hallux valgus group tending to demonstrate increased inversion across gait events (Fig. 3). The specific hypothesis called for making a pairwise group comparison at HO, believing the navicular would evert more in subjects with hallux valgus. A group difference ( $P < 0.05$ ) of 5.8° was identified at HO. However, those with hallux valgus had increased inversion, not eversion as was hypothesized. There was no group difference in the frontal plane navicular-world angle at HO (Table 2).

Hypothesis 2.iii tested for a condition effect in the frontal plane navicular-calcaneus angle. A condition effect ( $F = 20.00$ ;  $df = 2, 36$ ;  $P < 0.001$ ) was present indicating the navicular increasingly inverted across gait events (Fig. 3). Pairwise comparisons identified the navicular was more inverted ( $P < 0.05$ ) at TS as compared to MS in both groups. Inversion was significantly greater ( $P < 0.05$ ) at TS as compared to HO in subjects with deformity (Table 2). Inversion averaged 5.1° between TS and HO in the hallux valgus group and 4.3° (a non-significant amount) in controls. Inversion was  $< 2^\circ$  between HO and MS (Fig. 3), a nonsignificant amount (Table 2).

Sagittal plane positioning of the foot was controlled by the testing procedure. There was no group effect ( $F = 1.10$ ;  $df = 1, 18$ ;  $P = 0.31$ ) in the sagittal plane calcaneus-fibula angle. A group effect ( $F = 5.10$ ;  $df = 1, 18$ ;  $P = 0.037$ ) was found in the sagittal plane navicular-world angle. The difference was largest at HO, averaging  $1.7^\circ$ .

## 4. Discussion

### 4.1 Bone angle alignment

Hallux valgus is a progressive and disabling forefoot deformity.<sup>53</sup> Contrary to what the name would imply, deformity is not isolated to the hallux.<sup>1, 12, 15, 42</sup> Adduction of the first ray enlarges both the hallux and the intermetatarsal (IM) angles.<sup>42</sup> This was demonstrated (Table 1). Hallux angulation averaged  $36^\circ$  in subjects having deformity as compared to  $8^\circ$  in controls. A hallux angle measuring  $36^\circ$  indicates a moderate deformity, based on the clinical grading system where normal is  $15^\circ$  or less, mild is 15 to  $25^\circ$ , moderate is 25 to  $40^\circ$ , and severe is  $40^\circ$  or greater.<sup>1</sup> The IM angle averaged  $17^\circ$  in the hallux valgus group, as compared to  $11^\circ$  in controls. Normal in adults ranges between  $8^\circ$  and  $14^\circ$ .<sup>54, 55</sup> The comparisons show there was a difference in foot structure between groups, that alignment in the hallux valgus group would be considered a moderate to severe deformity, and that controls represented a population without foot deformity.

There was no group difference in arch angle. The angles measured (Table 1) ranged from 126° to 143°. Adult normal is  $132 \pm 2^\circ$ ,<sup>43, 56, 57</sup> with extremes of 104° and 166° reported for the cavus and planus foot, respectively.<sup>56</sup> Hallux valgus has been found associated with pes planus.<sup>32, 58, 59</sup> Thus we hypothesized the arch angle would be larger, indicating a lower arch in the hallux valgus group. In finding no group difference, we acknowledge that researchers<sup>25, 60</sup> have questioned whether any single measure of arch structure is sufficient to represent the complex architecture of the human foot. Therefore, surgeons use a series of radiographic accessory arch angle measurements to identify changes associated with hallux valgus.<sup>1</sup> The secondary types of angles could be quantified on the bone datasets but when reviewing the literature, we found no studies where such angles were measured to guide clinical decisions in the care for hallux valgus.

Our study was undertaken to measure the change in kinematics associated with hallux valgus. We hypothesized that arch height would be lower in the hallux valgus foot, knowing there is evidence to both support<sup>32, 58, 59</sup> and challenge<sup>1, 61</sup> the notion of pes planus being a causative factor of deformity progression. When attempting to understand our results, we reviewed Inman's paper that described the linkage between hallux valgus and "flat footedness". In the paper, he wrote that eversion of the heel and not necessary flatness of the arch to precipitate deformity. Our results support Inman's theory directly.

## **4.2 Angle – gait event comparisons**



We simulated gait to compare the kinematics of subjects having hallux valgus to controls. The calcaneus-fibula and the navicular-calcaneus angles computed across gait events were of primary interest. Each bone was defined by its own coordinate frame. Except for the navicular, this analysis preserved the anatomical relationship between the bones even while the foot was moved to simulate gait.

The coordinate frames defining the calcaneus and fibula aligned closely to the body planes. The bones shared no other known anatomical relevance. Thus we interpret the calcaneus-fibula angles in relative terms. The frontal plane angle averaged  $-27.8^\circ$  at MS in the hallux valgus group (Table 2; Fig. 3). The angle measured  $-21.2^\circ$  in controls. The negative values indicate eversion. So in relative terms, the calcaneus everted  $6.6^\circ$  more ( $P < 0.05$ ) in subjects with hallux valgus as compared to controls.

The anatomically based position angles (Table 2; Fig. 3) are more challenging to interpret. For example, the  $-21.2^\circ$  calcaneus-fibular position angle measured in controls tells the angle between the bone coordinate frames, not the ground. The distinction is made because gait studies often report data in reference to neutral stance.<sup>14, 16</sup> This gives meaning to the angles in relation to the ground, however, standing posture is made the same for all subjects. Consequently, group differences in foot posture cannot be tested. We prefer reporting position angles because the measure identifies subject variability in foot structure (type).

Unlike the fibula or calcaneus, the navicular coordinate frame was corrected to zero in the MR reference. The correction is seen in the data (Table 2; Figure 3). Regardless of group or body plane, all navicular-world angles record as zero at MS. The inertial coordinate frame originally embedded in the navicular aligned oblique to the body planes. Had we not corrected the navicular to the MR reference, any angle described relative to it would have been difficult to interpret. In a second manuscript we report first ray-navicular kinematics.<sup>62</sup> Besides the advantage gained in describing first ray-navicular kinematics, correcting the navicular to zero provided a more extensive understanding of hindfoot alignment.

The navicular-calcaneus frontal plane angle (Table 2; Fig. 3) measured 28.4° in subjects having hallux valgus at MS, and 21.4° in controls. A positive angle indicates the navicular inverted on the calcaneus. Thinking on this relationship in reverse and knowing the navicular coordinate frame aligned horizontal at MS, the calcaneus (coordinate frame) everted on the navicular. Thus eversion of the calcaneus on the navicular measured 28.4° in hallux valgus subjects and 21.4° in controls. These angles are nearly equivalent to the frontal plane calcaneal-fibular group angles computed at MS. The calcaneus everted 27.8° in the hallux valgus group, and 21.2° in controls (Table 2; Fig. 3). The nearly equivalent inter-tarsal anatomical relationship indicates the fibula aligned close to vertical in the MR reference. This was anticipated, as the shaft of the fibula aligned vertically when the subject stood for scanning.

The dataset of a single subject is shown in Figure 4. The rectangle surrounding the bone dataset represents the MR scanner field of view. It is shown here to give perspective for how the foot was placed in the scanner. The calcaneus is displayed with its coordinate frame embedded. Note the medial directed axis is angled down from horizontal (Fig. 4). The navicular-calcaneus angle for this subject measured  $13.2^\circ$ . A positive value indicates the navicular was inverted. It would also be correct and perhaps more representative of the anatomy to say the calcaneus (coordinate frame) everted  $13.2^\circ$  on the navicular. This reverse relationship is discussed to underscore that the position angle records the alignment of the coordinate frames, and not the bones themselves. And since the calcaneus coordinate frame (Fig. 4) did not align exact to the body planes, the position angle defining hindfoot alignment is difficult to assign with clinical meaning.

The navicular-world angle yielded orientation of the navicular in relation to the MR laboratory frame of reference. The angle was qualified by how the foot was placed for scanning. The platform upon which the subject stood was level, their foot was placed pointing forward. The image taken then partitioned the foot approximately into the cardinal body planes (Table 2; Fig. 3). Because the angle cannot discriminate rotation of the navicular from the foot itself, the sagittal plane rotations measured largest. This reflects how the foot was moved to simulate gait. The subject stood level at MS, on one  $15^\circ$  wedge at HO, and on two  $15^\circ$  wedges at TS (Fig. 1A). The wedge increments are seen as plantar flexion in the angle data (Table 2). A group effect ( $F = 5.1$ ;  $P = 0.037$ ) was found in the sagittal plane. The largest group difference was  $1.7^\circ$  at HO. Although

statistically significant, this magnitude of difference was not judged as being clinically meaningful.<sup>39</sup>

The transverse plane navicular-world angles changed by  $< 5^\circ$  from MS to TS. This rotation was small and influenced by the placement of the foot. Future studies intending to quantify this angle from static gait poses are advised to use procedures that assure the foot is placed in the same location in the MR reference between scanned events.

The frontal plane navicular-world angles changed a total of  $15^\circ$  across gait events (Fig. 3). The angles became increasingly inverted, with 75% of the rotation measured from HO to TS. The measure was consistent within group (95% CI =  $0.6$  to  $1.9^\circ$ ) and between groups ( $F = 0.58$ ;  $P = 0.45$ ). Such consistency gives evidence that the foot was placed in the same location between scanned events, except for the wedges added. Also, the consistency of measures indicates the foot was held stable on the wedge(s) for scanning. Therefore we attribute the condition effect ( $F = 91.82$ ;  $P < .001$ ) identified in the frontal plane navicular-world angle mostly to how the navicular oriented in the foot, and less to how the foot was (re)positioned between scanned gait events.

### **4.3 Calcaneus-to-fibula angles**

The reconstructed calcaneus and fibula gave representation of foot-to-leg alignment (Fig. 1.B). As hypothesized, the hallux valgus group demonstrated statistically ( $P < 0.05$ ) greater calcaneus-fibula eversion at each gait event (Table 2). Significant differences

ranged from 6.6° to 7.9° when compared to the control group across gait events. Assuming the fibula aligned vertical, the calcaneus everted these amounts relative to the ground. No group-by-condition interaction was found ( $F \leq 1.03$ ;  $P \geq 0.37$ ) meaning group differences were not dependent on gait event. These results can be directly applied to clinical practice. For clinicians using orthoses to manage hallux valgus, a custom appliance which corrects eversion of the calcaneus in standing (MS) may benefit across the gait cycle. Our reasoning does not suggest that orthoses could realign the calcaneus in a “non-fixed” foot deformity by as much as 7°, but that correction of the hindfoot in standing may benefit into terminal stance when load transfer between the foot and ground is highest.<sup>63</sup> Additionally, the finding of no group-by-condition interaction suggests hallux valgus affects foot posture more than joint motion. Thus we surmise, as Inman<sup>15</sup> did 40 years ago, orthoses used to shape the hindfoot may help combat deformity.<sup>12</sup>

Tanaka et al.<sup>31</sup> also found the calcaneus everted in the hallux valgus foot. They measured the frontal plane alignment of the calcaneus in reference to the tibia on radiographs taken on 58 consecutive patients seeking treatment for symptomatic deformity. The calcaneus everted 7° more ( $P < 0.001$ ) in patients having deformity as compared to controls. This amount of increased eversion was identical to the group difference we found in the calcaneus-fibula angle (Table 2). The corroborating results provide evidence that eversion of the calcaneus may be part of the larger sequelae of hallux valgus deformity.

The calcaneus was abducted relative to the fibula in both groups (Fig 3). The angle although not statistically different (Table 2), averaged  $-21.7^{\circ}$  in hallux valgus subjects and  $-17.0^{\circ}$  in controls with negative indicating abduction. Data reported in a previous imaging study gives meaning to this position angle result. Ledoux et al.<sup>25</sup> used imaging to develop a paradigm to classify foot type. Subjects were selected *a priori* as having a planus, neutral, or a cavus foot. The foot was then imaged with the subject positioned supine (assumed to replicate stance). The bones were reconstructed and inertial coordinate frames were embedded into the calcaneus and the fibula. They found the calcaneus-fibula angle abducted  $30.3^{\circ} (\pm 4.5)$  in the planus foot, abducted  $25.8^{\circ} (\pm 4.4)$  in the neutral foot, and abducted  $6.1^{\circ} (\pm 5.4)$  in the cavus foot. We found the calcaneus abducted  $21.7^{\circ}$  in the hallux valgus group and  $17.0^{\circ}$  in controls (Fig. 3). These group angles are midrange to what Ledoux reported.<sup>25</sup> Thus our subjects (N = 20), judged to have a normal arch height based on the measure of arch angle (Table 1) also displayed a calcaneus-fibula position angle of abduction consistent with a neutral (normal) foot-type.<sup>25</sup>

The ankle joint angle, measured with a goniometer while the subject stood in the scanner, was controlled as an independent test variable. Accordingly, the sagittal plane calcaneus-fibula angle did not differ between groups ( $F = 1.10$ ;  $P = 0.31$ ). The ankle angle, however, did not always equate to the calcaneus-fibula angle. A notable difference occurred between the MS and HO gait events. The ankle was dorsiflexed from MS ( $5^{\circ}$ ) to HO ( $10^{\circ}$ ) according to our testing protocol. By contrast, calcaneus-fibular group

angles plantar flexed ( $\sim 7^\circ$ ) between MS and HO (Fig. 3). The opposing directions of joint rotation did not overly surprise. The goniometric measures of ankle angle gave an estimate of the foot-to-leg alignment, which is different from the anatomical alignment of the calcaneus-fibula angle. Additionally, the calcaneus moves independent of the midfoot during gait loading.<sup>16, 18, 34</sup>

#### **4.4 Navicular-to-calcaneus angles**

Navicular-calcaneus angle data was recorded in the 3 body planes (Table 2; Fig. 3). We focused attention on analyzing the frontal plane rotations (hypothesis 2.ii). The measure of the navicular made in relation to the calcaneus captures a combination of subtalar and talonavicular joint motions. The joints act as the mechanical linkage between leg rotation and foot pronation/supination. Pronation is a triplanar motion, of which eversion is a component motion.

Eversion of the hallux and first ray is a chief characteristic of hallux valgus deformity.<sup>58, 64, 65</sup> Talbot et al<sup>65</sup> found the hallux everts by an average of  $12^\circ$  more ( $P < 0.01$ ) in patients having hallux valgus as compared to controls. Therefore it seemed reasonable to hypothesize that increased eversion would be measured in the navicular-calcaneus angle. Group difference ( $P < 0.05$ ) was identified at HO. The navicular demonstrated increased inversion of  $5.8^\circ$  more in the hallux valgus group, not eversion as hypothesized. We speculate the navicular inverted relative to the calcaneus to counteract the excess eversion

of the calcaneus (relative to leg and ground) to keep the metatarsals resting in level contact with the ground.<sup>66</sup> In separate study, we report first ray-navicular angles to more fully investigate the source of eversion of distal arch as commonly found in the severely deformed hallux valgus foot.<sup>58, 64, 65</sup>

Aside from testing for group differences, the frontal plane angle of the navicular measured relative to the calcaneus (hypothesis 2.iii) provided a marker by which the kinematics measured in this study could be compared to current and future published gait data.<sup>16, 17, 19, 20, 22, 34, 36, 39, 67</sup> A condition effect ( $F = 20.0$ ;  $P < 0.001$ ) was found in the frontal plane navicular-calcaneus angles with no significant interaction effects ( $P > 0.05$ ). The navicular-calcaneus angles were tested assuming that regardless of group, the navicular would evert more at HO as compared to MS, and invert more at TS as compared to HO. In subjects with hallux valgus the navicular inverted  $1.2^\circ$  from MS to HO, and inverted  $5.1^\circ$  from HO to TS. In controls the navicular inverted  $2^\circ$  from MS to HO, and  $4.7^\circ$  from HO to TS. The MS to HO change in the angle was not significant ( $P > 0.05$ ), in either group. Thus we cannot accept the hypothesis that the navicular would evert from MS to HO because frontal plane orientation did not change, statistically. The navicular did invert  $5.1^\circ$  from HO to TS ( $P < 0.05$ ) in the hallux valgus group, and  $4.7^\circ$  from HO to TS in controls, an amount that was not statistically significant.



The navicular-calcaneus angles we computed (Table 2; Fig. 3) are comparable to data previously reported. Rotation averaged  $6.3^{\circ}$  in hallux valgus subjects and  $6.7^{\circ}$  in controls. The magnitude of rotations are one third smaller than the  $9^{\circ}$  measured by Lundgren and Nester in the bone pin study<sup>20</sup> which reported navicular rotation across stance. Eversion of  $5^{\circ}$  occurred from heel strike to heel off, followed by a sharp reversal into inversion ( $4^{\circ}$ ) from heel off through push off.<sup>20</sup> The change in the direction of rotation at heel off is believed related to supination of the foot and the progressive tightening of the plantar fascia.<sup>34</sup> Navicular inversion did not change from MS to HO (Table 2; Fig. 3). Past studies<sup>19, 20, 36, 67</sup> have only reported navicular motions descriptively, so there remains no statistical evidence that supports the magnitude of navicular rotations between specified gait events. Timed with supination “twist” of the foot which starts at HO,<sup>66</sup> the navicular inverted about  $5^{\circ}$  in both groups (Table 2; Fig. 3). This magnitude and direction of navicular rotations were also reported in bone pin results.<sup>19, 20</sup> The measures navicular-calcaneus rotations generally agree with published gait data.<sup>16, 17, 19, 20, 22, 34, 36, 39, 67</sup>

#### **4.5 Limitations of the study**

The foot was imaged under static loading conditions. Standing does not replicate the transfer of kinetics between the foot and ground as occur in gait. Therefore limb accelerations and gait-timed muscle contractions may cause kinematics to differ from what we report. Despite this reality, the magnitude and direction of the inter-tarsal

rotations measured were comparable to kinematics collected in gait trials. Additionally, the superior accuracy of imaging allowed us to identify changes in hindfoot kinematics not detected in previous studies that used standard gait analysis to measure tarsal motion in subjects having hallux valgus.

The small sample of hallux valgus subjects ( $N = 10$ ) and controls ( $N = 10$ ), as well as scanning only 3 gait events reduces the generalizability of the results. The sample was kept small because of the costs associated with MR scanning, and because the computer processes involved in reconstructing the bone datasets are labor intensive. Although the sample was small, the study was sufficiently powered to detect group differences.

Another potential limitation was that subjects tested had a moderately sized hallux valgus foot deformity. They represent the population most apt to seek conservative care treatment. Results may not necessarily apply to the severe late-stage type of deformity. Subjects were not current patients. However, it seems reasonable to conclude that the kinematics measured would be the same in patients unless they were experiencing gait impairment due to pain of the 1-MTP joint.

## **5. Summary**

This study measured the change in tarsal kinematics associated with hallux valgus. From the imaged data, several measures were found statistically different between groups. The difference in the hallux and intermetatarsal (IM) angles was significant ( $P < 0.01$ ), but

not the arch angle. Subjects with hallux valgus had significantly greater ( $P < 0.05$ ) calcaneus-fibula eversion by an average of  $7^\circ$  across gait events. Group difference ( $P < 0.05$ ) in navicular-calcaneus angle was identified at HO. The navicular inverted (not everted as hypothesized) by  $5.8^\circ$  more in the hallux valgus group. In a secondary aim, we tested navicular to calcaneus rotations across gait events. The navicular angle became increasingly inverted across the gait progression. Clinicians may choose to consider these results in the treatment of hallux valgus.

**Table 4.1.** Group mean  $\pm$  SD (range) demographic and foot structure angle.

|                          | <b>Hallux Valgus (N=10)</b> | <b>Controls (N=10)</b>   | <b><i>P</i> Value</b> |
|--------------------------|-----------------------------|--------------------------|-----------------------|
| <b>Demographics</b>      |                             |                          |                       |
| Age (years)              | 43 $\pm$ 18 (22 to 73)      | 44 $\pm$ 19 (23 to 71)   | .82                   |
| Height (cm)              | 166 $\pm$ 6 (157 to 175)    | 167 $\pm$ 7 (157 to 180) | .61                   |
| BMI (kg/m <sup>2</sup> ) | 24 $\pm$ 3 (20 to 30)       | 26 $\pm$ 4 (19 to 32)    | .20                   |
| <b>*Bone Angles</b>      |                             |                          |                       |
| Hallux (°)               | 36 $\pm$ 7 (25 to 47)       | 8 $\pm$ 5 (-3 to 15)     | < 0.01                |
| Intermetatarsal (°)      | 17 $\pm$ 3 (14 to 20)       | 11 $\pm$ 1 (9 to 13)     | < 0.01                |
| Arch (°)                 | 135 $\pm$ 6 (126 to 143)    | 133 $\pm$ 6 (127 to 143) | .46                   |

\* Measured on the midstance (MS) bone datasets.

**Table 4.2.** Group angles recorded across gait events. Comparisons shown in the body planes. Dorsiflexion; adduction; inversion are the positive directions of measurement. Abbreviations: HV, hallux valgus; Cal, calcaneus; Fib, fibula; Nav, navicular; Wd, world. Abbreviation for gait events: MS, midstance; HO, heel off; TS, terminal stance.

|                   | <b>Sagittal</b><br>(°)        |                                 |              | <b>Transverse</b><br>(°)     |                              |              | <b>Frontal</b><br>(°)           |                                 |                              |
|-------------------|-------------------------------|---------------------------------|--------------|------------------------------|------------------------------|--------------|---------------------------------|---------------------------------|------------------------------|
|                   | <b>MS</b>                     | <b>HO</b>                       | <b>TS</b>    | <b>MS</b>                    | <b>HO</b>                    | <b>TS</b>    | <b>MS</b>                       | <b>HO</b>                       | <b>TS</b>                    |
| <b>Cal-to-Fib</b> |                               |                                 |              |                              |                              |              |                                 |                                 |                              |
| HV                | <sup>a,b</sup><br><b>16.2</b> | <sup>c</sup><br><b>6.8</b>      | <b>-13.1</b> | <sup>b</sup><br><b>-21.7</b> | <sup>b</sup><br><b>-20.8</b> | <b>-13.4</b> | <sup>*, b</sup><br><b>-27.8</b> | <sup>†, b</sup><br><b>-24.6</b> | <sup>§</sup><br><b>-15.2</b> |
| Controls          | <sup>a,b</sup><br><b>18.2</b> | <sup>c</sup><br><b>10.8</b>     | <b>-12.8</b> | <sup>b</sup><br><b>-17.0</b> | <sup>b</sup><br><b>-13.9</b> | <b>-9.0</b>  | <sup>b</sup><br><b>-21.2</b>    | <sup>b</sup><br><b>-17.2</b>    | <b>-7.3</b>                  |
| <b>Nav-to-Cal</b> |                               |                                 |              |                              |                              |              |                                 |                                 |                              |
| HV                | <b>-6.9</b>                   | <b>-7.9</b>                     | <b>-7.5</b>  | <sup>b</sup><br><b>11.4</b>  | <sup>b</sup><br><b>11.0</b>  | <b>17.6</b>  | <sup>b</sup><br><b>28.4</b>     | <sup>b</sup><br><b>29.6</b>     | <b>34.7</b>                  |
| Controls          | <b>-7.6</b>                   | <b>-8.5</b>                     | <b>-8.2</b>  | <sup>b</sup><br><b>11.3</b>  | <sup>b</sup><br><b>11.4</b>  | <b>15.8</b>  | <sup>b</sup><br><b>21.4</b>     | <b>23.8</b>                     | <b>28.1</b>                  |
| <b>Nav-to-Wd</b>  |                               |                                 |              |                              |                              |              |                                 |                                 |                              |
| HV                | <sup>a,b</sup><br><b>0.0</b>  | <sup>†, c</sup><br><b>-16.1</b> | <b>-31.6</b> | <b>0.0</b>                   | <b>-0.6</b>                  | <b>2.3</b>   | <sup>b</sup><br><b>0.0</b>      | <sup>b</sup><br><b>1.3</b>      | <b>13.9</b>                  |
| Controls          | <sup>a,b</sup><br><b>0.0</b>  | <sup>c</sup><br><b>-14.4</b>    | <b>-28.9</b> | <b>0.0</b>                   | <b>-0.1</b>                  | <b>3.7</b>   | <sup>b</sup><br><b>0.0</b>      | <sup>b</sup><br><b>2.5</b>      | <b>15.4</b>                  |

Statistical comparisons significant at  $P < 0.05$  for angles indicated with superscript symbols and letters. Group effect symbols: (\*) different at MS; (†) different at HO; (§) different at TS. Condition effect letters: (a) different from HO; (b) different from TS; (c) different from MS and TS.

### **Figure Legend (IV.)**

**Fig 4.1.** **A.** Weightbearing MR test conditions. The subject stood partially kneeling into a padded bolster fixed securely in the scanner. The ankle joint angle, measured with a goniometer, as well as standing on a standard sized wedge served as the reference for replicating the gait events. **B.** Sagittal view of a subject's reconstructed bone datasets at the midstance (MS), heel off (HO), and terminal stance (TS) gait events.

**Fig 4.2.** Bone angle alignment was measured on the midstance (MS) bone datasets.

**A.** Hallux Angle: Lines bisect the hallux and first metatarsal.

**B.** Intermetatarsal (IM) Angle: Lines bisect the first and second metatarsals.

**C.** Arch Angle: Lines connect the first metatarsal and calcaneus.

**Fig 4.3.** Group angles measured in the anatomical body planes. Rotations are plotted against gait midstance (MS), heel off (HO), and terminal stance (TS). Error bars are the 95% confidence interval of the mean data. Note: scale changes between graphs.

**Fig 4.4.** Hindfoot frontal view of a subject's bone dataset. The foot was imaged at midstance. The calcaneus is shown with its coordinate frame embedded. The medio-lateral axis of the frame was angled down from horizontal ( $13.2^\circ$  in this subject) indicating the calcaneus coordinate frame everted relative to horizontal, and relative to the navicular.

Figure 4.1.

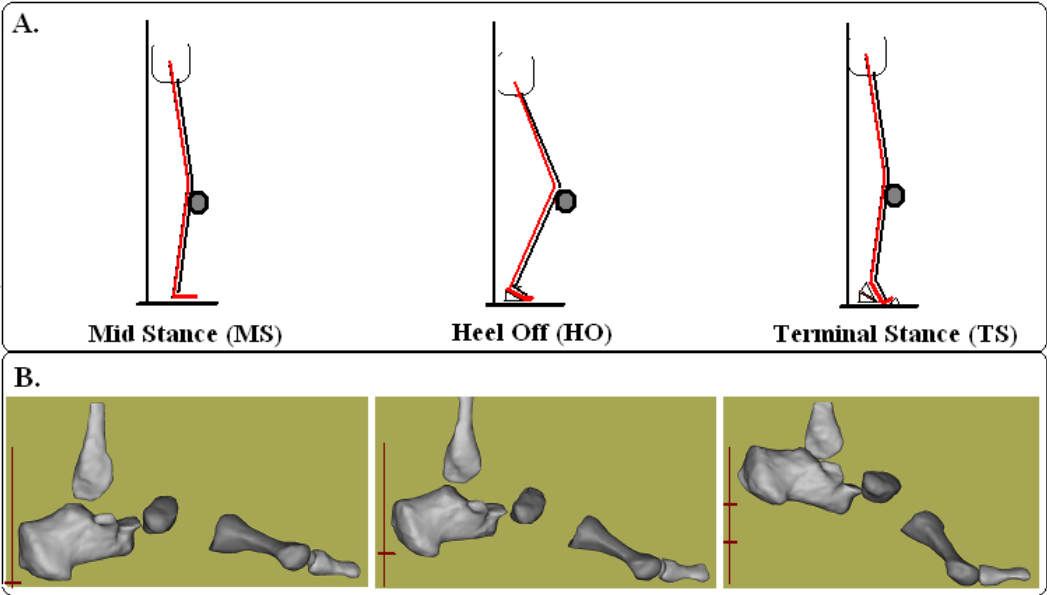
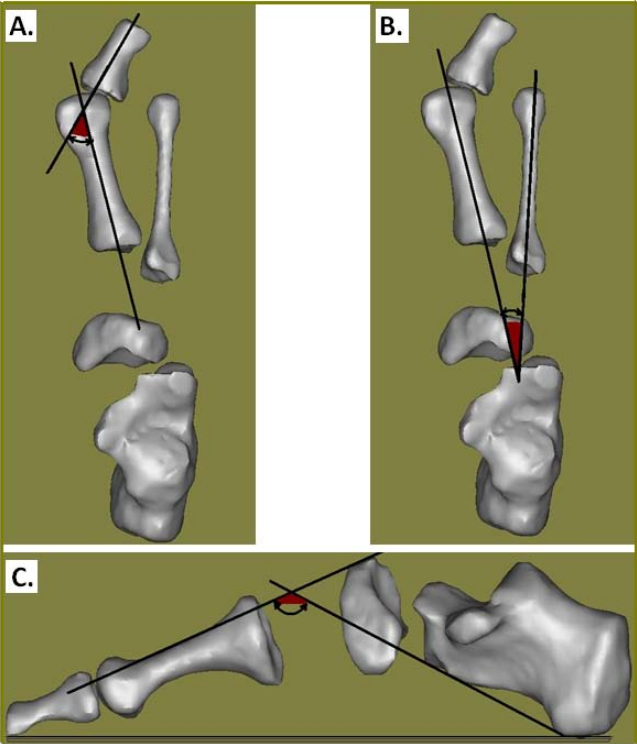
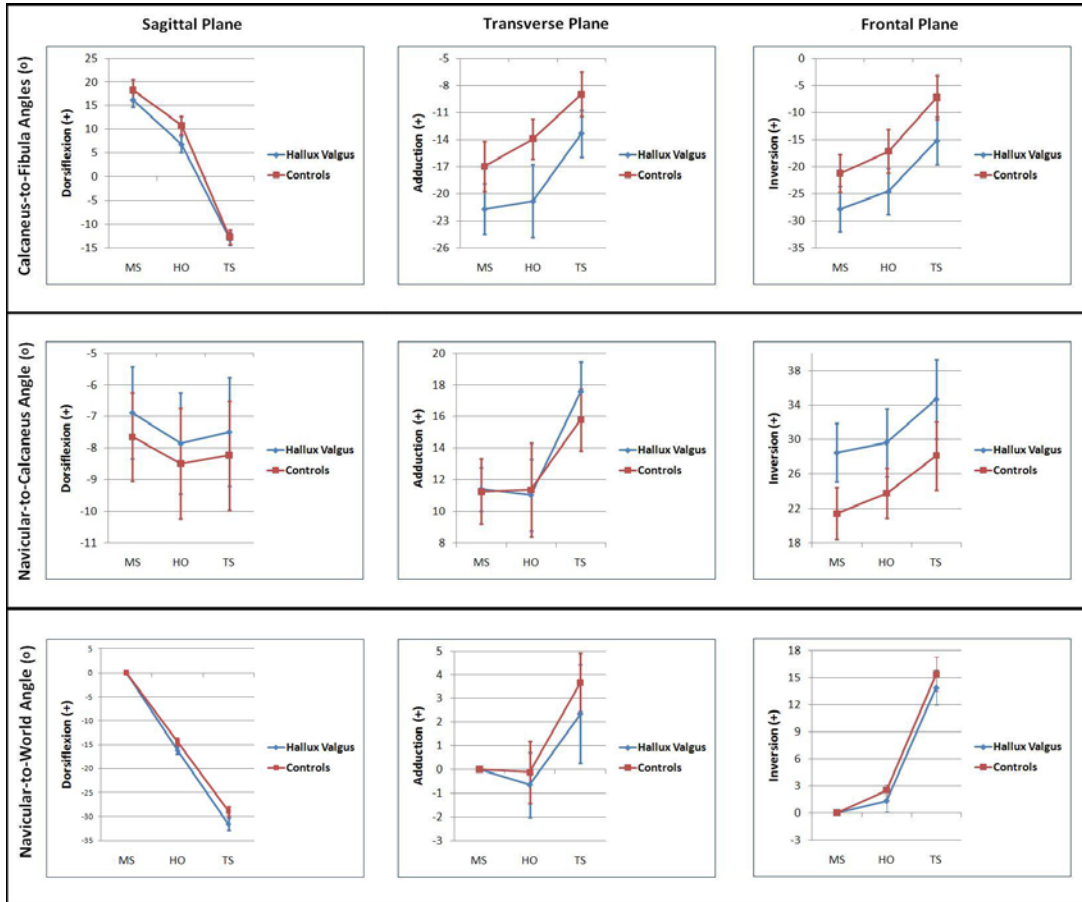


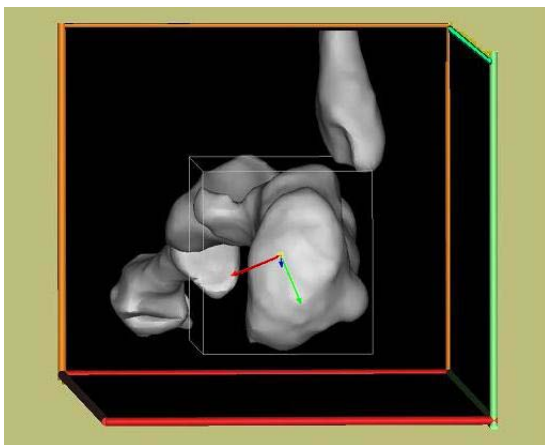
Figure 4.2.



**Figure 4.3.**



**Figure 4.4.**





## References (Chapter IV.)

1. Coughlin M, Jones C. Hallux valgus: demographics, etiology, and radiographic assessment. *Foot Ankle Int.* 2007;28:759-777.
2. Menz H, Morris M. Determinants of disabling foot pain in retirement village residents. *J Am Podiatr Med Assoc.* 2005;95:573-579.
3. Ferrari J, Higgins J, Prior T. Interventions for treating hallux valgus (abductovalgus) and bunions. *Cochrane Database of Systematic Reviews.* 2004;Issue 1. Art. No.:CD000964.DOI:10.1002/14651858.CD000964.pub2.
4. Budiman-Mak E, Conrad K, Roach K, et al. Can foot orthoses prevent hallux valgus deformity in rheumatoid arthritis? A randomized clinical trial. *J Clin Rheumatoid.* 1995;1:313-321.
5. Kilmartin T, Barrington R, Wallace W. A controlled prospective trial of a foot orthosis for juvenile hallux valgus. *J Bone Joint Surg.* 1994;76-B:210-214.
6. Torkki M, Malmivaara A, Scitsalo S, Hoikka V, Laippala P, Paavolainen P. Surgery vs orthosis vs watchful waiting for hallux valgus. *J Am Med Assoc.* 2001(285):2474-2480.
7. Torkki M, Malmivaara A, Seitsalo S, Hoikka V, Laippala P, Paavolainen P. Hallux valgus: immediate operation versus 1 year of waiting with and without orthoses. *Acta Orthop Scand.* 2003;74(2):209-215.
8. Groiso J. Juvenile hallux valgus. A conservative approach to treatment. *J Bone Joint Surg.* 1992;74-A:1367-1374.
9. Schuh R, Hofstaetter S, Adams S, Pichler F, Kristen K, Trnka H. Rehabilitation after hallux valgus surgery: importance of physical therapy to restore weight bearing of the first ray during the stance phase. *Phys Ther.* 2009;89:Epub ahead of print.
10. Caselli M, George D. Foot deformities: biomechanical and pathomechanical changes associated with aging, part 1. *Clin Podiatr Med Surg.* 2003;20:487-509.
11. Hart E, deAsla R, Grottkau B. Current concepts in the treatment of hallux valgus. *Orthopaedic Nursing.* 2008;27(5):274-280.
12. Glasoe W, Nuckley D, Ludewig P. Hallux valgus and the first metatarsal arch segment: a theoretical biomechanical perspective. *Phys Ther.* 2010;90:110-120.
13. Canseco K, Rankine L, Long L, Smedberg T, Marks R, Harris G. Motion of the multisegmental foot in hallux valgus. *Foot Ankle Int.* 2010;31:146-152.
14. Deschamps K, Birch I, Desloovere K, Matricali G. The impact of hallux valgus on foot kinematics: A cross-sectional. *Gait Posture.* 2010;32:102-106.
15. Inman V. Hallux valgus: a review of etiologic factors. *Orthop Clin N Amer.* 1974;5(1):59-66.
16. Nester C, Jones R, Liu A, et al. Foot kinematics during walking measured using bone and surface mounted markers. *J Biomech.* 2007;40:3412-3423.

17. Wolf P, Stacoff A, Liu A, et al. Functional units of the human foot. *Gait Posture*. 2008;28:434-431.
18. Nester C, Liu A, Ward E, et al. In vitro study of foot kinematics using a dynamic walking cadaver model. *J Biomech*. 2007;40:1927-1937.
19. Lundgren P, Nester C, Liu A, et al. Invasive in vivo measurement of rear-, mid- and forefoot motion during walking. *Gait Posture*. 2008;28:93-100.
20. Nester C, Liu A, Ward E, Howard D, Cocheba J, Derrick T. Error in the description of foot kinematics due to violation of rigid body assumptions. *J Biomech*. 2010;43:666-672.
21. Easley M, Trnka H. Current concepts review: hallux valgus Part 1: pathomechanics, clinical assessment, and nonoperative management. *Foot Ankle Int*. 2007;28(5):654-659.
22. Arndt A, Westblad P, Winson I, Hashimoto T, Lundberg A. Ankle and subtalar kinematics measured with intracortical pins during the stance phase of walking. *Foot Ankle Int*. 2004;25(5):357-363.
23. Beimers L, Tuijthof G, Blankevoort L, Jonges R, Maas M, Van Dijk C. In-vivo range of motion of the subtalar joint using computed tomography. *J Biomech*. 2008;41(7):1390-1397.
24. Hirsch B, Udupa J, Samarasekera S. New method of studying joint kinematics from three-dimensional reconstructions of MRI data. *J Am Podiatr Med Assoc*. 1996;86(1):4-15.
25. Ledoux W, Rohr E, Ching R, Sangeorzan B. Effect of foot shape on the three-dimensional position of the foot bones. *J Orthop Res*. 2006;24:2176-2186.
26. Cargill S, Pearcy M, Barry M. Three-dimensional lumbar spine postures measured by magnetic resonance imaging reconstruction. *Spine*. 2007;32:1242-1248.
27. Mattingly B, Talwalker V, Tylkowski C, Stevens D, Hardy P, Pienkowski D. Three-dimensional in vivo motion of adult hind foot bones. *J Biomech*. 2006;39:726-733.
28. Wolf P, Stacoff A, Liu A, et al. Does a specific MR imaging protocol with a supine-lying subject replicate tarsal kinematics seen during upright standing? *Biomed Tech*. 2007;52:290-294.
29. Hawke F, Burns J, Radford J, Toit V. Custom-made foot orthoses for the treatment of foot pain. *Cochrane Database of Systematic Reviews* 2008;July(1):1-91.
30. Schoenhaus H, Cohen R. Etiology of the bunion. *J Foot Ankle Surg*. 1992;31(1):25-29.
31. Tanaka Y, Takakura Y, Tadashi F, Sugimoto K. Hindfoot alignment of hallux valgus evaluated by a weightbearing subtalar x-ray view. *Foot Ankle Int*. 1999;20(10):640-645.
32. Scranton P, McDermott J. Prognostic factors in bunion surgery. *Foot Ankle Int*. 1995;16(11):698-704.
33. Saltzman CL, Nawoczenski DA. Complexities of foot architecture as a base of support. *J Orthop Sports Phys Ther*. 1995;21(6):354-360.
34. Wilken J, Rao S, Saltzman C, Yack H. The effect of arch height on kinematic coupling during walking. *Clin Biomech*. 2011;26(3):318-323.

35. Brown K, Bursey D, Arneson L, Andrews C, Ludewig P, Glasoe W. Consideration of digitization precision when building local coordinate axes for a foot model. *J Biomech.* 2009;42:1263-1239.
36. Allen M, Cuddeford T, Glasoe W, et al. Relationship between static mobility of the first ray and first ray, midfoot, and hindfoot motion during gait. *Foot Ankle Int.* 2004;25(6):391-396.
37. Cornwall M, McPoil T. Motion of the calcaneus, navicular, and first metatarsal during the stance phase of walking. *J Am Podiatr Med Assoc.* 2002;92(2):67-76.
38. Coughlin M, Shurnas P. Hallux Rigidus: demographics, etiology, and radiographic assessment. *Foot Ankle Int.* 2003;24(10):731-743.
39. Neville C, Flemister A, Houck J. Deep posterior compartment strength and foot kinematics in subjects with stage II posterior tibial tendon dysfunction. *Foot Ankle Int.* 2010;31(4):320-327.
40. Mueller M, Minor S, Diamond J, Blair V. Relationship of foot deformity to ulcer location in patients with diabetes mellitus. *Phys Ther.* 1990;70(6):356-362.
41. Arnett F, Edworthy S, Bloch D, McShane D, Frieo J, et al. The American Rheumatism Association 1987 revised criteria for the classification of rheumatoid arthritis. *Arthritis Rheum.* 1988;31(3):315-324.
42. Glasoe W, Allen M, Saltzman C. First ray dorsal mobility in relation to hallux valgus deformity and first intermetatarsal angle. *Foot Ankle Int.* 2001;22(2):98-101.
43. Saltzman C, Nawoczenski D, Talbot K. Measurement of the medial longitudinal arch. *Arch Phys Med Rehabil.* 1995;76(1):45-49.
44. Glasoe W, Phadke V, Nuckley D, Pena F, Ludewig P. First metatarsal helical axis and angle measurements in subjects having bunion as compared to controls *J Foot Ankle Res Suppl.* 2011 (in press).
45. Glasoe W, Pena F, Phadke V, Ludewig P. Arch height and first metatarsal joint axis orientation as related variables in foot structure and function: theory related to bunion. *Foot Ankle Int.* 2008;29(6):647-655.
46. Hunt A, Smith R, Torode M, Keenan A. Inter-segment foot motion and ground reaction forces over stance phase of walking. *Clin Biomech.* 2001;16:592-600.
47. Rattanaprasert U, Smith R, Sullivan M, Gilleard W. Three-dimensional kinematics of the forefoot, rearfoot, and leg without function of tibialis posterior in comparison with normals during stance phase of walking. *Clin Biomech.* 1999;14:14-23.
48. Camacho D, Ledoux W, Rohr E, Sangeorzan B, Ching R. A three-dimensional, anatomically detailed foot model: a foundation for a finite element simulation and means of quantifying foot-bone position. *J Rehab Res Develop.* 2002;39(3):401-410.
49. Stindel E, Udupa J, Hirsch B, Odhner D, Couture C. MR image analysis of the morphology of the rear foot: application to classification of bones. *Comput Med Imaging Graph.* 1999;23:75-83.

50. Wolff K, Wicks A, Shaw A, Smith J, Ludewig P, Glasoe W. Clinical measurement correlates of the first metatarsal axis leading to intervention strategies for hallux valgus. *Foot Ankle Int.* 2010;In Review.
51. Wu G, Siegler S, Allard P, et al. ISB recommendation on definitions of joint coordinate system of various joints for the reporting of human joint motion--part I: Ankle, hip, and spine. *J Biomech.* 2002;35:543-548.
52. Glasoe W. Kinematic Study of Hallux Valgus Foot Deformity. *Ph.D Dissertation, Univ of Minnesota, USA.* 2011.
53. Menz H, Roddy E, Thomas E, Croft P. Impact of hallux valgus severity on general and foot-specific health-related quality of life. *Arthritis Care & Res.* 2011;63(3):396-404.
54. Bryant A, Tinley P, Singer K. A comparison of radiographic measurements in normal, hallux valgus, and hallux limitus feet. *J Foot Ankle Surg.* 2000;39:39-43.
55. Scott G, Wilson D, Bently G. Roentgenographic assessment in hallux valgus. *Clin Orthop.* 1991;267:143-147.
56. Menz H, Munteanu S. Validity of 3 clinical techniques for the measurement of static foot posture in older people. *J Orthop Sport Phys Ther.* 2005;35(8):479-486.
57. Wearing S, Smeathers J, Sullivan P, Yates B, Urry S, Dubois P. Plantar fasciitis: are pain and fascial thickness associated with arch shape and loading. *Phys Ther.* 2007;87:1002-1008.
58. Eustace S, Byrne J, Beausang O, Codd M, Stack J, Stephens M. Hallux valgus, first metatarsal pronation and collapse of the medial longitudinal arch - a radiological correlation. *Skeletal Radiol.* 1994;23:191-194.
59. Scranton P, Rutkowski R. Anatomic variations in the first ray: Part I. Anatomic aspects related to bunion surgery. *Clin Orthop Rel Res.* 1980;151:244-255.
60. Stindel E, Udupa J, Hirsch B, Odhner D. A characterization of the geometric architecture of the peritalar joint complex via MRI: an aid to classification of foot type. *IEEE Trans. Med. Imag.* 1999;18(9):753-762.
61. Coughlin M, Shurnas P. Hallux valgus in men part II: first ray mobility after bunionectomy and factors associated with hallux valgus deformity. *Foot Ankle Int.* 2003;24(1):73-78.
62. Glasoe W, et al. First ray kinematics in hallux valgus: a weightbearing imaging study. *TBD.* 2011:Ready for Journal Submission.
63. Hayafune N, Hayafune Y, Jacob H. Pressure and force distribution characteristics under the normal foot during the push-off phase in gait. *The Foot.* 1999;9:88-92.
64. Saltzman CL, Brandser EA, Anderson BS, Berbaum KS, Brown TD. Coronal plane rotation of the first metatarsal. *Foot Ankle.* 1996;17(3):157-161.

65. Talbot K, Saltzman C. Hallucal rotation: a method of measurement and relationship to bunion deformity. *Foot Ankle Int.* 1997;18(9):550-556.
66. Sarrafian SK. Functional characteristics of the foot and plantar aponeurosis under tibiotalar loading. *Foot Ankle.* 1987;8(1):4-18.
67. Cornwall M, McPoil T. Three-dimensional movement of the foot during the stance phase of walking. *J Am Podiatr Med Assoc.* 1999;89(2):56-66.

## CHAPTER V.

### FIRST RAY KINEMATICS IN SUBJECTS WITH HALLUX VALGUS

#### **Introductory Summary**

The hindfoot study (Chapter IV) found the calcaneus everted  $7^{\circ}$  more in subjects having hallux valgus as compared to controls. Arch angle did not differ between groups. The work continues (Chapter V) by computing first ray kinematics on the same imaged bone datasets. Theory advanced for testing was that collapse of the arch tilts the first ray axis more vertical in subjects with hallux valgus, consistent with the first ray arch segment adducting into deformity. Similar to the methods used to analyze the data collected on cadavers (Chapter III), the change in the angular position of the first ray was computed in relation to the navicular both as Cardan angles and as helical axis parameters. Data was then compared between groups and across gait event conditions. Additionally, multiple regression analysis evaluated the relationship between arch angle and first ray kinematics. For completeness, this study also reported hallux-first metatarsal (1-MTP) joint angles, descriptively, across gait events.

Malalignment of the first ray is a determinant of hallux valgus. **Methods:** This imaging study scanned the foot of 10 subjects each with and without hallux valgus. Subjects stood to simulate gait midstance (MS), heel off (HO), and terminal stance (TS) in an open

MR scanner. Data were processed to reconstruct the first metatarsal (ray), navicular, and other selected tarsals. Each bone was embedded with its own coordinate frame. First ray angles and finite helical axis (FHA) parameters were computed relative to the navicular frame. **Analysis:** First ray angles and helical axis orientation parameters decomposed into the  $Y$ ,  $Z$ ,  $X$  components were analyzed between groups and across conditions using a 2-way mixed model analysis of variance (ANOVA). Multiple regression analysis assessed the relationship of arch angle and change in navicular-to-world eversion angle measured during middle (MS to HO) and late (HO to TS) stance to vertical orientation of the first ray axis. **Results:** Adduction of the first ray was greater ( $F = 44.17$ ,  $P < 0.001$ ) in the hallux valgus group. Group-by-condition interaction for the vertical  $Y$  component of helical axis was statistically significant ( $F = 5.06$ ,  $P = 0.037$ ). In the hallux valgus group, the  $Y$  component ( $Y_c$ ) was larger before (0.40) as compared to after (-0.05) the HO gait event. The regression models found no significance ( $P \geq 0.68$ ) among variables investigated. **Conclusion:** Adduction of the first ray was increased ( $\geq 9.3^\circ$ ) in subjects having deformity, with orientation of the axis inclined  $23^\circ$  ( $Y_c = 0.40$ ) during middle stance as compared to  $6^\circ$  ( $Y_c = 0.10$ ) in controls. Results support previous theory and compliment existing research. **Key words:** Bunion, First Metatarsal, Helical Axis, Arch.

## 1. Introduction

Debate surrounds the etiology of hallux valgus foot deformity<sup>1-4</sup> and its recurrence following surgery.<sup>5,6</sup> Referred to as a bunion, the condition is characterized by abduction

of the hallux with corresponding adduction of the first ray.<sup>1,7</sup> This research investigates the first ray.<sup>7</sup>

The first ray is formed by the first metatarsal and the medial cuneiform.<sup>8,9</sup> The first metatarsal also articulates with the second metatarsal providing added structural support. The connecting plantar ligaments are thick and dense, with the first metatarsocuneiform joint surfaces uniquely configured to stiffen the arch and carry load.<sup>10-12</sup> Past imaging results<sup>10</sup> and studies of cadavera<sup>11,12</sup> have been confirmed *in vivo*.<sup>13,14</sup> Bone-pin measurement of tarsal motion show the first metatarsal and cuneiform move as a single segment during gait.<sup>13,14</sup>

Hallux valgus foot deformity adducts, elevates, and everts the first ray.<sup>15,16</sup> This alters the kinetic and kinematic behaviors of the medial longitudinal arch.<sup>15-18</sup> Plantar pressures are most studied.<sup>19-22</sup> Patients having deformity demonstrate reduced loading of the first ray, timed with the lateral displacement of forefoot pressures. Kinematic studies<sup>23,24</sup> using standard video analysis and surface marker methods modeled the foot as 3 segments (hallux, forefoot, hindfoot), and described motion of the distal segment relative to the proximal segment.<sup>23,24</sup> Canseco et al.<sup>23</sup> identified greater ( $P \leq 0.002$ ) dorsiflexion ( $5^\circ$ ) and eversion ( $10^\circ$ ) fore-on-hindfoot joint motions in patients with hallux valgus as compared to controls. Deschamps et al.<sup>24</sup> reported similar data, identifying group difference ( $P < 0.05$ ) in hallux-on-forefoot joint angles. Subjects with deformity had a  $5^\circ$  decrease in hallux dorsiflexion from gait midstance to heel off. Because the hallux rests



on the ground during middle stance, the group difference detected in hallux dorsiflexion was due to the arch flattening more in patients with deformity. Both studies<sup>23, 24</sup> showed the stability of the arch to be compromised.

Collapse of the arch may precipitate deformity.<sup>3, 7, 25</sup> Inman's teachings on the topic are well accepted.<sup>3</sup> By attaching a pendulum to the hallux, he demonstrated how standing in a pronated foot position everted the arch relative to the ground. This shifts the ground reaction forces to the medial side of the first metatarsophalangeal (1-MTP) joint increasing the net valgus moment acting on the hallux. The just described ground reaction moments have been modeled to explain the progression of deformity.<sup>4, 26</sup>

Foot kinematics may also be tracked with imaging methods.<sup>27-29</sup> Called Kinematic Imaging,<sup>30</sup> the technique quantifies 3D bone morphology. When a series of images are linked (registered) together across a sequence of time-instances, the change in bone position can be measured as "motion". Error associated with the image measurement of tarsal motion is  $< 3^\circ$ ,<sup>27-29</sup> about half the error assigned to surface sensors and foot modeling procedures.<sup>13, 31</sup> Besides allowing for the measurement of bone angles, helical axis parameters can be derived from imaged datasets to provide a complete definition of 3D joint kinematics.<sup>32</sup>

In a previous study,<sup>30</sup> we measured hindfoot kinematics from scanned images of subjects placed in standing to simulate gait (Fig. 1.A). The bones were reconstructed and

registered, and inter-tarsal angles were computed across gait events. Hallux valgus subjects had greater ( $P < 0.05$ ) eversion of the calcaneus by  $6.6^\circ$  at midstance,  $7.4^\circ$  at heel off, and  $7.9^\circ$  at terminal stance. The result is similar to what Tanaka and colleagues published.<sup>33</sup> Research<sup>30, 33</sup> supports Inman's most basic observation.<sup>3</sup> The calcaneus everts in the hallux valgus foot.

Our hindfoot study<sup>30</sup> also measured the navicular-calcaneus angles across gait events. Eversion was tested believing the "pronated twist" of the hallux valgus deformity<sup>15-17</sup> might be traced to the navicular. This was not found. Eversion of the navicular was not statistically different ( $F = 1.57$ ;  $P = 0.27$ ) in subjects with deformity. The calcaneus, not the navicular, was everted.<sup>30</sup> Using the same bone datasets, the first ray-navicular kinematics are now analyzed in this study.

The first ray rotates independent of the midfoot tarsals about a single oblique axis. Hicks<sup>9</sup> and others<sup>25, 34, 35</sup> demonstrated the axis runs from the navicular across the midfoot horizontal. The navicular is the centermost bone of the arch. Its orientation is dependent on foot type and arch height.<sup>7</sup> Glasoe and colleagues<sup>34</sup> simulated gait loading in 9 cadaver specimens. Using a finite helical axis (FHA) approach to measure first ray-navicular joint rotation, they demonstrated orientation of the axis to be a function of arch height. Axis orientation was variable among specimens, tilt was inversely related to arch height ( $r = -0.73$ ), and when the axis inclined towards vertical, the first ray adducted

under conditions of vertical load. These measures made on subjects with hallux valgus may lead to improved understanding of deformity progression.

The purpose of this study was to investigate the change in first ray kinematics associated with hallux valgus. Subjects with and without deformity were imaged in an open-upright magnetic resonance (MR) scanner. Each stood to simulate gait midstance (MS), heel off (HO), and terminal stance (TS).<sup>30</sup> MS to HO events represented gait middle stance; HO to TS represented gait late stance.<sup>34</sup> Data were processed to address the following hypotheses: 1) The first ray would adduct more in relation to the navicular in subjects having hallux valgus and accordingly, the first ray axis would orient more vertical in middle, and in late stance; 2) Subjects having hallux valgus would demonstrate greater eversion of the first ray-navicular angle at HO as compared to controls; 3) Arch angle considered in combination with the change in navicular-to-world (MR world reference) eversion angle measured in middle and late stance as variables in a regression model would relate at level  $R^2 \geq 0.30$  to vertical orientation of the first ray axis evaluated during the same gait timing. Arch angle was quantified by the first metatarsal-to-calcaneus angle of alignment measured from a sagittal planar view of the imaged foot.<sup>30</sup> A relationship found may distinguish arch angle as a factor of deformity.<sup>34</sup>

## **2. Methods**

### **2.1 Subjects**

The data of 20 female subjects were studied. Ten subjects had hallux valgus, ten served as controls. A power calculation made from pilot results indicated that a group difference of 0.15 in the orientation of the first ray helical axis direction cosine vector, computed with a between subject SD of 0.09, had 80% power to reach significance if 9 subjects were sampled per group. Subject demographics (N = 20): age =  $44.3 \pm 17.9$  years; height =  $166.9 \pm 6.4$  cm; weight =  $68.4 \pm 9.3$  kg; BMI =  $24.7 \pm 3.9$  kg/m<sup>2</sup>. There was no group difference in the demographics ( $P \geq 0.20$ ).<sup>30</sup>

The hallux angle (Table 1) averaged 36° on subjects with deformity (N = 10) and 8° in controls (N = 10).<sup>30</sup> The complete description of the selection and screening procedures were detailed previously.<sup>30</sup> In brief, the participants were physically able to stand for one hour, and all had  $\geq 10^\circ$  ankle joint dorsiflexion and  $\geq 50^\circ$  1- MTP joint dorsiflexion. Subjects having contraindications to MR imaging, previous foot surgery, or observed deformity other than hallux valgus were excluded. Informed consent was obtained in accordance with University of Minnesota IRB guidelines.

## **2.2 Scanning and image reconstruction procedures**

The kinematics were computed from MR images. The scanner was a FONAR (Melville, NY, USA) Upright 0.6 Tesla magnet. Images were acquired in the sagittal plane, using a T1-weighted 3D gradient-recall-echo sequence with fat suppression (flip angle = 60°, NEX = 1) scanning protocol. The scan captured the entire foot (Fig. 1.B) in a 256 x 256 matrix. The scanner field-of-view could be rotated from level to follow the foot into late

stance. Imaging was carried out in 1mm slice thickness; each scan took 6 minutes to complete.

The subject stood with their weight distributed equally on both feet while partially kneeling into a padded bolster fixed securely in the scanner (Fig. 1.A). The foot was posed to simulate gait midstance (MS), heel off (HO), and terminal stance (TS).<sup>30</sup> Conditions were standardized by the position of the ankle angle.<sup>36, 37</sup> The ankle was dorsiflexed 5° at MS, dorsiflexed 10° at HO, and plantar flexed 10° at TS. Midstance (MS) was achieved by positioning the leg while the foot rested level on the scanner platform (Fig. 1.A). To simulate HO and TS, the subject stood on one or two hard rubber wedges. Each wedge was angled at 15°, and sized to support the hindfoot (Fig. 1.B). An additional wedge angled at 10° was placed beneath the toes at TS. The wedge dorsiflexed the toes, tightening the plantar fascia as should happen in gait.<sup>30</sup>

Images were exported as a DICOM (Digital Imaging and Communication in Medicine) file in 128 slices that allowed for sagittal, transverse, and frontal plane viewing.

Processing of the image data was done using MIMICS (Materialise, Leuven, Belgium) software.

Segmentation and subsequent 3D objects were created after custom smoothing techniques. Six separate bone “masks” were segmented: the proximal phalanx of the hallux, the first and second metatarsals, the navicular, calcaneus, and the distal end of the

fibula. Once reconstructed, the bone dataset (Fig. 2) gave spatial representation of the foot in the MR laboratory frame of reference, hence forth called the “MR reference”. Mattingly et al.<sup>28</sup> used a similar method. They reported a 0.26° mean difference in the orientation of a navicular model as compared to the bone measured in situ.<sup>28</sup>

Registration was performed to link together the datasets of each subject in the MR reference.<sup>27</sup> This avoided variability associated with reconstruction of the same bone in multiple scans. First, the MS bone object was exported in stereolithograph (.stl) file format. The bone.stl file was next imported into the MIMICS projects at HO, and at TS. Computer registration then translated and rotated the MS bone object to the HO/TS masks of that same bone. The registration output a 4 X 4 transformation matrix which recorded the change in the orientation of the bone.stl file between gait events. Computer registration has been shown reliable and valid to within 1°.<sup>27</sup>

Each “bone” 3D object was embedded with an inertial axis coordinate frame.<sup>38,39</sup> A computer algorithm calculated the centroid of the bone volume, and its smallest and largest moments of inertial rotations.<sup>38,39</sup> The bone and coordinate frame was then displayed for viewing. The frames embedded between subjects and across bone datasets with consistency. The coordinate frame axes (fixed to each bone) were relabeled X, Y, Z following International Society of Biomechanics (ISB) recommendations.<sup>40</sup> The frame embedded in the first metatarsal, for example, was labeled so the axis of least moment of inertia (aligned with the shaft) became X positive pointing approximately forward, the

axis of greatest moment of inertia became *Y* positive pointing superior, and *Z* positive pointing lateral was calculated as a common perpendicular to *X* and *Y* axis using Matlab Software Version 7.6 (Mathworks Inc., Natick, USA).

The hallux and first metatarsal coordinate frames aligned close to the anatomical body planes. Whereas the frame fixed in the navicular aligned out-of-plane. So that angles measured in relation to the navicular could be described with clinical notation, the navicular coordinate frame was mathematically aligned to the MR reference at midstance (MS). The correction factor was applied to the navicular reconstructed at HO and TS, before calculating its change in orientation from MS.

A tag-tracking adjustment<sup>41</sup> was performed to compute the FHA in a constant MR reference. Tags are saturation markings in the MR image. Tracking the tag-line provided a method to keep the MR reference constant when the scanner field-of-view was rotated.<sup>41</sup> The adjustment made is shown in Figure 3. The field-of-view rotated forward to capture the foot and ankle at TS, was corrected to the MS tag line position prior to solving for the helical axis. See Figure 3. This subject's foot, scanned in TS (Fig. 1.B.), has been rotated back to horizontal in the MR reference.

Bone alignments (Fig. 2) gave measurement of the overall shape of the foot and arch (Table 1). Additionally, selected inter-tarsal angles extracted from transformation matrices were computed on each subject (Table 2). The first ray-navicular joint angles

were of primary interest. The hallux-first ray (1-MTP joint) angles are reported as mean data but not evaluated further.

Subjects were grouped with and without deformity according to the size of the hallux angle. The angle defines the transverse plane alignment of the proximal phalanx of the hallux and the first metatarsal (Fig. 2.A). The angle is positive when the hallux turns lateral (valgus) and is negative when the hallux turns medial.<sup>1</sup> A single examiner (WG) measured the angle from a transverse plane view of the MS bone datasets. The examiner also measured the intermetatarsal (IM) and arch angles.<sup>42</sup> The IM angle (Fig 2.B) was formed by lines bisecting the metatarsals. The arch angle (Fig 2.C), formed by lines connecting the first metatarsal and the calcaneus quantified sagittal plane arch height.<sup>43</sup> Measurement reliability was excellent ( $ICC \geq 0.97$ ;  $SEM \leq 2^\circ$ ).<sup>37</sup>

Error does occur with image data processing.<sup>27, 28</sup> Segmentation may distort the anatomy, extraction of coordinate frame locations may be imprecise, and the optimization surface fitting techniques used for registration are not exact. The collective magnitude of the errors was assessed by computing the difference in the tarsal rotations for 3 trials on one subject across the succession of gait events (Appendix B.3). The difference was  $\leq 3^\circ$ .<sup>44</sup>

### **2.3 Kinematic measurement procedures**

The coordinate frame  $X$ ,  $Y$ ,  $Z$  axes described the mutually perpendicular planes. Sagittal dorsi/plantar flexion was in the  $X$ - $Y$  plane, transverse ad/abduction was in the  $Z$ - $X$  plane,



and frontal in/eversion was in the  $Y$ - $Z$  plane. The positive directions were adduction, dorsiflexion, and inversion.

Data were processed as Cardan angles. The ISB recommended angular descriptors for calculating ankle rotations but not for the foot joints.<sup>40</sup> The  $Z$ -axis rotation is computed first because the sagittal plane angles are largest. In recognition that subjects with hallux valgus have positional add/abduction ( $Y$ -axis) deformity of the 1-MTP joint, we calculated the hallux and first ray-navicular rotations using a  $Y, Z', X''$  sequence. In final analysis, left-sided data was converted to right-sided equivalency.

Orientation of the first ray axis was estimated using a finite helical axis (FHA) approach.<sup>34, 45-48</sup> The calculation output a vector (axis) having unit length that defines the path about which two segments rotate, interpolated between two sequential postures.<sup>46-48</sup> The axis expressed the change in angular position of the first ray relative to the navicular, calculated between MS and HO, and again between HO and TS.<sup>34</sup> Research has located the axis in the navicular.<sup>25, 35</sup> The basis for gait event interpolation was because the arch lowers in early stance until heel off.<sup>49</sup>

The FHA calculation output direction cosine parameters computed in the MR reference.<sup>47, 48</sup> Only the orientation components (3 cosines of the angles between the helical axis and the MR laboratory reference frame) and total rotation ( $\Phi$ ) were analyzed (Table 3).<sup>34, 45</sup> The  $Y$  component ( $Y_c$ ) was the primary dependent variable. It

defined vertical orientation of the axis. Total rotation was reported descriptively but not analyzed further.

Matrix transformations were computed from a custom-written Matlab code. Angles were determined at each successive gait event from the direction cosine matrices to compute the 3D orientation of the hallux relative to the first ray, and the first ray relative to the navicular. One matrix represented the orientation of the hallux in the MR reference, one represented the first ray in the MR reference, and one represented the navicular in the MR reference. Matrix transformations then solved for the hallux (1-MTP) joint angles, and first ray-navicular angles.

## **2.4 Data analysis**

Statistical parameters for the variables were calculated using NCSS (Kaysville, Utah) Edition 2007 software. All data were explored for normal distribution by evaluating skewness and kurtosis.

Parametric analyses were performed on the first ray-navicular angles as two separate 2-way mixed design analysis of variance (ANOVA). Analysis determined group-by-condition effects and interaction of the first ray angles ( $Y$ ,  $Z$ ,  $X$ ) taken from each gait event (Table 2). The gait event conditions (MS, HO, TS) were treated as distinct within-subject independent variables that affected the Cardan angles (dependent variables). Analysis also assessed for group-by-condition main effects and interaction for the  $Y$

component helical axis. In this model, the periods between successive gait events (middle stance; late stance) were treated as the independent variables that affected the Y component (Table 3). If an interaction was identified, Tukey post hoc pairwise comparisons for condition were evaluated. Significance was set at alpha  $P < 0.05$ .

Multiple regression analysis was used to assess the linear relationship in the measures of arch angle and change in navicular-to-world eversion angular position to the Y component first ray helical axis measured during the middle, and late stance gait conditions.

### **3. Results**

The hallux-metatarsal (1-MTP joint) angles computed across conditions are reported in Table 2. In both groups, the mean hallux rotations became increasingly dorsiflexed, abducted, and inverted with the progression of gait events. The angle changed the most in the sagittal plane. For subjects with deformity, the hallux dorsiflexed  $11.6^\circ$  in middle stance (MS to HO) and  $33.4^\circ$  in late stance (HO to TS). For controls, the hallux dorsiflexed  $11.3^\circ$  and  $31.4^\circ$  during the same gait timing. Dorsiflexion of the hallux occurred in response to the subject's foot being placed level at MS, and then wedged forward into late stance (Table 2).

Table 2 also records the first ray-navicular angles computed by group and condition. Our hypotheses called for making group comparisons in the transverse and frontal plane

angles. A group effect ( $F = 44.17$ ,  $df = 1, 18$ ;  $P < 0.001$ ) was found in the transverse plane. Statistically greater adduction was measured across gait events in the hallux valgus group ( $P < 0.05$ ); the mean difference was as large as  $12^\circ$  at HO (Fig. 4). The group difference was one of positional malalignment; there was no group-by-condition interaction in the adduction angle.

A statistically significant group-by-condition interaction was found in the frontal plane angle ( $F = 3.56$ ,  $df = 2, 36$ ;  $P < 0.04$ ). Pairwise comparisons did not identify a group effect (Table 2; Fig. 4). We cannot accept the hypothesis that the first ray everts more on the navicular at HO in subjects having deformity. The pairwise comparisons did show the angle of eversion at MS and HO was different from TS in both groups ( $P < 0.05$ ). Eversion increased across gait with most rotation occurring in late stance (Table 2).

First ray-navicular total rotation (Table 3) and the complementary directional cosine components were computed between gait events. Rotation measured in middle stance ( $\leq 5.6^\circ$ ) was small in relative size as compared to late stance ( $\geq 11.3^\circ$ ) in both groups. In subjects with deformity, rotation averaged  $5.6^\circ$  (direction cosines averaged  $Y_c = 0.40$ ,  $Z_c = 0.08$ ,  $X_c = -0.20$ ) during middle stance. The larger positive helical Y (0.40) component indicates adduction was the dominant motion, the negative X (-0.20) component indicates eversion occurred to a lesser degree, and the positive Z (0.08) component indicates dorsiflexion contributed minimally. In hallux valgus subjects, rotation averaged  $11.3^\circ$  in late stance (Table 3) with the respective mean Y, Z, X directional cosine components

measuring -0.05, -0.33, and -0.62. The relatively large X (-0.62) component indicates eversion was dominant; the smaller Y (-0.33) component indicates plantar flexion occurred to a lesser degree, and the smallest Y (-0.05) component indicates the abduction contributed minimally to the total rotation measured. Mean helical axis parameters for controls are shown in Table 3.

The Y component (helical axis) was the primary dependent variable of interest (Table 3). The 2-way ANOVA identified a significant group-by-condition interaction ( $F = 5.06$ ,  $df = 1, 18$ ;  $P = 0.037$ ). The  $Y_c$  was statistically larger ( $P < 0.05$ ) for subjects with deformity in middle stance ( $Y_c = 0.40$ ) as compared to late stance ( $Y_c = -0.05$ ).  $Y_c$  did not change across gait in controls. See Figure 5.

Multiple regression analysis (Table 4) revealed no significant in the relationship in arch angle considered in combination with the change in navicular-to-world eversion angle measured during middle stance (MS to HO), and during late stance (HO to TS) to the helical axis Y component. The hypothesis that variables would relate was not supported.

## **4. Discussion**

### **4.1 Rationale for data interpretation**

This study investigated first ray kinematics using a weightbearing imaging technique. Subjects stood in an MR scanner, their foot/ankle placed to simulate gait postures. Tarsal geometries were segmented from the scanned images, and coordinate systems were

embedded into each bone. First ray angles and helical axis parameters were computed with respect to the navicular in the MR reference. The data were then analyzed between groups and across gait conditions (Fig. 4). The discussion now synthesizes the results, and compares the data measured to the relevant gait and clinical literature.<sup>13, 14, 43, 50-52</sup>

The criterion standard for kinematic comparisons comes from research that tracked tarsal motion from fixed bone-pins while subjects walked barefoot.<sup>13, 14, 52</sup> Results illuminate the complexity of tarsal motion, while providing a rationale for how the foot should be modeled to preserve a realistic representation of weightbearing kinematics.<sup>13, 14, 52</sup> Of importance to this study, the first metatarsal and medial cuneiform were found to move in synchrony. This led the researchers to recommend future studies model the bones together as one segment,<sup>13, 14, 52</sup> called the first ray.<sup>8, 9</sup>

Further discussion of bone-pin results give context to first ray motions.<sup>13, 52</sup> In young healthy males (N = 5), component rotations (transverse, sagittal, frontal) averaged no more than 6° in any plane as subjects stepped from heel strike to heel off. Component rotations measured through the remainder of stance averaged less than 13°.<sup>13, 52</sup> These results are discussed in reference to heel off because at this instant of gait, the direction of the component rotations changed abruptly. And for this reason, HO was simulated as the middle gait event (MS, HO, TS) in this study.

## **4.2 First ray-navicular angles and rotations**

The first ray kinematics measured (Fig. 4) are consistent with data published in the gait literature.<sup>13, 14, 50-52</sup> Change measured largest in the sagittal plane angles (Fig. 4). The greatest change occurred from HO to TS (late stance) with the first ray plantar flexing 6°. In comparison, the sagittal plane angle changed less than 1° from MS to HO (middle stance). Leardini et al.<sup>51</sup> reported similar data. Other studies<sup>13, 50, 51</sup> however, report the first ray dorsiflexes (~3°) during weight acceptance until heel off, timed with the lowering of the arch.<sup>43, 50</sup> We simulated heel off (HO) by standing the subject on a wedge. There was no acceleration, and the hindfoot shared in carrying the load. Thus, when reviewing our data critically we speculate that our method of simulating HO may not have flattened the arch fully. All other angles reported in this imaging study (Table 2; Fig. 4) closely compare to data collected in gait trails.<sup>13, 50, 51</sup>

The change in first ray angles generally measured largest from HO to TS. A wedge was placed beneath the toes at TS (Fig. 1.A). This tightened the plantar fascia and was observed to elevate the arch, represented as first ray plantar flexion in the angle data (Fig. 4).

Besides angles, we measured rotation of the first ray as helical axis parameter (Table 3). Total rotation summed to 16.9° in the hallux valgus group, and 19.3° in controls. We highlight this output to make one final comparison to the published bone-pin results.<sup>13, 14, 52</sup> Nester and colleagues reported first ray-navicular component rotations averaged 5.4°, 11.6°, and 11.0° in the respective transverse, sagittal, and frontal planes.<sup>13</sup> Although

component angles give only a representation of the motion measured,<sup>53</sup> the angles are similar in magnitude to the rotations reported here (Table 3). Such comparison supports the construct validity of our results.

Adduction deformity is a primary characteristic of hallux valgus. As hypothesized, adduction of the first ray was increased ( $P < 0.01$ ) by as much as  $12^\circ$  in the group having deformity (Table 2). Adduction of first ray disrupts the “truss” framework upon which the plantar fascia gains mechanical advantage to produce tension.<sup>54</sup> The plantar fascia originates on the calcaneus and inserts into the toes.<sup>55, 56</sup> Dorsiflexion of the toes winds the fascia around the metatarsal heads.<sup>55</sup> This stiffens the foot in preparation for push off, when forces transmitted between the first ray and the ground approach 30% of weight.<sup>57, 58</sup> Adduction isolates the first ray, moving it away from the foot’s center-of-pressure.<sup>19, 20, 22</sup> Conjecture offered by others<sup>54, 59</sup> is that adduction reduces the capacity of the plantar fascia to produce tension which in turn, destabilize the arch<sup>54</sup> causing the first ray arch segment to carry a smaller proportion of weight.<sup>19, 20, 22</sup>

Eversion of the hallux is a progressive trait of hallux valgus deformity.<sup>15-17</sup> Therefore, we hypothesized the first ray would evert more in subjects with deformity at HO.<sup>54, 60</sup> This specified pairwise comparisons (Table 2) revealed no group difference in the eversion angle. Canseco et al<sup>23</sup> found what could be interpreted as a different result. Using standard gait analysis, they compared fore-on-hindfoot angles in patients having deformity to a control group. Eversion was increased  $10^\circ$  in patients with hallux valgus



into late stance gait. Our hindfoot study<sup>30</sup> showed deformity everted the calcaneus. Since modeling the foot as rigid segments does not isolate the measure of joint motion, Canseco's<sup>23</sup> findings of increased eversion may have actually detected changes in the hindfoot alignment, and not the first ray. More research is needed.

### **4.3 First ray axis orientation**

A joint axis is a line that varies in 3D orientation about which body segments rotate in a perpendicular plane. In a previous study<sup>34</sup> we calculated a finite helical axis (FHA) direction cosine vector<sup>47, 48</sup> to quantify orientation of the first ray axis in cadavers. The specimens did not have obvious foot deformity, but the study provided us opportunity to test these methods.<sup>34</sup>

The Y, Z, X components measured to define the orientation of the first ray axis were computed in the MR reference.<sup>47, 48</sup> The directional cosine vector calculates as positive or negative (Table 3). The sign indicates the direction of joint rotation. The calculation is bounded by an absolute value of 1.00. For example, should the Yc axis = 1.00 then Zc and Xc compute as zero. This defined vector would orient vertical and point up, with adduction being the rotation expressed. The example just given was hypothetical, as well as improbable because the axes of the foot joints do not align perpendicular to the cardinal planes. Accordingly, the components reported in Table 3 do not approach the bounded limits of plus or minus 1. The foot joints are “triplanar”. Meaning the joints rotate in an oblique plane that passes through some portion of all three cardinal planes.

For example, should the directional cosine components compute as equal and as positive, the array of parameters would present  $Y_c = 0.33$ ,  $Z_c = 0.33$ , and  $X_c = 0.33$ . Orientation of this particular direction cosine vector would indicate that rotation, regardless of its magnitude, occurred in equal proportions of adduction, dorsiflexion, and inversion. Directions designate positive based on how the coordinate systems are defined.

The first ray helical axis exhibited some degree of inclination in both groups (Table 3). The Y component averaged 0.40 in the hallux valgus group during middle stance, with adduction being dominant motion.  $Y_c$  averaged 0.10 in controls, with adduction now being the smallest motion. In late stance,  $Y_c$  averaged -0.05 in hallux valgus subjects as compared to 0.13 in controls. The Y component measured smallest in both cases.

We hypothesized the axis would orient more vertical in subjects with hallux valgus. Group differences were not found, but group-by-condition interaction (Fig. 5) was identified as being statistically significant ( $F = 5.06$ ;  $P = 0.037$ ). The Y component was larger in the hallux valgus group during middle (0.40) as compared to late (-0.05) stance. To aid our interpretation of this result, we converted the mean directional cosines into angles using an arccosine trigonometric function. Middle stance conversion was  $\arccosine\ 0.40 = 66^\circ$ . Late stance conversion was  $\arccosine\ -0.05 = 93^\circ$ . Recall, the orientation of the axis was computed in relation to the true vertical MR laboratory frame of reference. Thus  $Y_c = 0.40$  tilted  $66^\circ$  from vertical;  $Y_c = -0.05$  tilted  $93^\circ$  from vertical. Staying consistent with language used throughout, this indicates the first ray axis in the

hallux valgus group inclined  $23^\circ$  (from horizontal) during middle stance, and declined  $3^\circ$  during late stance. The same conversion applied to the control Y component means (Table 3) equates to the axis being inclined  $6^\circ$  at middle stance, and  $3^\circ$  at late stance.

To summarize, the axis orientation was statistically dependent ( $P = 0.037$ ) on gait event. The first ray axis inclined  $23^\circ$  in the hallux valgus group and  $6^\circ$  in controls at middle stance. At gait mid-stance the foot assumes its most natural alignment, when Glasoe et al<sup>7</sup> theorized the first ray axis would be more inclined in subjects with hallux valgus. This result does not decide the issue, but does show the first ray axis is physical trait that can be quantified. Results, in general support theory<sup>7</sup> and existing research.<sup>30, 34</sup>

We make one final observation in discussing the angular data. Agreement exists between mean helical axis components (Table 3) and mean group angles (Table 2; Fig. 4). To give an example, the Yc computed positive both groups ( $Yc = 0.40$ ;  $Yc = 0.10$ ) for middle stance. This positive Y component indicates the first ray adducted from MS to HO, as displayed in the angle data (Fig. 4). This proof in kinematic outputs helps verify that matrix transformations were made correctly.

#### **4.4 Regression analysis measurements**

Degradation of the arch foot structure may initiate hallux valgus.<sup>7</sup> To investigate, a series of bone angle alignments were measured on the MS bone datasets (Fig. 2). Subjects with deformity had significantly larger hallux/IM angles ( $36^\circ/17^\circ$ ) as compared to controls

(8°/11°).<sup>30</sup> The size of the angles indicates the severity of deformity. Normal hallux/IM angles range from 5-15°/8-12°. <sup>61, 62</sup> Mild deformity ranges from 15-25°/12-14°, moderate from 25-40°/14-20°, and severe is > 41°/20°. <sup>1, 62</sup> Subjects sampled generally had a moderately sized deformity, representing a population that would seek conservative care treatment.

There was no group difference in arch angle (Table 1).<sup>30</sup> The angle averaged 135° in the hallux valgus group and 133° in controls. Adult normal is  $132 \pm 2^\circ$ . <sup>42, 63</sup> Because deformity has been associated with pes planus, <sup>17, 64</sup> and because our *in vitro* experiment<sup>34</sup> found the first ray axis to be more inclined in the low-arched foot, multiple regression analysis assessed the relationship of arch angle and change in navicular-to-world eversion angle to vertical orientation of the first ray axis (Table 4). Since navicular eversion angle is often reported in gait studies, <sup>13, 14, 50, 65</sup> we considered it useful in predicting the helical axis Y component.

Multiple regression analysis (Table 4) output two coefficient of determination  $R^2$  values. The coefficients estimated the variance explained by the arch angle and navicular eversion in predicting  $Y_c$  for middle ( $R^2 = 0.04$ ), and late stance ( $R^2 = 0.00$ ). The predictors explained a nonsignificant ( $P \geq 0.68$ ) amount of the overall variance of the computed  $Y_c$  causing us to reject the hypothesis put forth for testing. The larger results revealed that neither arch angle nor navicular-world eversion were statistically different between groups. Therefore, when considered in combination, there was not surprise the

variables did not predict the orientation of the first ray axis. In our hindfoot study of kinematics,<sup>30</sup> the calcaneus was found everted 7° more in subjects with deformity. Thus, we now conclude that eversion of the calcaneus, not arch angle or navicular eversion, to better predict vertical orientation of the first ray axis.

#### **4.5 Limitations of the study**

The imaging measurement of first ray kinematics has limitations. Categorized as: i. Modeling gait with static foot postures. ii. Small sample size. iii. Complexities involved in representing first ray rotation with a single oblique axis

i. Modeling gait with static loading eliminated the need for the muscles to control or propel body accelerations. While acknowledging this as a limitation, our methods replicated the foot/ankle positions of gait (Fig 1.B) and overall, the data reported in this study was shown comparable to data published in the gait literature.<sup>13, 50, 51</sup>

ii. The sample was small because of the costs associated with imaging. The sample size had sufficient power to detect group differences in first ray angles, but not for the follow-up of the Y component directly. A post hoc power calculation estimates recruitment of 3 more hallux valgus subjects would have been required to achieve an 80% chance to detect a 0.3 difference over the control group. In addition, results reported are generalized to all females having hallux valgus. A group of 10 may not in all ways represent the population, as the severity of deformity varies widely in the general public.

iii. The helical axis computation was made under the assumption that the first ray rotation can be modeled to occur about a single oblique axis. This assumes the two bones (first metatarsal and cuneiform) behave as a single segment. We cannot know how group differences in the stability of the first metatarsocuneiform joint may have affected the results.

## 5. Summary

Imaging was used to compare first ray kinematics in subjects grouped with and without hallux valgus. From the imaged datasets, first ray angles and helical axis parameters were computed. Adduction was increased ( $\geq 9.3^\circ$ ) in those having deformity, with orientation of the first ray axis inclined  $23^\circ$  ( $Y_c = 0.40$ ) during middle stance, as compared to  $6^\circ$  ( $Y_c = 0.10$ ) in controls. Arch angle and navicular eversion were explored using regression analysis as predictors that may relate to vertical orientation of the first ray axis. No relationship was found. The kinematics defined, especially the computation of the first ray helical axis parameters, may be useful in developing improved treatment strategies for hallux valgus.

**Table 5.1.** Group mean  $\pm$  SD (range) for the measurement of bone angles.

| <b>Group</b>                      | <b>*Hallux Angle<br/>(°)</b> | <b>*IM 1-2 Angle<br/>(°)</b> | <b>Arch Angle<br/>(°)</b> |
|-----------------------------------|------------------------------|------------------------------|---------------------------|
| <b>Hallux Valgus<br/>(N = 10)</b> | 36 $\pm$ 7 (25 to 47)        | 17 $\pm$ 3 (14 to 20)        | 135 $\pm$ 6 (126 to 143)  |
| <b>Controls<br/>(N = 10)</b>      | 8 $\pm$ 5 (-3 to 15)         | 11 $\pm$ 1 (9 to 13)         | 133 $\pm$ 6 (127 to 143)  |

\*Group differences ( $P < 0.01$ ) were determined in a previous study.<sup>30</sup>

**Table 5.2.** Group angles recorded in the body planes at midstance (MS), heel off (HO), and terminal stance (TS). Comparisons are angles for the 1-MTP joint, and first ray-navicular. Adduction, dorsiflexion, and inversion are positive.

|                         | <b>Transverse<br/>(°)</b> |                  |                  | <b>Sagittal<br/>(°)</b> |                  |                  | <b>Frontal<br/>(°)</b> |                  |                  |
|-------------------------|---------------------------|------------------|------------------|-------------------------|------------------|------------------|------------------------|------------------|------------------|
|                         | <b><u>MS</u></b>          | <b><u>HO</u></b> | <b><u>TS</u></b> | <b><u>MS</u></b>        | <b><u>HO</u></b> | <b><u>TS</u></b> | <b><u>MS</u></b>       | <b><u>HO</u></b> | <b><u>TS</u></b> |
| <b><u>1-MTP</u></b>     |                           |                  |                  |                         |                  |                  |                        |                  |                  |
| HV                      | -34.2                     | -37.0            | -53.3            | 3.8                     | 15.4             | 48.8             | -12.7                  | -7.9             | 10.8             |
| Controls                | -9.9                      | -12.2            | -30.3            | 3.7                     | 15.0             | 46.4             | -4.2                   | -2.4             | 14.5             |
| <b><u>First Ray</u></b> |                           |                  |                  |                         |                  |                  |                        |                  |                  |
| HV                      | *<br>18.1                 | †<br>20.1        | §<br>18.9        | -14.2                   | -13.8            | -19.7            | a<br>-4.0              | a<br>-6.6        | -12.7            |
| Controls                | *<br>7.8                  | †<br>8.2         | §<br>9.6         | -12.5                   | -13.2            | -19.7            | a<br>-4.4              | a<br>-4.5        | -17.5            |

Statistical comparisons made at gait events in each body plane for the first ray-navicular angles only. Differences at  $P < 0.05$  indicated by superscript symbols. Group symbols: (\*) different at MS; (†) different at HO; (§) different at TS. Condition letters: (a) different for both groups from TS.

**Table 5.3.** First ray rotations (Phi) and helical axis components computed relative to the navicular in the MR reference. Data is displayed as group means (SE).

| <b>Middle Stance (MS to HO)</b> |            |              |              |              |
|---------------------------------|------------|--------------|--------------|--------------|
|                                 | <b>Phi</b> | <b>Yc</b>    | <b>Zc</b>    | <b>Xc</b>    |
| <b>Hallux Valgus</b>            | 5.6°       | 0.40 (0.10)  | 0.08 (0.20)  | -0.20 (0.20) |
| <b>Controls</b>                 | 4.0°       | 0.10 (0.12)  | -0.11 (0.19) | -0.25 (0.23) |
| <b>Late Stance (HO to TS)</b>   |            |              |              |              |
|                                 | <b>Phi</b> | <b>Yc</b>    | <b>Zc</b>    | <b>Xc</b>    |
| <b>Hallux Valgus</b>            | 11.3°      | -0.05 (0.11) | -0.33 (0.13) | -0.62 (0.16) |
| <b>Controls</b>                 | 15.3°      | 0.13 (0.06)  | -0.30 (0.10) | -0.86 (0.05) |

The positive direction for the Y, Z, X components: adduction, dorsiflexion, inversion.

**Table 5.4.** Multiple regression analysis results. Arch angle ( $X_1$ ) and change in navicular-to-world eversion angles ( $X_2$ ) are predictor variables for the Y component first ray helical axis.

|               |                 | <b>Predictor Variables</b> |                           |                      |          |          |
|---------------|-----------------|----------------------------|---------------------------|----------------------|----------|----------|
| <b>Stance</b> | <b>Constant</b> | <b>X<sub>1</sub> (SE)</b>  | <b>X<sub>2</sub> (SE)</b> | <b>R<sup>2</sup></b> | <b>F</b> | <b>P</b> |
| Middle        | -1.229          | 0.023 (0.01)               | -0.012 (0.03)             | 0.04                 | 0.39     | 0.68     |
| Late          | 0.329           | -0.002 (0.01)              | -0.001 (0.01)             | 0.00                 | 0.02     | 0.98     |

Abbreviations: SE, standard error; R<sup>2</sup>, coefficient of determination; F, F-ratio; P, P-value.



**Figure Legend (Chapter V.)**

**Fig. 5.1.** **A.** Gait (MS, HO, TS) was simulated with the subject standing while partially kneeling into a bolster fixed in the scanner. **B.** Shows the sagittal view of the reconstructed bone dataset. The bone models represented are the proximal phalanx of the hallux, the first metatarsal, navicular, calcaneus, and fibula.

**Fig. 5.2.** Bone angles measured on the midstance (MS) bone datasets. **A.** Hallux Angle. **B.** Intermetatarsal (IM) Angle. **C.** Arch Angle.

**Fig. 5.3.** Sagittal view of a single subject bone dataset. The foot was scanned at terminal stance (TS). The surrounding dark-shaded rectangle represents the scanner field-of-view. Shown here, the foot and scanner field-of-view have been rotated back to horizontal in the MR reference.

**Fig. 5.4.** Group angles plotted in the body planes across gait midstance (MS), heel off (HO), and terminal stance (TS). Error bars are the 95% confidence interval (CI) of the mean data. Note: scale changes between graphs.

**Fig. 5.5.** Significant\* group-by-condition interaction ( $P = 0.037$ ). The Y component was larger in middle stance (0.40) as compared to late stance (-0.05) in subjects having hallux valgus. Error bars indicate 95% confidence interval.

**Figure 5.1.**

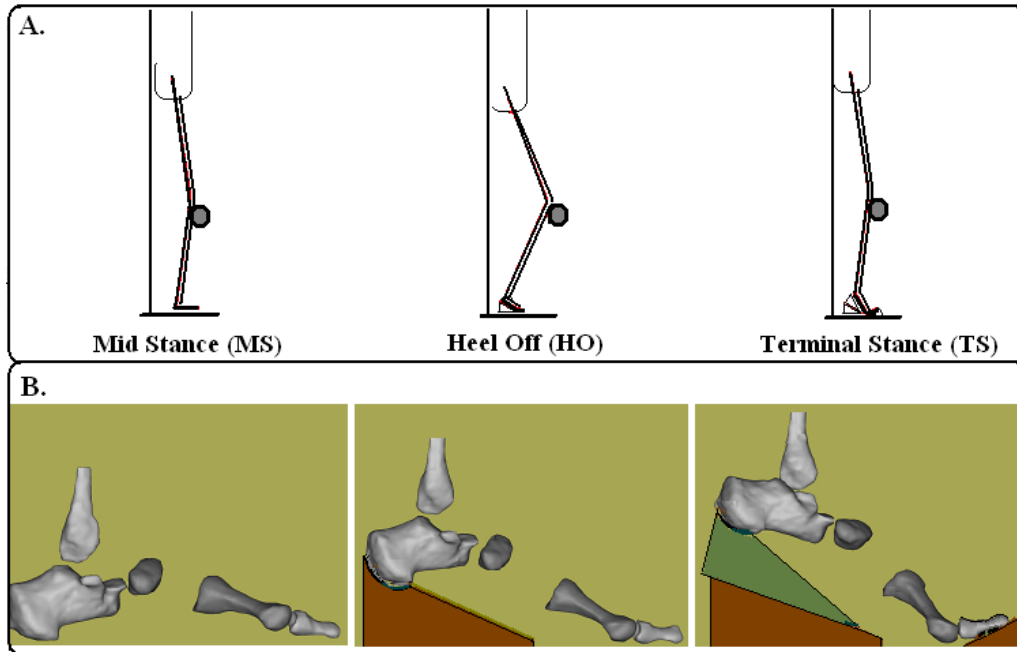


**Figure 5.2.**

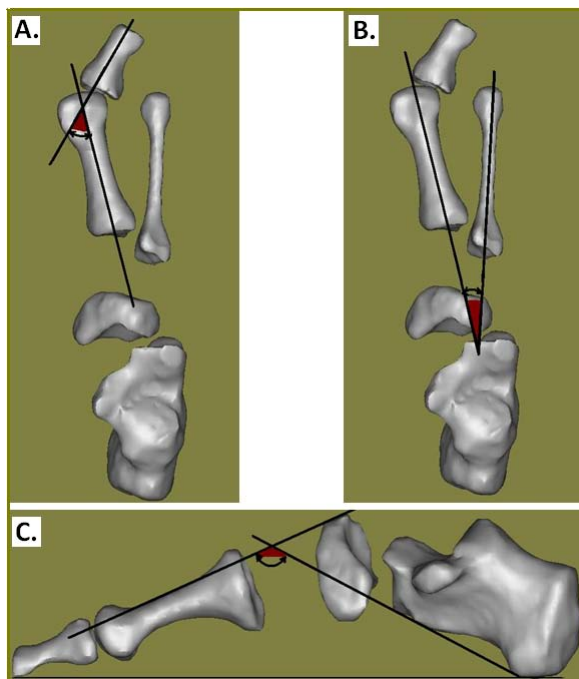


**Figure 5.3.**

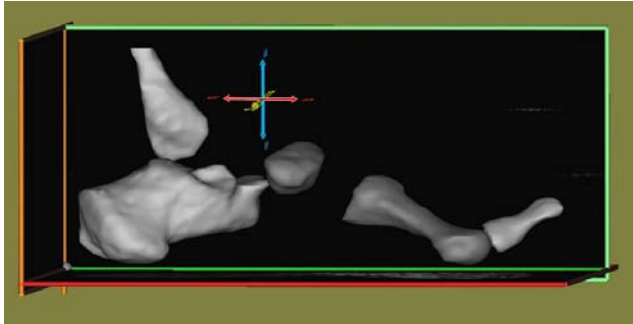


**Figure 5.4.**

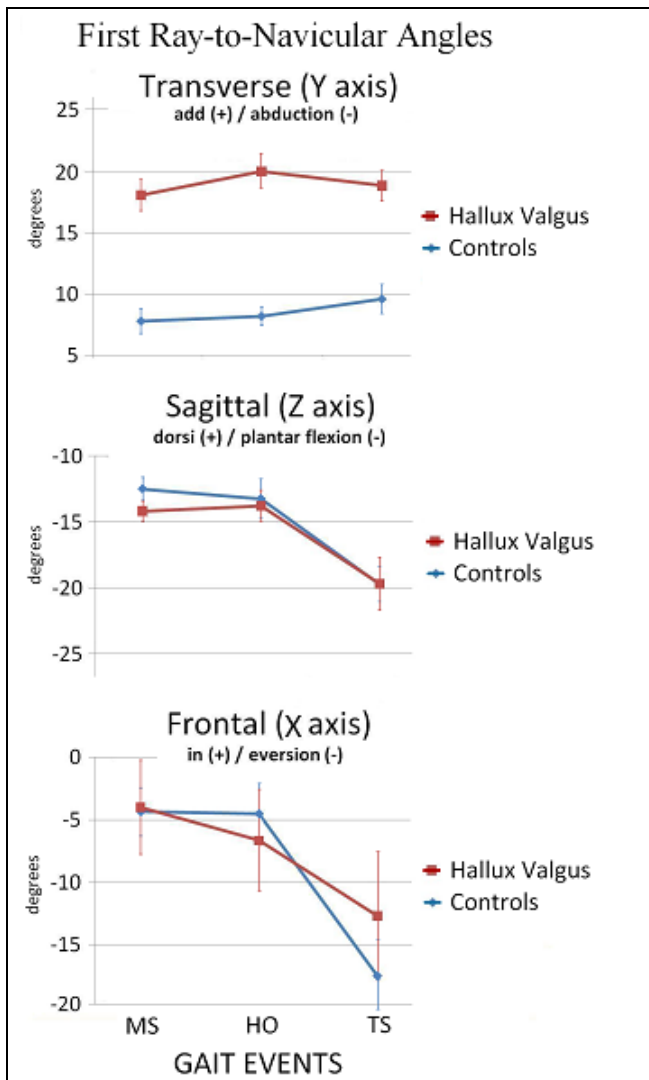
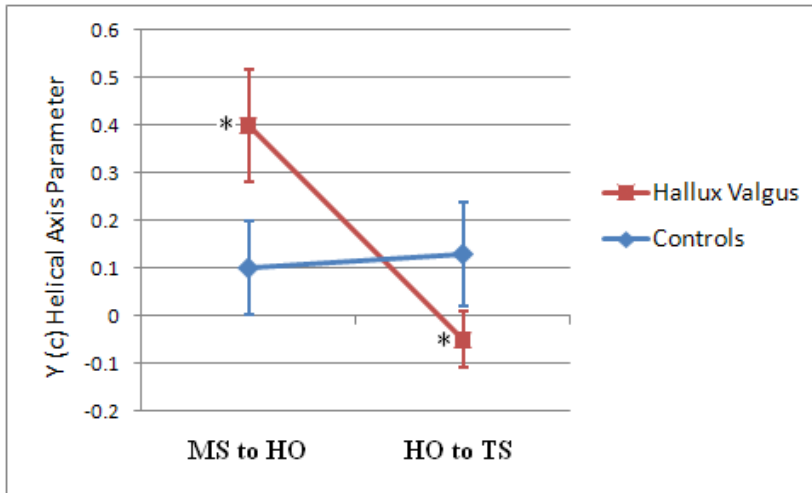


**Figure 5.5.**



## References (Chapter V.)

1. Coughlin M, Jones C. Hallux valgus: demographics, etiology, and radiographic assessment. *Foot Ankle Int.* 2007;28:759-777.
2. Ferrari J, Higgins J, Prior T. Interventions for treating hallux valgus (abductovalgus) and bunions. *Cochrane Database of Systematic Reviews.* 2004;Issue 1. Art. No.:CD000964.DOI:10.1002/14651858.CD000964.pub2.
3. Inman V. Hallux valgus: a review of etiologic factors. *Orthop Clin N Amer.* 1974;5(1):59-66.
4. Snijder C, Snijder J, Philippens M. Biomechanics of hallux valgus and spread foot. *Foot Ankle.* 1986;7:26-39.
5. Coetzee J, Wickum D. The Lapidus procedure: a prospective cohort outcome study. *Foot Ankle Int.* 2004;25:526-531.
6. Spruce M, Bowling F, Metcalfe S. A longitudinal study of hallux valgus surgical outcomes using a validated patient centered outcome measure. *Foot (Edinb)* 2011 Feb 11. [Epub ahead of print].
7. Glasoe W, Nuckley D, Ludewig P. Hallux valgus and the first metatarsal arch segment: a theoretical biomechanical perspective. *Phys Ther.* 2010;90:110-120.
8. Glasoe W, Yack H, Saltzman C. Anatomy and biomechanics of the first ray. *Phys Ther.* 1999;79(9):854-859.
9. Hicks J. The mechanics of the foot. I. The joints. *J Anat.* 1953;87:345-357.
10. Ferrari J, Hopkinson D, Linney A. Size and shape differences between male and female foot bone. Is the female foot predisposed to hallux abducto valgus deformity? *J Am Podiatr Med Assoc.* 2004;94(5):434-452.
11. Romash M, Fugate D, Yanklowit B. Passive motion of the first metatarsal cuneiform joint: preoperative assessment. *Foot Ankle.* 1990;10(6):293-298.
12. Wanivenhaus A, Pretterklieber M. First tarsometatarsal joint: anatomical biomechanical study. *Foot Ankle Int.* 1989;9(4):153-157.
13. Nester C, Jones R, Liu A, et al. Foot kinematics during walking measured using bone and surface mounted markers. *J Biomech.* 2007;40:3412-3423.
14. Wolf P, Stacoff A, Liu A, et al. Functional units of the human foot. *Gait Posture.* 2008;28:434-431.
15. Saltzman CL, Brandser EA, Anderson BS, Berbaum KS, Brown TD. Coronal plane rotation of the first metatarsal. *Foot Ankle.* 1996;17(3):157-161.
16. Talbot K, Saltzman C. Hallucal rotation: a method of measurement and relationship to bunion deformity. *Foot Ankle Int.* 1997;18(9):550-556.
17. Eustace S, Byrne J, Beausang O, Codd M, Stack J, Stephens M. Hallux valgus, first metatarsal pronation and collapse of the medial longitudinal arch - a radiological correlation. *Skeletal Radiol.* 1994;23:191-194.

18. Saltzman C, Aper R, Brown T. Anatomic determinants of first metatarsophalangeal flexion moments in hallux valgus. *Clin Orthop*. 1997;339(6):261-269.
19. Hutton W, Dhanendran M. The mechanics of normal and hallux valgus feet: a quantitative study. *Clin Orthop Related Res*. 1981;157:7-13.
20. Kernozek T, Elfessi A, Sterriker S. Clinical and biomechanical risk factors of patients diagnosed with hallux valgus. *J Am Podiatr Med Assoc*. 2003;93(2):97-103.
21. Schuh R, Hofstaetter S, Adams S, Pichler F, Kristen K, Trnka H. Rehabilitation after hallux valgus surgery: importance of physical therapy to restore weight bearing of the first ray during the stance phase. *Phys Ther*. 2009;89:Epub ahead of print.
22. Waldecker U. Pedographic analysis of hallux valgus deformity. *Foot Ankle Surg*. 2004;10(3):121-124.
23. Canseco K, Rankine L, Long L, Smedberg T, Marks R, Harris G. Motion of the multisegmental foot in hallux valgus. *Foot Ankle Int*. 2010;31:146-152.
24. Deschamps K, Birch I, Desloovere K, Matricali G. The impact of hallux valgus on foot kinematics: A cross-sectional. *Gait Posture*. 2010;32:102-106.
25. Ebisui J. The first ray axis and first metatarsophalangeal joint. *J Am Podiatr Assoc*. 1968;58(4):160-168.
26. Sanders A, Snijders C, Linge B. Medial deviation of the first metatarsal head as a result of flexion forces in hallux valgus. *Foot Ankle Int*. 1992;13(9):515-522.
27. Cargill S, Pearcy M, Barry M. Three-dimensional lumbar spine postures measured by magnetic resonance imaging reconstruction. *Spine*. 2007;32:1242-1248.
28. Mattingly B, Talwalker V, Tylkowski C, Stevens D, Hardy P, Pienkowski D. Three-dimensional in vivo motion of adult hind foot bones. *J Biomech*. 2006;39:726-733.
29. Wolf P, Stacoff A, Liu A, et al. Does a specific MR imaging protocol with a supine-lying subject replicate tarsal kinematics seen during upright standing? *Biomed Tech*. 2007;52:290-294.
30. Glasoe W, et al. Calcaneus and navicular kinematics in hallux valgus: a weightbearing imaging study. *TBD*. 2011:Ready for Journal Submission.
31. Nester C, Liu A, Ward E, Howard D, Cocheba J, Derrick T. Error in the description of foot kinematics due to violation of rigid body assumptions. *J Biomech*. 2010;43:666-672.
32. Hirsch B, Udupa J, Samarasekera S. New method of studying joint kinematics from three-dimensional reconstructions of MRI data. *J Am Podiatr Med Assoc*. 1996;86(1):4-15.
33. Tanaka Y, Takakura Y, Tadashi F, Sugimoto K. Hindfoot alignment of hallux valgus evaluated by a weightbearing subtalar x-ray view. *Foot Ankle Int*. 1999;20(10):640-645.

34. Glasoe W, Pena F, Phadke V, Ludewig P. Arch height and first metatarsal joint axis orientation as related variables in foot structure and function: theory related to bunion. *Foot Ankle Int.* 2008;29(6):647-655.
35. Johnson C, Christensen J. Biomechanics of the first ray part 1. The effects of peroneus longus function: a three-dimensional kinematic study on a cadaver model. *J Foot Ankle Surg.* 1999;38(5):313-321.
36. Glasoe W, et al. First ray kinematics in hallux valgus: a weightbearing imaging study. *TBD.* 2011:Ready for Journal Submission.
37. Glasoe W, Phadke V, Nuckley D, Pena F, Ludewig P. First metatarsal helical axis and angle measurements in subjects having bunion as compared to controls *J Foot Ankle Res Suppl.* 2011 (in press).
38. Camacho D, Ledoux W, Rohr E, Sangeorzan B, Ching R. A three-dimensional, anatomically detailed foot model: a foundation for a finite element simulation and means of quantifying foot-bone position. *J Rehab Res Develop.* 2002;39(3):401-410.
39. Ledoux W, Rohr E, Ching R, Sangeorzan B. Effect of foot shape on the three-dimensional position of the foot bones. *J Orthop Res.* 2006;24:2176-2186.
40. Wu G, Siegler S, Allard P, et al. ISB recommendation on definitions of joint coordinate system of various joints for the reporting of human joint motion--part I: Ankle, hip, and spine. *J Biomech.* 2002;35:543-548.
41. Deng X, Denny T. Combined tag tracking and strain reconstruction from tagged cardiac MR images without use defined myocardial contours. *J Magn Reson Imaging.* 2005;21:12-22.
42. Saltzman C, Nawoczenski D, Talbot K. Measurement of the medial longitudinal arch. *Arch Phys Med Rehabil.* 1995;76(1):45-49.
43. Wilken J, Rao S, Saltzman C, Yack H. The effect of arch height on kinematic coupling during walking. *Clin Biomech.* 2011;26(3):318-323.
44. Glasoe W. Kinematic Study of Hallux Valgus Foot Deformity. *Ph.D Dissertation, Univ of Minnesota, USA.* 2011.
45. Engsberg J, Andrews J. Kinematic analysis of the talocalcaneal/talocrural joint during running support. *Med Sci Sports Exerc.* 1987;19(3):275-284.
46. Tuijthof G, Zengerink M, Beimers L, et al. Determination of consistent patterns of range of motion in the ankle joint with a computed tomography stress-test. *Clin Biomech.* 2009;24:517-523.
47. Woltring H. Representation and calculation of 3-D joint movement. *Human Movement Science.* 1991;10:603-616.
48. Woltring H. 3-D attitude representation of human joints: a standardization proposal. *J Biomech.* 1994;27:1399-1414.

49. Wearing S, Urry S, Pearlman P, Smeathers J, Dubois P. Sagittal plane motion of the human arch during gait: a videofluoroscopic analysis. *Foot Ankle Int.* 1998;19(11):738-742.
50. Allen M, Cuddeford T, Glasoe W, et al. Relationship between static mobility of the first ray and first ray, midfoot, and hindfoot motion during gait. *Foot Ankle Int.* 2004;25(6):391-396.
51. Leardini A, Benedetti M, Berti L, Bettinelli D, Nativo R, Giannini S. Rear-foot, mid-foot and fore-foot motion during the stance phase of gait. *Gait Posture.* 2006;25:453-462.
52. Lundgren P, Nester C, Liu A, et al. Invasive in vivo measurement of rear-, mid- and forefoot motion during walking. *Gait Posture.* 2008;28:93-100.
53. Karduna A, McClure P, Michener L. Scapular kinematics: effects of altering the Euler angle sequence of rotations. *J Biomech.* 2000;33:1063-1068.
54. Coughlin M, Jones C. Hallux valgus and first ray mobility. *J Bone Joint Surg.* 2007;89A(9):1887-1898.
55. Hamel A, Donahue S, Sharkey N. Contributions of active and passive toe flexion to forefoot loading. *Clin Orthop.* 2001;393:326-334.
56. Thordarson DB, Schmotzer H, Chon J, Peters J. Dynamic support of the human longitudinal arch. *Clinical Orthopaedics and Related Research.* 1995;316:165-172.
57. Hayafune N, Hayafune Y, Jacob H. Pressure and force distribution characteristics under the normal foot during the push-off phase in gait. *The Foot.* 1999;9:88-92.
58. Jacob H. Forces acting in the forefoot during normal gait - an estimate. *Clin Biomech.* 2001;16:783-792.
59. Coughlin M, Jones C, Viladot R, et al. Hallux valgus and first ray mobility: a cadaveric study. *Foot Ankle Int.* 2004;25(8):537-544.
60. Grebing B, Coughlin M. The effect of ankle position on the exam for first ray mobility. *Foot Ankle Int.* 2004;25(7):467-475.
61. Bryant A, Tinley P, Singer K. A comparison of radiographic measurements in normal, hallux valgus, and hallux limitus feet. *J Foot Ankle Surg.* 2000;39:39-43.
62. Robinson A, Limbers J. Modern concepts in the treatment of hallux valgus. *J Bone Joint Surg.* 2005;87-B:1038-1045.
63. Wearing S, Smeathers J, Sullivan P, Yates B, Urry S, Dubois P. Plantar fasciitis: are pain and fascial thickness associated with arch shape and loading. *Phys Ther.* 2007;87:1002-1008.
64. Scranton P, McDermott J. Prognostic factors in bunion surgery. *Foot Ankle.* 1995;16(11):698-704.
65. Cornwall M, McPoil T. Motion of the calcaneus, navicular, and first metatarsal during the stance phase of walking. *J Am Podiatr Med Assoc.* 2002;92(2):67-76.



CHAPTER VI.  
OVERALL SUMMARY AND DISCUSSION

*Whether the first ray axis is intimately related to hallux valgus is a matter of conjecture.*

**Introduction**

John Ebisui <sup>1(P168)</sup> penned the above quote 45 years ago when calling for research to investigate the mechanics of hallux valgus foot deformity. In response, this three-part study of cadaver feet<sup>2</sup> and human subjects<sup>3,4</sup> measured tarsal kinematics and quantified orientation of the first ray axis in subjects having hallux valgus deformity.

The initial cadaveric experiment simulated gait midstance (MS), heel off (HO), and terminal stance (TS) while measuring first ray kinematics both as Cardan angles and helical axis parameters.<sup>2</sup> The methods were next integrated with imaging to compare the kinematics of subjects with hallux valgus to age-matched controls. From the imaged data, selected bones were reconstructed and foot posture and joint motion were measured. A mixed effect ANOVA model compared the variables tested between group (hallux valgus vs. controls) and across conditions (MS, HO, TS). The collective work is now summarized.

Chapter I. titled *Hallux Valgus Foot Kinematics: A Weightbearing Study* introduced the surrounding health care issues associated with hallux valgus deformity, and recorded the aims and hypotheses offered for testing.

Chapter II., titled *Hallux Valgus and the First Metatarsal Arch Segment: A Theoretical Biomechanical Perspective*<sup>5</sup> reviewed the literature. The perspective described the progressive nature of hallux valgus deformity and the ineffectiveness of currently available non-surgical treatments. Theory proposed for testing was that collapse of the arch orients (tilts) the first ray axis toward vertical allowing the first ray to adduct into deformity. The perspective concluded that treatment with orthoses has yet untested potential to shape the foot and slow the progression of hallux valgus.

Theory has now been tested.<sup>2-4</sup> Data was collected on cadavera (N = 9) and on human subjects (N = 20). The experimental methods and results were written as separate research reports.<sup>2-4</sup> The initial *in vitro* investigation<sup>2</sup> was written as Chapter III. in this thesis. The testing of human subjects followed. Write-up of the *in vivo* work was parsed into two manuscripts. One manuscript reported hindfoot and arch kinematics,<sup>3</sup> the other reported first ray kinematics.<sup>4</sup> The separate papers were written as Chapters IV. and V. for thesis distribution.

Chapter VI titled the *Overall Summary and Discussion* brings the thesis to conclusion. Part I discusses the choice for using weightbearing imaging to measure tarsal kinematics.

My method of simulating gait in an upright MR scanner was original.<sup>3,4</sup> To counter criticisms related to the construct validity of the “gait” data reported,<sup>3,4</sup> a section written in each of the three manuscripts<sup>2-4</sup> compared the angles measured to corresponding kinematic data published in the literature.<sup>6-8</sup> Part 1 concludes by listing the advantages and disadvantages associated with using Kinematic Imaging to measure foot posture and joint motions, and highlight related limitations of the methods. Part 2 summarizes the key findings and states the potential implications that this research has on clinical practice.

### **Part 1. Imaging Measurement of Tarsal Kinematics**

Two approaches are currently used by researchers to measure foot kinematics without skin motion artifact. One approach involves the surgical implantation of metallic markers or pins to indentify the spatial orientation of the tarsals individually. In my experiment on cadavers,<sup>2</sup> for example, the motion sensors were fixed to the bones. Such methods are not easily used on patients or large sample studies. The other approach is image-based modeling.<sup>9-12</sup> Its growing use in foot research<sup>10-12</sup> can be traced to recent advancements in scanning and computer software technology. Commercially available software now makes it easier to render bones as 3D objects,<sup>9</sup> with computerized registration used to spatially link datasets together leading to the measurement of joint motion.<sup>11,12</sup> As with pins screwed into the bone, imaging eliminates skin motion artifact and rigid-modeling error assumptions.<sup>9</sup>

Imaging was used to measure kinematics in this study.<sup>3,4</sup> Subjects grouped with (N = 10) and without (N = 10) hallux valgus were placed standing in a MR scanner on wedges to simulate a progression of gait events (MS, HO, TS). Standing on wedges standardized the test conditions.<sup>13,14</sup>

The images were reconstructed using MIMICS (Materialise, Leuven, Belgium). A software procedure reconstructed and embedded each bone with a “principal axes” inertial coordinate frame.<sup>9</sup> A potential problem here is that alignment of a bone’s coordinate frame may not conform to common clinical descriptions, as happened for the navicular.<sup>3,4</sup> The issue was managed mathematically by correcting the navicular coordinate frame to zero in the MR reference. A different solution would have been to build the coordinate frame from bony landmarks selected to express the cardinal plane direction of joint motions.<sup>15</sup> With imaging, landmark identification becomes a visual process, and seeing the anatomy should reduce this potential source of error.<sup>16</sup>

Additionally, imaging offered the advantage of measuring both foot posture and motion.<sup>3,</sup>

<sup>4</sup> The measurement of posture had particular importance, because posture defines the severity of deformity; i.e. hallux valgus.

Kinematic Imaging measurements of joint motion are highly accurate<sup>8,12,17,18</sup> which may, in part, explain why this study of hallux valgus identified group difference not detected in previous gait studies.<sup>19,20</sup> The combined error of data acquisition, reconstruction, and registration was  $\leq 3^\circ$  (Thesis Appendix 2) in this study. This degree

of accuracy is nearly three times better than tarsal motion measured from skin mounted markers when the data collected is modeled as non-anatomical rigid body segments.<sup>8, 18</sup>

There were limitations in the methods used.<sup>3, 4</sup> Perhaps most critical, the ground reaction forces could not be quantified within the narrow confines of the upright MR scanner. A side-experiment was conducted on 5 subjects to estimate the forces involved in standing in the scanner. Loading was measured in a research laboratory with PEDAR insoles (Novel Inc., St Paul, MN, USA) and force plates (Bertec Corp., Columbus, OH, USA), with subjects posed to replicate the sequence of scanned gait events. As expected, the foot-to-ground loading differed from physiological gait (Fig. A.3, Thesis Appendix 3). The foot carried half of body weight, the direction of ground reaction force (GRF) was mostly vertical and stayed constant across gait events with the heel supporting the majority of the load, and center-of-pressure (CoP) did not track forward in the foot as would occur during gait (Fig. A.4, Thesis Appendix 3). These differences in kinetics were accepted in trade-off for the accuracy gained in quantifying kinematics from a subject's reconstructed anatomy.

The cost of scanning and the time required to segment the anatomy are the disadvantages of imaging. As dynamic scanning technology become more available, and as data processing software continues to improve, imaging studies will measure tarsal motion during gait.

## Part 2. Results Synthesized

Part 2 is organized to report the hypothesis testing results, followed by a discussion of the key findings and the related clinical implications of this work. The chapter concludes in summary.

### Hypothesis testing results

Hypotheses are listed by Chapter, and designated by Study (1, 2, 3) and hypothesis number (1, 2, ...). The system of numbering for each hypothesis comes from Chapter I.

Chapter III. Study 1. <sup>(1)</sup>*Arch Height and First Ray Joint Axis Orientation.*

Hypothesis <sub>1,1)</sub> correctly predicted that a decomposition of finite helical axis parameters could quantify the orientation of the first ray axis between gait events. These descriptive results are presented in Figure 3.2 and Table 3.3.

Hypothesis <sub>1,2)</sub> correctly predicted that arch height and vertical orientation of the first ray axis are related to the increased intermetatarsal (IM) angle and increased adduction of the first ray. Arch height and inclination of the axis were related at a level of  $r = -0.73$ . The negative relationship indicates the first ray axis was more inclined in the low arched foot. Considered in combination, arch height and first ray axis orientation accounted for 69% of the variance of the IM angle and change in first ray adduction positioning (Table 3.4.). Results supported the hypothesis.

Chapter IV. Study 2. (2) *Calcaneus Kinematics in Subjects with Hallux Valgus.*

Hypothesis 2.1) investigated group difference in IM and arch angle measurements, with angles predicted to be larger in subjects with deformity. The group with hallux valgus demonstrated a larger mean IM angle ( $17^\circ$ ) as compared to controls ( $11^\circ$ ). There was no group difference in arch angle. Results (Table 4.1) partially supported the hypothesis.

Hypothesis 2.2) correctly predicted that the calcaneus in subjects with deformity would evert more in relation to the fibula at each gait event (MS, HO, TS). Significant group difference ranged from  $6.6^\circ$  to  $7.9^\circ$  (Table 4.2.) across gait events, with the group having deformity demonstrating significantly ( $P < 0.05$ ) more calcaneal eversion at each gait event. No interaction was found. The hypothesis was supported.

Hypothesis 2.3) predicted the navicular would evert more at HO in relation to the calcaneus, and with respect to the MR laboratory in subjects with deformity. No group difference was found (Table 4.2). The hypothesis was not supported.

Hypothesis 2.4) predicted that for both groups, the navicular would evert more in relation to the calcaneus at HO as compared to MS, and the navicular would invert more TS as compared to HO. A condition effect was found. The navicular inverted (not everted as predicted) a significant amount ( $\sim 5^\circ$ ) with respect to calcaneus from

MS to TS (Table 4.2). There was no interaction, meaning the change in angle across gait events was consistent between groups. The hypothesis was not supported.

Chapter V. Study 3.<sup>(3)</sup> *First Ray Kinematics in Subjects with Hallux Valgus.*

Hypothesis 3.1) correctly predicted the first ray would adduct more in relation to the navicular in subjects having hallux valgus. Group difference averaged  $\geq 9.3^\circ$  across gait events (Table 5.2). Related to predicting the first ray would be more adducted, the full hypothesis predicted the first ray axis would be more inclined in subjects with deformity as compared to controls. Although a group difference was not found, group-by-condition interaction (Fig. 5.5) was statistically significant ( $P = 0.037$ ). Follow-up comparisons identified the axis was more ( $P \leq 0.05$ ) inclined in middle stance ( $23^\circ$ ) as compared to late stance ( $-3^\circ$ ) in the hallux valgus group. Whereas for controls, the first ray axis remained oriented nearly horizontal (tilted  $\leq 6^\circ$ ) across gait events. The hypothesis was partially supported.

Hypothesis 3.2) predicted subjects with deformity would have greater eversion of the first ray relative to the navicular at the HO gait event. No group difference was found (Fig. 5.4). The hypothesis was not supported.

Hypothesis 3.3) predicted arch angle in combination with the change in navicular-to-world eversion angle measured between MS and HO, and between HO and TS as variables in a regression model would relate to vertical orientation of the first ray axis



measured between the same gait events. The relationship between arch height and first ray axis, although identified when testing cadavers ( $r = -0.73$ ),<sup>2</sup> could not be verified in subjects (Table 5.5). The hypothesis was not supported.

### **Key findings**

Collapse of the hindfoot and arch predisposes hallux valgus.<sup>5</sup> The theoretical concept here argues that deformity originates from within the foot, instead of the hallux. The premise advanced makes a paradigm shift for how the onset of deformity is currently described and treated. To investigate, imaging methods were devised to output measures of tarsal kinematics as Cardan angles and helical axis parameters.<sup>21</sup> While helical axis parameters are useful in characterizing joint rotations, the result proved challenging to describe with clinical language. Agreement was shown between first ray-navicular angles and helical axis direction cosine results and reporting both,<sup>2,4</sup> aided in the interpretation of the data.

The first ray axis was modeled using a finite helical axis (FHA) approach. Angular kinematics were initially measured on cadaver feet (Chapter III.). The study *Arch Height and First Metatarsal Joint Axis Orientation as Related Variables in Foot Structure and Function* found large variation in axis inclination among specimens, axis inclination was inversely related to arch height ( $r = -0.73$ ), and the first ray adducted when the axis inclined towards vertical. Perhaps more important, this preliminary experiment on cadavers ( $N = 9$ ) showed orientation of the first ray axis could be modeled as a direction

cosine vector. The technique had been used in previous research to quantify the orientation of the subtalar joint axis.<sup>22,23</sup>

The study continued by next measuring tarsal kinematics in subjects grouped with and without hallux valgus. Foot posture and motion were quantified from reconstructed imaged datasets with an ANOVA statistical model used to compare the kinematic variables between groups and across gait events, and multiple regression analysis used to assess arch angle and navicular eversion as predictors of vertical orientation of the first ray axis. Considering the number of hypotheses tested (and number of inter-tarsal angles measured) the write-up was broken into two research manuscripts.<sup>3,4</sup> One titled *Calcaneus and Navicular Kinematics in Subjects with Hallux Valgus*<sup>3</sup> (Chapter IV.); the other titled *First Ray Kinematics in Subjects with Hallux Valgus*<sup>4</sup> (Chapter V.).

The collective *in vivo* data was analyzed by first interpreting the hindfoot kinematics (Chapter IV.). Subjects with hallux valgus had greater ( $P < 0.05$ ) eversion of calcaneus by  $6.6^\circ$  at midstance,  $7.4^\circ$  at heel off, and  $7.9^\circ$  at terminal stance. Tanaka et al<sup>24</sup> published a similar finding. They recorded eversion of the calcaneus (in relation to the tibia) from radiographs taken on 58 consecutive patients seeking treatment for hallux valgus. The calcaneus everted  $7^\circ$  more in patients with deformity in comparison to controls ( $P < 0.01$ ). Clinicians may incorporate this result<sup>3,24</sup> when fitting orthoses or when prescribing exercises in the management of deformity.

Theory tested was that collapse of the arch inclines the first ray axis to precipitate deformity. The belief reflected the teachings of Verne Inman,<sup>25</sup> with the underlying concept supported by other primary sourced data.<sup>26-28</sup> Inman wrote that excess pronation of the subtalar joint everts the arch, shifting the ground reaction forces to the medial side of the hallux which increases the valgus moment acting across the first-metatarsophalangeal joint. My research,<sup>3</sup> however, found no group difference in arch height which caused me to again review Inman's teachings.<sup>25</sup> To clarify, Inman observed "eversion of the heel" not "flatness of the arch" as the predisposition of hallux valgus.<sup>25</sup> The difference here is subtle, because eversion of the calcaneus often manifests as a flat arch. Now in summary, I more concisely conclude that calcaneal eversion and arch height represent two distinctly different foot characteristics. Treatment aimed at slowing hallux valgus should prioritize controlling eversion of the calcaneus, not arch height.

The study next proceeded to analyze the first ray-navicular angular data on the same bone datasets.<sup>4</sup> Chapter V. tested two primary hypotheses. First, that the first ray would adduct more in hallux valgus subjects and related, the first ray axis would orient more vertical between gait events. Second, that arch angle paired with the change in navicular-to-world eversion angle (measured between gait events) would relate at level  $R^2 \geq 0.30$  to the vertical (Y component) orientation of the first ray axis measured during the same gait timing. Results demonstrated that adduction was indeed increased in the hallux valgus group, with orientation of the axis inclined  $23^\circ$  from the horizontal during middle stance as compared to  $6^\circ$  in controls. The finding gave evidence that inclination of the axis may

allow the first ray to adduct with less anatomical resistance and initiate hallux valgus deformity.

Multiple regression analysis identified no statistical significance ( $P \geq 0.68$ ) among arch angle, navicular eversion, and first ray axis relationship.<sup>4</sup> Further analysis revealed that neither arch angle nor change in navicular eversion angle were statistically different between groups. Thus when considered in combination in the regression model, there was no surprise the set of variables did not predict the Y (vertical) component axis at a significant level. Because eversion of the calcaneus was statistically different between groups ( $P < 0.05$ ),<sup>3</sup> the measure of calcaneus eversion, not arch angle, might better predict vertical orientation of the first ray axis.

Subsequent to this, a *post hoc* regression analysis was performed to examine the relationship between the eversion of calcaneus (measured with respect to the fibula at midstance) to the Y component helical axis computed from MS to HO. The linear model output  $R^2 = 0.12$ ;  $F = 2.62$ ;  $P = 0.12$ . Despite the small number of subjects tested ( $N = 20$ ), the result approached statistical significance ( $P = 0.12$ ) indicating a possible link between hindfoot posture and first ray axis orientation. Eversion of the calcaneus corresponded with increased tilt of the axis. Applied to practice, treatment aimed at controlling hindfoot eversion should keep the first ray axis from tilting vertical, and assist in limiting adduction of first ray arch segment.

Even though the *post hoc* exploratory regression analysis result trended towards significance ( $P = 0.12$ ), considerable unexplained variance ( $R^2 = 0.12$ ) remained. Because the calcaneus influences the arch by acting on the talus, individual variability in talar torsion or in alignment of the subtalar and talonavicular joints may have contributed to the unexplained variance in the model. Future study intending to investigate the strength in relationship between calcaneal eversion and first ray kinematics should describe the role of the talus, as this bone, not the calcaneus, articulates with the first ray arch segment.

### **Clinical implications**

Watchful waiting, that is what Torkki et al<sup>29</sup> called the practice of not treating hallux valgus until, eventually, the severity of impairments justified surgery. Surgery yields good results<sup>30-33</sup> although recurrence is a common complication.<sup>34</sup> Few studies, however, report outcomes on the non-operative management of hallux valgus, which explains Torkki's<sup>29</sup> decision to withhold conservative treatment during the early stages of hallux valgus progression.

Strengthening exercises<sup>35,36</sup> and orthoses<sup>29,37-39</sup> are the therapies most prescribed. A study by Schuh et al.<sup>36</sup> reported on 30 patients treated with physical therapy following the surgical correction of hallux valgus. Therapy included the strengthening of the fibularis longus. This muscle counters adduction while plantar flexing the first ray.

Correspondingly, progressing hallux valgus reduces the capacity of the fibularis longus to produce force as demonstrated in plantar pressure gait studies.<sup>40, 41</sup> Schuh<sup>36</sup> measured plantar pressures prior to surgery and 6 months later. Load carried by the hallux increased from 66 N to 87 N.<sup>36</sup> The change indicated improved weightbearing of the first ray, and the restoration of a near normal plantar pressure distribution.<sup>41</sup> A control group was not tested. Thus it is not known if therapy improved the surgical outcome.

Research<sup>29, 39, 42</sup> has investigated the use of orthoses in the management of hallux valgus. Kilmartin et al.<sup>42</sup> published the first randomized controlled trial (RCT) in 1994. They sampled 122 children aged 9 or 10 having juvenile hallux valgus. Half of the children were fit with rigid, partial contact, custom orthoses while controls received no treatment. Follow-up radiographs performed 3 years after enrollment showed the hallux angle increased most in children treated with orthoses. Compliance in wearing the orthoses was not verified, and the orthoses supposedly worn by the children for 3 years were never re-made to accommodate for the child's growth. Kilmartin's<sup>42</sup> finding that orthoses make deformity worse stands apart from all other RCT results,<sup>29, 37, 39</sup> as does his controversial choice of treating children with rigid orthoses.<sup>5, 43</sup>

More recently published randomized controlled trials<sup>29, 37, 39</sup> demonstrate good results. Budiman-Mak et al.<sup>37</sup> reported on 102 patients having rheumatoid arthritis and foot pain. Subjects receiving orthoses were 73% less likely to develop hallux valgus as compared to

a control group. Torkki et al.<sup>29, 39</sup> reported on 209 consecutive patients seeking care for symptomatic hallux valgus. Patients fit with orthoses described themselves improved on global assessment scale at year-one.<sup>29</sup> At two years, the same patients treated with orthoses were as satisfied as those having surgery, and more satisfied than controls.<sup>39</sup>

Clinicians may choose to construct orthoses and prescribe strengthening exercises to address the progressive changes in foot kinematics now identified.<sup>2-4</sup> Treatment should aim to keep the calcaneus from excessively everting which in theory, should keep the first ray axis oriented towards horizontal and optimize the truss mechanics of the arch and stabilize the first ray.<sup>2-4</sup> Orthoses offer the most immediate way to decrease eversion of the calcaneus.<sup>44, 45</sup> Custom-fit appliances constructed for the task should be inserted into supportive shoes and complimented with strength exercise.<sup>46</sup>

Strengthening treatments should ideally be prescribed control both hindfoot eversion and first ray adduction. The posterior tibialis has this potential. The muscle originates from the middle third of the tibia and interosseous membrane. Its tendon travels behind the medial malleolus making attachment to the navicular tuberosity.<sup>47-49</sup> The tendon branches distally into the cuneiforms, cuboid, the middle three metatarsals and makes shared attachment to the flexor hallucis brevis<sup>47</sup> and sometimes, onto the fibularis longus tendon at the base of the first metatarsal.<sup>48, 49</sup> While the importance of the posterior tibialis in supporting hindfoot posture has garnered attention,<sup>46, 50</sup> its relationship with

hallux valgus has never been investigated. Because of its expansive attachment into the midfoot, the posterior tibialis is ideally positioned to limit first ray loading displacements. As well, the fibularis longus should be strengthened.<sup>36</sup> Research on cadavers demonstrated the pull of the fibularis longus counters adduction of the first ray arch segment.<sup>51</sup> Based on the anatomy, exercise aimed at strengthening the posterior tibialis and fibularis longus muscles should benefit in the management of hallux valgus. Clinical research is needed.

In recommending treatment, we acknowledge that altered biomechanics are one of many factors associated with hallux valgus. Regardless, when considering the promising results documented for treating with orthoses,<sup>29, 37, 39</sup> the yet untested possible benefits of muscle strengthening exercises,<sup>35, 36</sup> and the eventual debilitating nature of hallux valgus, clinicians should not wait for deformity to worsen, but instead, should intervene early.

### **Summary**

The series of studies<sup>2-5</sup> culminated in using imaging to measure the change in kinematics associated with hallux valgus deformity. The calcaneus everted 7° more in subjects having deformity as compared to controls.<sup>3</sup> The first ray adducted 10° more in the group having hallux valgus, with orientation of the first ray axis inclined 23° during middle stance as compared to 6° in controls.<sup>4</sup> Results generally support the theory tested.

Inclination of the first ray axis may contribute to adduction of the first ray and of related



importance, eversion of the calcaneus, not flatness of the arch, was demonstrated in the subjects with deformity. Footwear/orthoses and strengthening exercises designed to keep the calcaneus from everting and the first ray segment from adducting may counteract deformity.

## References (Chapter VI.)

1. Ebisui J. The first ray axis and first metatarsophalangeal joint. *J Am Podiatr Assoc.* 1968;58(4):160-168.
2. Glasoe W, Pena F, Phadke V, Ludewig P. Arch height and first metatarsal joint axis orientation as related variables in foot structure and function: theory related to bunion. *Foot Ankle Int.* 2008;29(6):647-655.
3. Glasoe W, et al. Calcaneus and navicular kinematics in hallux valgus: a weightbearing imaging study. *TBD.* 2011:Ready for Journal Submission.
4. Glasoe W, et al. First ray kinematics in hallux valgus: a weightbearing imaging study. *TBD.* 2011:Ready for Journal Submission.
5. Glasoe W, Nuckley D, Ludewig P. Hallux valgus and the first metatarsal arch segment: a theoretical biomechanical perspective. *Phys Ther.* 2010;90:110-120.
6. Allen M, Cuddeford T, Glasoe W, et al. Relationship between static mobility of the first ray and first ray, midfoot, and hindfoot motion during gait. *Foot Ankle Int.* 2004;25(6):391-396.
7. Leardini A, Benedetti M, Berti L, Bettinelli D, Nativo R, Giannini S. Rear-foot, mid-foot and fore-foot motion during the stance phase of gait. *Gait Posture.* 2006;25:453-462.
8. Nester C, Jones R, Liu A, et al. Foot kinematics during walking measured using bone and surface mounted markers. *J Biomech.* 2007;40:3412-3423.
9. Hirsch B, Udupa J, Samarasekera S. New method of studying joint kinematics from three-dimensional reconstructions of MRI data. *J Am Podiatr Med Assoc.* 1996;86(1):4-15.
10. Ledoux W, Rohr E, Ching R, Sangeorzan B. Effect of foot shape on the three-dimensional position of the foot bones. *J Orthop Res.* 2006;24:2176-2186.
11. Mattingly B, Talwalker V, Tylkowski C, Stevens D, Hardy P, Pienkowski D. Three-dimensional in vivo motion of adult hind foot bones. *J Biomech.* 2006;39:726-733.
12. Wolf P, Stacoff A, Liu A, et al. Does a specific MR imaging protocol with a supine-lying subject replicate tarsal kinematics seen during upright standing? *Biomed Tech.* 2007;52:290-294.
13. Hunt A, Smith R, Torode M, Keenan A. Inter-segment foot motion and ground reaction forces over stance phase of walking. *Clin Biomech.* 2001;16:592-600.
14. Kidder S, Abuzzahab F, Harris G, Johnson J. A system for the analysis of foot and ankle kinematics during gait. *IEEE Trans Rehabil Eng.* 1996;4(1):25-32.
15. Cargill S, Percy M, Barry M. Three-dimensional lumbar spine postures measured by magnetic resonance imaging reconstruction. *Spine.* 2007;32:1242-1248.
16. Brown K, Bursley D, Arneson L, Andrews C, Ludewig P, Glasoe W. Consideration of digitization precision when building local coordinate axes for a foot model. *J Biomech.* 2009;42:1263-1239.

17. Lundgren P, Nester C, Liu A, et al. Invasive in vivo measurement of rear-, mid- and forefoot motion during walking. *Gait Posture*. 2008;28:93-100.
18. Nester C, Liu A, Ward E, Howard D, Cocheba J, Derrick T. Error in the description of foot kinematics due to violation of rigid body assumptions. *J Biomech*. 2010;43:666-672.
19. Canseco K, Rankine L, Long L, Smedberg T, Marks R, Harris G. Motion of the multisegmental foot in hallux valgus. *Foot Ankle Int*. 2010;31:146-152.
20. Deschamps K, Birch I, Desloovere K, Matricali G. The impact of hallux valgus on foot kinematics: A cross-sectional. *Gait Posture*. 2010;32:102-106.
21. Woltring H. Representation and calculation of 3-D joint movement. *Human Movement Science*. 1991;10:603-616.
22. Arndt A, Westblad P, Winson I, Hashimoto T, Lundberg A. Ankle and subtalar kinematics measured with intracortical pins during the stance phase of walking. *Foot Ankle Int*. 2004;25(5):357-363.
23. Engsberg J, Andrews J. Kinematic analysis of the talocalcaneal/talocrural joint during running support. *Med Sci Sports Exerc*. 1987;19(3):275-284.
24. Tanaka Y, Takakura Y, Tadashi F, Sugimoto K. Hindfoot alignment of hallux valgus evaluated by a weightbearing subtalar x-ray view. *Foot Ankle Int*. 1999;20(10):640-645.
25. Inman V. Hallux valgus: a review of etiologic factors. *Orthop Clin N Amer*. 1974;5(1):59-66.
26. Eustace S, Byrne J, Beausang O, Codd M, Stack J, Stephens M. Hallux valgus, first metatarsal pronation and collapse of the medial longitudinal arch - a radiological correlation. *Skeletal Radiol*. 1994;23:191-194.
27. Scranton P, McDermott J. Prognostic factors in bunion surgery. *Foot Ankle Int*. 1995;16(11):698-704.
28. Scranton P, Rutkowski R. Anatomic variations in the first ray: Part I. Anatomic aspects related to bunion surgery. *Clin Orthop Rel Res*. 1980;151:244-255.
29. Torkki M, Malmivaara A, Scitsalo S, Hoikka V, Laippala P, Paavolainen P. Surgery vs orthosis vs watchful waiting for hallux valgus. *J Am Med Assoc*. 2001;285:2474-2480.
30. Coetzee J, Wickum D. The Lapidus procedure: a prospective cohort outcome study. *Foot Ankle Int*. 2004;25:526-531.
31. Easley M, Trnka H. Current concepts review: hallux valgus Part 1: pathomechanics, clinical assessment, and nonoperative management. *Foot Ankle Int*. 2007;28(5):654-659.
32. Thordarson D, Ebramzadeh E, Moorthy M, Lee J, Rduicel S. Correlation of hallux valgus surgical outcomes with AOFAS forefoot score and radiological parameters. *Foot Ankle Int*. 2005;26:698-703.
33. Trnka H, Hofstaetter S, Easley M. Intermediate-term results of the Ludloff osteotomy in one hundred and eleven feet. Surgical technique. *J Bone Joint Surg Am*. 2009;1(91):Suppl 2 Pt 1:156-168.

34. Okuda R, Kinoshita M, Yasuda T, Jotoku T, Shima H, Takamura M. Hallux valgus angle as a predictor of recurrence following proximal metatarsal osteotomy. *J Orthop Sci.* 2011;Aug 5. [Epub ahead of print].
35. Groiso J. Juvenile hallux valgus. A conservative approach to treatment. *J Bone Joint Surg.* 1992;74-A:1367-1374.
36. Schuh R, Hofstaetter S, Adams S, Pichler F, Kristen K, Trnka H. Rehabilitation after hallux valgus surgery: importance of physical therapy to restore weight bearing of the first ray during the stance phase. *Phys Ther.* 2009;89(9):934-945.
37. Budiman-Mak E, Conrad K, Roach K, et al. Can foot orthoses prevent hallux valgus deformity in rheumatoid arthritis? A randomized clinical trial. *J Clin Rheumatoid.* 1995;1:313-321.
38. Kilmartin TE, Wallace WA, Hill TW. Orthotic effect on metatarsophalangeal joint extension. *J Am Podiatr Assoc.* 1991;81(8):414-417.
39. Torkki M, Malmivaara A, Seitsalo S, Hoikka V, Laippala P, Paavolainen P. Hallux valgus: immediate operation versus 1 year of waiting with and without orthoses. *Acta Orthop Scand.* 2003;74(2):209-215.
40. Kernozek T, Elfessi A, Sterriker S. Clinical and biomechanical risk factors of patients diagnosed with hallux valgus. *J Am Podiatr Med Assoc.* 2003;93(2):97-103.
41. Stokes I, Hutton W, Stott J. Forces acting on the metatarsals during normal walking. *J Anat.* 1979;129:579-590.
42. Kilmartin T, Barrington R, Wallace W. A controlled prospective trial of a foot orthosis for juvenile hallux valgus. *J Bone Joint Surg.* 1994;76-B:210-214.
43. Ferrari J, Higgins J, Prior T. Interventions for treating hallux valgus (abductovalgus) and bunions. *Cochrane Database of Systematic Reviews.* 2004;Issue 1. Art. No.:CD000964.DOI:10.1002/14651858.CD000964.pub2.
44. Davis I, Zifchock R, Deleo A. A comparison of rearfoot motion control and comfort between custom and semicustom foot orthotic devices. *J Am Podiatr Med Assoc.* 2008;98(5):394-403.
45. Zifchock R, Davis I. A comparison of semi-custom and custom foot orthotic devices in high- and low-arched individuals during walking. *Clin Biomech.* 2008;23(10):1287-1293.
46. Neville C, Flemister A, Houck J. Deep posterior compartment strength and foot kinematics in subjects with stage II posterior tibial tendon dysfunction. *Foot Ankle Int.* 2010;31(4):320-327.
47. Fernandes R, Aguiar R, Trudell D, Resnick D. Tendons in the plantar aspect of the foot: MR imaging and anatomic correlation in cadavers. *Skeletal Radiol.* 2007;36(2):115-122.
48. Sanal H, Nico M, Chen L, Haghighi P, Trudell D, Resnick D. A slip connecting the peroneus longus and tibialis posterior tendons at the forefoot: MRI, anatomic and histologic findings in a cadaver. *Diagn Interv Radiol.* 2010;10.4261/1305-3825.DIR.3996-10.2. Epub ahead of print

49. Sarrafian S. *Anatomy of the Foot and Ankle: Descriptive, Topographic, Functional*. 2 ed. Philadelphia: Lippincott. Williams and Wilkins; 1993.
50. Tome J, Flemister S, Nawoczinski D, Houck J. Comparison of foot kinematics between subjects with posterior tibial tendon dysfunction and healthy controls. *J Orthop Sport Phys Ther*. 2006;36:635-644.
51. Johnson C, Christensen J. Biomechanics of the first ray part I. The effects of peroneus longus function: a three-dimensional kinematic study on a cadaver model. *J Foot Ankle Surg*. 1999;38(5):313-321.

## REFERENCES

1. Allen M, Cuddeford T, Glasoe W, et al. Relationship between static mobility of the first ray and first ray, midfoot, and hindfoot motion during gait. *Foot Ankle Int.* 2004;25:391-396.
2. Arnett F, Edworthy S, Bloch D, McShane D, Frieo J, et al. The American Rheumatism Association 1987 revised criteria for the classification of rheumatoid arthritis. *Arthritis Rheum.* 1988;31:315-324.
3. Arndt A, Westblad P, Winson I, Hashimoto T, Lundberg A. Ankle and subtalar kinematics measured with intracortical pins during the stance phase of walking. *Foot Ankle Int.* 2004;25:357-363.
4. Barnicott N, Hardy R. The position of hallux in Western Africans. *J Anat.* 1952;89:355-361.
5. Beimers L, Tuijthof G, Blankevoort L, Jonges R, Maas M, Van Dijk C. In-vivo range of motion of the subtalar joint using computed tomography. *J Biomech.* 2008;41:1390-1397.
6. Belt E, Kaarela K, Lehto M. Destruction and arthroplasties of the metatarsophalangeal joints in seropositive rheumatoids arthritis. *Scand H Rheumatol.* 1998;27:194-196.
7. Brown K, Bursey D, Arneson L, Andrews C, Ludewig P, Glasoe W. Consideration of digitization precision when building local coordinate axes for a foot model. *J Biomech.* 2009;42:1263-1239.
8. Bryant A, Tinley P, Singer K. A comparison of radiographic measurements in normal, hallux valgus, and hallux limitus feet. *J Foot Ankle Surg.* 2000;39:39-43.
9. Budiman-Mak E, Conrad K, Roach K, et al. Can foot orthoses prevent hallux valgus deformity in rheumatoid arthritis? A randomized clinical trial. *J Clin Rheumatoid.* 1995;1:313-321.
10. Cargill S, Percy M, Barry M. Three-dimensional lumbar spine postures measured by magnetic resonance imaging reconstruction. *Spine.* 2007;32:1242-1248.

11. Carl A, Ross S, Evanski P, Waugh T. Hypermobility in hallux valgus. *Foot Ankle Int.* 1988;8:264-270.
12. Camacho D, Ledoux W, Rohr E, Sangeorzan B, Ching R. A three-dimensional, anatomically detailed foot model: a foundation for a finite element simulation and means of quantifying foot-bone position. *J Rehab Res Develop.* 2002;39:401-410.
13. Canseco K, Rankine L, Long L, Smedberg T, Marks R, Harris G. Motion of the multisegmental foot in hallux valgus. *Foot Ankle Int.* 2010;31:146-152.
14. Caselli M, George D. Foot deformities: biomechanical and pathomechanical changes associated with aging, part 1. *Clin Podiatr Med Surg.* 2003;20:487-509.
15. Coetzee J, Wickum D. The Lapidus procedure: a prospective cohort outcome study. *Foot Ankle Int.* 2004;25:526-531.
16. Cornwall M, McPoil T. Three-dimensional movement of the foot during the stance phase of walking. *J Am Podiatr Med Assoc.* 1999;89:56-66.
17. Cornwall M, McPoil T. Motion of the calcaneus, navicular, and first metatarsal during the stance phase of walking. *J Am Podiatr Med Assoc.* 2002;92:67-76.
18. Cornwall M, Fishco W, McPoil T, Lane C, O'Donnell D, Hunt L. Reliability and validity of the clinically assessing first-ray mobility of the foot. *J Am Podiatr Med Assoc.* 2004;94:470-476.
19. Coughlin M. Juvenile hallux valgus: etiology and treatment. *Foot Ankle Int.* 1995;16:682-697.
20. Coughlin M. Hallux valgus: an instructional course lecture. *J Bone Joint Surg.* 1996;78A:932-966.
21. Coughlin M. Hallux valgus in men: effect of the distal metatarsal articular angle on hallux valgus correction. *Foot Ankle Int.* 1997;18:463-470.
22. Coughlin M, Shurnas P. Hallux valgus in men part II: first ray mobility after bunionectomy and factors associated with hallux valgus deformity. *Foot Ankle Int.* 2003;24:73-78.
23. Coughlin M, Shurnas P. Hallux Rigidus: demographics, etiology, and radiographic assessment. *Foot Ankle Int.* 2003;24:731-743.

24. Coughlin M, Jones C, Viladot R, et al. Hallux valgus and first ray mobility: a cadaveric study. *Foot Ankle Int.* 2004;25:537-544.
25. Coughlin M, Saltzman C, Nunley J. Angular measurements in the evaluation of hallux valgus deformities: a report of the ad hoc committee of the American Orthopaedic Foot and Ankle Society on Angular Measurements. *Foot Ankle Int.* 2002;23:68-74.
26. Coughlin M, Jones C, Viladot R, et al. Hallux valgus and first ray mobility: a cadaveric study. *Foot Ankle Int.* 2004;25:537-544.
27. Coughlin M. *Adult Hallux Valgus.* In: Coughlin MJ, Mann RA, Saltzman CL, eds. *Surgery of the Foot and Ankle. Vol 1. 8th ed.* Philadelphia: Mosby; 2007.
28. Coughlin M, Jones C. Hallux valgus: demographics, etiology, and radiographic assessment. *Foot Ankle Int.* 2007;28:759-777.
29. D'Amico J, Schuster R. Motion of the first ray. *J Am Podiatr Assoc.* 1979;69:17-23.
30. Davis I, Zifchock R, Deleo A. A comparison of rearfoot motion control and comfort between custom and semicustom foot orthotic devices. *J Am Podiatr Med Assoc.* 2008;98:394-403.
31. Deng X, Denny T. Combined tag tracking and strain reconstruction from tagged cardiac MR images without use defined myocardial contours. *J Magn Reson Imaging.* 2005;21:12-22.
32. Deschamps K, Birch I, Desloovere K, Matricali G. The impact of hallux valgus on foot kinematics: A cross-sectional. *Gait Posture.* 2010;32:102-106.
33. Dunn J, Link C, Felson D, Crincoli M, Keysor J, McKinley J. Prevalence of foot and ankle conditions in a multiethnic community sample of older adults. *Am J Epidemiol.* 2004;159:491-498.
34. Easley M, Trnka H. Current concepts review: hallux valgus Part 1: pathomechanics, clinical assessment, and nonoperative management. *Foot Ankle Int.* 2007;28:654-659.
35. Ebisui J. The first ray axis and first metatarsophalangeal joint. *J Am Podiatr Assoc.* 1968;58:160-168.



36. Eustace S, Byrne J, Beausang O, Codd M, Stack J, Stephens M. Hallux valgus, first metatarsal pronation and collapse of the medial longitudinal arch - a radiological correlation. *Skeletal Radiol.* 1994;23:191-194.
37. Engsberg J, Andrews J. Kinematic analysis of the talocalcaneal/talocrural joint during running support. *Med Sci Sports Exerc.* 1987;19:275-284.
38. Faber F, Kleinrensink G, Mulder P, Verhaar J. Mobility of the first tarsometatarsal joint in hallux valgus patients: a radiographic analysis. *Foot Ankle Int.* 2001;22:965-969.
39. Fernandes R, Aguiar R, Trudell D, Resnick D. Tendons in the plantar aspect of the foot: MR imaging and anatomic correlation in cadavers. *Skeletal Radiol.* 2007;36:115-122.
40. Ferrari J, Higgins J, Prior T. Interventions for treating hallux valgus (abductovalgus) and bunions. *Cochrane Database of Systematic Reviews.* 2004;Issue 1.:1-124.
41. Ferrari J, Hopkinson D, Linney A. Size and shape differences between male and female foot bone. Is the female foot predisposed to hallux abducto valgus deformity? *J Am Podiatr Med Assoc.* 2004;94:434-452.
42. Ferrari J, Malone-Lee J. The shape of the metatarsal head as a cause of hallux abductovalgus. *Foot Ankle Int.* 2002;23:236-242.
43. Fritz G, Prieskorn D. First metatarsocuneiform motion: a radiographic and statistical analysis. *Foot Ankle Int.* 1995;16:117-123.
44. Glasoe W, Yack H, Saltzman C. Anatomy and biomechanics of the first ray. *Phys Ther.* 1999;79:854-859.
45. Glasoe W, Allen M, Saltzman C. First ray dorsal mobility in relation to hallux valgus deformity and first intermetatarsal angle. *Foot Ankle Int.* 2001;22:98-101.
46. Glasoe W, Allen M, Kepros T, Stonewall L, Ludewig P. Dorsal first ray mobility in women athletes with a history of stress fracture of the second or third metatarsal. *J Orthop Sports Phys Ther.* 2002;32:560-567.

47. Glasoe W, Allen M, Saltzman C, Ludewig P, Sublett S. Comparison of two methods used to assess first ray mobility. *Foot Ankle Int.* 2002;23:248-252.
48. Glasoe W, Nuckley D, Ludewig P. Hallux valgus and the first metatarsal arch segment: a theoretical biomechanical perspective. *Phys Ther.* 2010;90:110-120.
49. Glasoe W, Coughlin M. A critical analysis of Dudley Morton's concept of disordered foot function. *J Foot Ankle Surg.* 2006;45:147-155.
50. Glasoe W, Allen M, Ludewig P, Saltzman C. Dorsal mobility and first ray stiffness in patients with diabetes mellitus. *Foot Ankle Int.* 2004;25:250-555.
51. Glasoe W, Pena F, Phadke V, Ludewig P. Arch height and first metatarsal joint axis orientation as related variables in foot structure and function: theory related to bunion. *Foot Ankle Int.* 2008;29:647-655.
52. Glasoe W, et al. Calcaneus and navicular kinematics in hallux valgus: a weightbearing imaging study. *TBD.* 2011:Ready for Journal Submission.
53. Glasoe W, Nuckley D, Ludewig P. Hallux valgus and the first metatarsal arch segment: a theoretical biomechanical perspective. *Phys Ther.* 2010;90:110-120.
54. Glasoe W, et al. First ray kinematics in hallux valgus: a weightbearing imaging study. *TBD.* 2011:Ready for Journal Submission.
55. Glasoe W. Kinematic Study of Hallux Valgus Foot Deformity. *Ph.D Dissertation, Univ of Minnesota, USA.* 2011.
56. Gould N, Schneider W, Ashikaga T. Epidemiological survey of foot problems in the continental United States. *Foot Ankle.* 1980;1:8-10.
57. Grebing B, Coughlin M. The effect of ankle position on the exam for first ray mobility. *Foot Ankle Int.* 2004;25:467-475.
58. Groiso J. Juvenile hallux valgus. A conservative approach to treatment. *J Bone Joint Surg.* 1992;74-A:1367-1374.
59. Hamel A, Donahue S, Sharkey N. Contributions of active and passive toe flexion to forefoot loading. *Clin Orthop.* 2001;393:326-334.
60. Hardy R, Clapham J. Observations on hallux valgus: based on a controlled series. *J Bone Joint Surg.* 1951;33-B:376-391.

61. Hardy R, Clapham J. Hallux valgus, predisposing anatomical causes. *Lancet*. 1952;1180-1183.
62. Harris M-C, Beeson P. Generalized hypermobility: Is it a predisposing factor towards the development of juvenile hallux abducto-valgus? Part 2. *The Foot*. 1998;8:203-209.
63. Hart E, deAsla R, Grottkau B. Current concepts in the treatment of hallux valgus. *Orthop Nursing*. 2008;27:274-280.
64. Hawes M, Nachbauer W, Sovak D, Nigg B. Footprint parameters as a measure of arch height. *Foot Ankle*. 1992;13:22-26.
65. Hawke F, Burns J, Radford J, Toit V. Custom-made foot orthoses for the treatment of foot pain. *Cochrane Database of Systematic Reviews* 2008;July:1-91.
66. Hayafune N, Hayafune Y, Jacob H. Pressure and force distribution characteristics under the normal foot during the push-off phase in gait. *The Foot*. 1999;9:88-92.
67. Hicks J. The mechanics of the foot. I. The joints. *J Anat*. 1953;87:345-357.
68. Hirsch B, Udupa J, Samarasekera S. New method of studying joint kinematics from three-dimensional reconstructions of MRI data. *J Am Podiatr Med Assoc*. 1996;86:4-15.
69. Ho I, Hou Y, Yang C, Wu W, Chen S, Guo L. Comparison of plantar pressure distribution between different speed and incline during treadmill jogging. *J Sport Science Med*. 2010;9:154-160.
70. Hunt A, Smith R, Torode M, Keenan A. Inter-segment foot motion and ground reaction forces over stance phase of walking. *Clin Biomech*. 2001;16:592-600.
71. Hutton W, Dhanendran M. The mechanics of normal and hallux valgus feet: a quantitative study. *Clin Orthop Rel Res*. 1981;157:7-13.
72. Inman V. Hallux valgus: a review of etiologic factors. *Orthop Clin N Amer*. 1974;5:59-66.
73. Jacob H. Forces acting in the forefoot during normal gait - an estimate. *Clin Biomech*. 2001;16:783-792.

74. Johnson C, Christensen J. Biomechanics of the first ray part I. The effects of peroneus longus function: a three-dimensional kinematic study on a cadaver model. *J Foot Ankle Surg.* 1999;38:313-321.
75. Johnson K, Kile T. Hallux valgus due to cuneiform-metatarsal instability. *J South Orthop Assoc.* 1994;3:273-282.
76. Kalen V, Breecher A. Relationship between adolescent bunions and flatfeet. *Foot Ankle.* 1988;8:331-336.
77. Karduna A, McClure P, Michener L. Scapular kinematics: effects of altering the Euler angle sequence of rotations. *J Biomech.* 2000;33:1063-1068.
78. Kato S, Watanabe S. The etiology of hallux valgus in Japan. *Clin Orthop.* 1981;157:188-191.
79. Kelso S, Richie D, Cohen I, Weed J, Root M. Direction and range of the first ray. *J Am Podiatr Med Assoc.* 1982;72:600-605.
80. Kernozek T, Elfessi A, Sterriker S. Clinical and biomechanical risk factors of patients diagnosed with hallux valgus. *J Am Podiatr Med Assoc.* 2003;93:97-103
81. Khaw F, Mak P, Johnson G, Briggs P. Distal ligamentous restraints of the first metatarsal. An in vitro biomechanical study. *Clin Biomech.* 2005;20:653-658.
82. Kidder S, Abuzzahab F, Harris G, Johnson J. A system for the analysis of foot and ankle kinematics during gait. *IEEE Trans Rehabil Eng.* 1996;4:25-32.
83. Kilmartin T, Wallace W. First metatarsal head shape in juvenile hallux abducto valgus. *J Foot Surg.* 1991;30:506-508.
84. Kilmartin T, Barrington R, Wallace W. A controlled prospective trial of a foot orthosis for juvenile hallux valgus. *J Bone Joint Surg.* 1994;76-B:210-214.
85. Kilmartin TE, Wallace WA, Hill TW. Orthotic effect on metatarsophalangeal joint extension. *J Am Podiatr Assoc.* 1991;81:414-417.
86. Kim J, Park J, Hwang S, Young K, Sung I. Mobility changes of the first ray after hallux valgus surgery: clinical results after proximal metatarsal chevron osteotomy and distal soft tissue procedure. *Foot Ankle Int.* 2008;29:468-472.

87. Klaue K, Hansen S, Masquelet A. Clinical, quantitative assessment of first tarsometatarsal mobility in the sagittal plane and its relation to hallux valgus deformity. *Foot Ankle Int.* 1994;15:9-13.
88. LaPrade R, Bollom T, Wentorf F, Wills N, Meister K. Mechanical properties of posterolateral structures of the knee. *Am J Sports Med.* 2005;33:1386-1391.
89. Lapidus P. The operative correction of the metatarsus varus primus in hallux valgus. *Surg Gynecol Obstet.* 1934;58:183-191.
90. Leardini A, Benedetti M, Cantani F, Simoncini L, Giannini S. An anatomically based protocol for the description of foot segment kinematics during gait. *Clin Biomech.* 1999;14:528-536.
91. Leardini A, Benedetti M, Berti L, Bettinelli D, Nativo R, Giannini S. Rear-foot, mid-foot and fore-foot motion during the stance phase of gait. *Gait Posture.* 2006;25:453-462.
92. Ledoux W, Rohr E, Ching R, Sangeorzan B. Effect of foot shape on the three-dimensional position of the foot bones. *J Orthop Res.* 2006;24:2176-2186.
93. Lee K, Young K. Measurement of first-ray mobility vs. hallux valgus patients. *Foot Ankle Int.* 2001;22:960-964.
94. Lundgren P, Nester C, Liu A, et al. Invasive in vivo measurement of rear-, mid- and forefoot motion during walking. *Gait Posture.* 2008;28:93-100.
95. MacLennan R. Prevalence of hallux valgus in neolithic New Guinea population. *Lancet.* 1966;1:1398-1400.
96. Mancuso J, Abramow S, Landsman M, Waldman M, Carioscia M. The zero-plus first metatarsal and its relationship to bunion deformity. *J Foot Ankle Surg.* 2003;42:319-326.
97. Mann R, Coughlin M. Hallux valgus - etiology, anatomy, treatment, and surgical considerations. *Clin Orthop Rel Res.* 1981;157:31-41.
98. Mathieson I, Upton D, Prior T. Examining the validity of selected measures of foot type. *J Am Podiatr Med Assoc.* 2004;94:275-281.

99. Mattingly B, Talwalker V, Tylkowski C, Stevens D, Hardy P, Pienkowski D. Three-dimensional in vivo motion of adult hind foot bones. *J Biomech.* 2006;39:726-733.
100. Menz H, Morris M. Determinants of disabling foot pain in retirement village residents. *J Am Podiatr Med Assoc.* 2005;95:573-579.
101. Menz H, Munteanu S. Validity of 3 clinical techniques for the measurement of static foot posture in older people. *J Orthop Sport Phys Ther.* 2005;35:479-486.
102. Menz H, Roddy E, Thomas E, Croft P. Impact of hallux valgus severity on general and foot-specific health-related quality of life. *Arthritis Care Res.* 2011;63:396-404.
103. Milne A, Chess D, Johnson J, King G. Accuracy of an electromagnetic tracking device: a study of optimal range and metal interference. *J Biomech.* 1996;29:791-793.
104. Mueller M, Minor S, Diamond J, Blair V. Relationship of foot deformity to ulcer location in patients with diabetes mellitus. *Phys Ther.* 1990;70:356-362.
105. Myerson M. Metatarsocuneiform arthrodesis for treatment of hallux valgus and metatarsus primus varus. *Orthopedics.* 1990;13:1025-1031.
106. Nawoczenski D, Ludewig P. The effect of forefoot and arch posting orthotic designs on first metatarsophalangeal joint kinematics during gait. *J Orthop Sports Phys Ther.* 2004;34:317-327.
107. Nester C, Liu A, Ward E, et al. In vitro study of foot kinematics using a dynamic walking cadaver model. *J Biomech.* 2007;40:1927-1937.
108. Nester C, Jones R, Liu A, et al. Foot kinematics during walking measured using bone and surface mounted markers. *J Biomech.* 2007;40:3412-3423.
109. Nester C, Liu A, Ward E, Howard D, Cocheba J, Derrick T. Error in the description of foot kinematics due to violation of rigid body assumptions. *J Biomech.* 2010;43:666-672.
110. Neville C, Flemister A, Houck J. Deep posterior compartment strength and foot kinematics in subjects with stage II posterior tibial tendon dysfunction. *Foot Ankle Int.* 2010;31:320-327.

111. Okuda R, Kinoshita M, Yasuda T, Jotoku T, Shima H, Takamura M. Hallux valgus angle as a predictor of recurrence following proximal metatarsal osteotomy. *J Orthop Sci.* 2011;Aug 5. [Epub ahead of print].
112. Oldenbrook L, Smith C. Metatarsal head motion secondary to rearfoot pronation and supination. *J Am Podiatr Assoc.* 1979;69:24-28.
113. Piazza S, Cavanagh P. Measurement of the screw-home motion of the knee is sensitive to errors in axis alignment. *J Biomech.* 2000;33:1029-1034.
114. Pohl M, Messenger N, Buckley J. Forefoot, rearfoot and shank coupling: effect of variations in speed and mode of gait. *Gait Posture.* 2006;25:1-8.
115. Rattanaprasert U, Smith R, Sullivan M, Gilleard W. Three-dimensional kinematics of the forefoot, rearfoot, and leg without function of tibialis posterior in comparison with normals during stance phase of walking. *Clin Biomech.* 1999;14:14-23.
116. Robinson A, Limbers J. Modern concepts in the treatment of hallux valgus. *J Bone Joint Surg.* 2005;87-B:1038-1045.
117. Romash M, Fugate D, Yanklowit B. Passive motion of the first metatarsal cuneiform joint: preoperative assessment. *Foot Ankle.* 1990;10:293-298.
118. Ross-Smith N. Hallux valgus and rigidus treated by arthrodesis of the metatarsophalangeal joint. *Br Med J.* 1952;2:1385-1387.
119. Roukis T, Landsman A. Hypermobility of the first ray: a critical review of the literature. *J Foot Ankle Surg.* 2003;42:377-390.
120. Roukis T, Weil LJ, Weil LS, Landsman A. Predicting articular erosion in hallux valgus: clinical, radiographic, and intraoperative analysis. *J Foot Ankle Surg.* 2005;44:13-21.
121. Saltzman C, Brandser E, Berbaum K, et al. Reliability of standard foot radiographic measurements. *Foot Ankle Int.* 1994;15:661-665.
122. Saltzman C, Nawoczenski D, Talbot K. Measurement of the medial longitudinal arch. *Arch Phys Med Rehabil.* 1995;76:45-49.
123. Saltzman CL, Nawoczenski DA. Complexities of foot architecture as a base of support. *J Orthop Sports Phys Ther.* 1995;21:354-360.

124. Saltzman CL, Brandser EA, Anderson BS, Berbaum KS, Brown TD. Coronal plane rotation of the first metatarsal. *Foot Ankle*. 1996;17:157-161.
125. Saltzman C, Aper R, Brown T. Anatomic determinants of first metatarsophalangeal flexion moments in hallux valgus. *Clin Orthop*. 1997;339:261-269.
126. Sanal H, Nico M, Chen L, Haghighi P, Trudell D, Resnick D. A slip connecting the peroneus longus and tibialis posterior tendons at the forefoot: MRI, anatomic and histologic findings in a cadaver. *Diagn Interv Radiol*. 2010;10.4261/1305-3825.DIR.3996-10.2. Epub ahead of print
127. Sarrafian SK. Functional characteristics of the foot and plantar aponeurosis under tibiotalar loading. *Foot Ankle*. 1987;8:4-18.
128. Sarrafian S. *Anatomy of the Foot and Ankle: Descriptive, Topographic, Functional*. 2 ed. Philadelphia: Lippincott. Williams and Wilkins; 1993.
129. Sangeorzan B, Hansen S. Modified Lapidus procedures for hallux valgus. *Foot Ankle Int*. 1989;9:262-266.
130. Sanders A, Snijders C, Linge B. Medial deviation of the first metatarsal head as a result of flexion forces in hallux valgus. *Foot Ankle Int*. 1992;13:515-522.
131. Schoenhaus H, Cohen R. Etiology of the bunion. *J Foot Ankle Surg*. 1992;31:25-29.
132. Schuh R, Hofstaetter S, Adams S, Pichler F, Kristen K, Trnka H. Rehabilitation after hallux valgus surgery: importance of physical therapy to restore weight bearing of the first ray during the stance phase. *Phys Ther*. 2009;89:Epub ahead of print.
133. Scott G, Wilson D, Bently G. Roentgenographic assessment in hallux valgus. *Clin Orthop*. 1991;267:143-147.
134. Scranton P, Rutkowski R. Anatomic variations in the first ray: Part I. Anatomic aspects related to bunion surgery. *Clin Orthop Rel Res*. 1980;151:244-255.
135. Scranton P. Adolescent bunions: diagnosis and management. *Pediatr Ann*. 1982;11:518-520.
136. Scranton P, McDermott J. Prognostic factors in bunion surgery. *Foot Ankle Int*. 1995;16:698-704.



137. Sim-Fook. A comparison of foot forms among the non-shoe and shoe-wearing Chinese people. *J Bone Joint Surg.* 1958;40A:1058-1062.
138. Shereff M. Pathology, anatomy and biomechanics of hallux valgus. *Orthopaedics.* 1990;13:939-945.
139. Small C, Pichora D, Bryant J, Griffiths P. Precision and accuracy of bone landmarks in characterizing hand and wrist positions. *J Biomed Eng.* 1993;15:371-378.
140. Snijder C, Snijder J, Philippens M. Biomechanics of hallux valgus and spread foot. *Foot Ankle.* 1986;7:26-39.
141. Spruce M, Bowling F, Metcalfe S. A longitudinal study of hallux valgus surgical outcomes using a validated patient centered outcome measure. *Foot (Edinb)* 2011 Feb 11. [Epub ahead of print].
142. Stindel E, Udupa J, Hirsch B, Odhner D. A characterization of the geometric architecture of the peritalar joint complex via MRI: an aid to classification of foot type. *IEEE Trans. Med. Imag.* 1999;18:753-762.
143. Stokes I, Hutton W, Stott J. Forces acting on the metatarsals during normal walking. *J Anat.* 1979;129:579-590.
144. Tabachnick B, Fidell L. *Using Multivariate Statistics.* 5th ed. Boston: Pearson Education; 2007.
145. Takane Y, Hwang H. Generalized constrained canonical correlation analysis. *Multivariate Behav Res.* 2002;37:163-195.
146. Talbot K, Saltzman C. Hallucal rotation: a method of measurement and relationship to bunion deformity. *Foot Ankle Int.* 1997;18:550-556.
147. Tanaka Y, Takakura Y, Sugimoto K, Kumai T, Sakamoto T, Kadono K. Precise anatomic configuration changes in the first ray of the hallux valgus. *Foot Ankle Int.* 2000;21:651-656.
148. Thompson F, Coughlin M. The high price of high-fashion footwear. *J Bone Joint Surg.* 1994;10A:1586-1593. Truslow W. Metatarsus primus varus or hallux valgus? *J Bone Joint Surg.* 1925;7:98-108.

149. Thordarson DB, Schmotzer H, Chon J, Peters J. Dynamic support of the human longitudinal arch. *Clin Orthop Rel Res.* 1995;316:165-172.
150. Thordarson D, Ebramzadeh E, Moorthy M, Lee J, Rduicel S. Correlation of hallux valgus surgical outcomes with AOFAS forefoot score and radiological parameters. *Foot Ankle Int.* 2005;26:698-703.
151. Tome J, Flemister S, Nawoczinski D, Houck J. Comparison of foot kinematics between subjects with posterior tibial tendon dysfunction and healthy controls. *J Orthop Sport Phys Ther.* 2006;36:635-644.
152. Torkki M, Malmivaara A, Scitsalo S, Hoikka V, Laippala P, Paavolainen P. Surgery vs orthosis vs watchful waiting for hallux valgus. *J Am Med Assoc.* 2001;285:2474-2480.
153. Torkki M, Malmivaara A, Seitsalo S, Hoikka V, Laippala P, Paavolainen P. Hallux valgus: immediate operation versus 1 year of waiting with and without orthoses. *Acta Orthop Scand.* 2003;74:209-215.
154. Turner D, Woodburn J, Helliwell P, Cornwall M, Emery P. Pes planovalgus in rheumatoid arthritis: a descriptive and analytical study of foot function determined by gait analysis. *Musculoskeletal Care.* 2003;1:21-33.
155. Turner D, Helliwell P, Lohmann Siegel K, Woodburn J. Biomechanics of the foot in rheumatoid arthritis: identifying abnormal function and the factors associated with localized disease 'impact'. *Clin Biomech.* 2008;23:93-100.
156. Trnka H, Hofstaetter S, Easley M. Intermediate-term results of the Ludloff osteotomy in one hundred and eleven feet. Surgical technique. *J Bone Joint Surg Am.* 2009;1:Suppl 2 Pt 1:156-168.
157. Tuijthof G, Zengerink M, Beimers L, et al. Determination of consistent patterns of range of motion in the ankle joint with a computed tomography stress-test. *Clin Biomech.* 2009;24:517-523.
158. Uchiyama E, Kitaoka H, Luo Z, Grande J, Kura H, An K. Pathomechanics of hallux valgus: biomechanical and immunohistochemical study. *Foot Ankle Int.* 2005;26:732-738.

159. Umberger B, Nawoczenski D, Baumhauer J. Reliability and validity of first metatarsophalangeal joint orientation measured with an electromagnetic tracking device. *Clin Biomech.* 1999;14:74-76.
160. Viladot A. Metatarsalgia due to biomechanical alterations of the forefoot. *Orthop Clin N Am.* 1973;4:165-178.
161. Valderrabano V, Hintermann B, Nigg B, Stefanyshyn P. Kinematic changes after fusion and total replacement of the ankle part 1: range of motion. *Foot Ankle Int.* 2003;24:881-887.
162. Waldecker U. Pedographic analysis of hallux valgus deformity. *Foot Ankle Surg.* 2004;10:121-124.
163. Wanivenhaus A, Pretterklieber M. First tarsometatarsal joint: anatomical biomechanical study. *Foot Ankle Int.* 1989;9:153-157.
164. Wearing S, Urry S, Pearlman P, Smeathers J, Dubois P. Sagittal plane motion of the human arch during gait: a videofluoroscopic analysis. *Foot Ankle Int.* 1998;19:738-742.
165. Wearing S, Urry S, Pearlman P, Dubois P, Smeathers J. Serial measurement of calcaneal pitch during midstance. *J Am Podiatr Med Assoc.* 1999;89:188-193.
166. Wearing S, Smeathers J, Sullivan P, Yates B, Urry S, Dubois P. Plantar fasciitis: are pain and fascial thickness associated with arch shape and loading. *Phys Ther.* 2007;87:1002-1008.
167. Wilken J, Rao S, Saltzman C, Yack H. The effect of arch height on kinematic coupling during walking. *Clin Biomech.* 2011;26:318-323.
168. Wu G, Siegler S, Allard P, et al. ISB recommendation on definitions of joint coordinate system of various joints for the reporting of human joint motion--part I: Ankle, hip, and spine. *J Biomech.* 2002;35:543-548.
169. Wolf P, Stacoff A, Liu A, et al. Functional units of the human foot. *Gait Posture.* 2008;28:434-431.

170. Wolf P, Stacoff A, Liu A, et al. Does a specific MR imaging protocol with a supine-lying subject replicate tarsal kinematics seen during upright standing? *Biomed Tech.* 2007;52:290-294.
171. Wolff K, Wicks A, Shaw A, Smith J, Ludewig P, Glasoe W. Clinical measurement correlates of the first metatarsal axis leading to intervention strategies for hallux valgus. *Foot Ankle Int.* 2010:In Review.
172. Woltring H. Representation and calculation of 3-D joint movement. *Human Movement Science.* 1991;10:603-616.
173. Woltring H. 3-D attitude representation of human joints: a standardization proposal. *J Biomech.* 1994;27:1399-1414.
174. Woodburn J, Nelson K, Siegel K, Kepple T, Gerber L. Multisegment foot motion during gait: proof of concept in rheumatoid arthritis. *J Rheumatol.* 2004;31:1918-1927.
175. Zatsiorsky V. *Kinematics of Human Motion:* Human Kinetics; 1998.
176. Zifchock R, Davis I. A comparison of semi-custom and custom foot orthotic devices in high- and low-arched individuals during walking. *Clin Biomech.* 2008;23:1287-1293.

## APPENDIX 1

### Introduction

**Appendix 1. *Introduces*** the experiments or analysis conducted to support the research.

**Appendix 2. *Measurement Error Experiments*** detailed experiments that quantified the collective errors of measuring tarsal kinematics from MR imaged data. Two experiments quantified the error of using MIMICS to reconstruct and register bone models; one experiment explored the degree to which the subject's foot or wedge deformed.

**2.1. *Image Processing Basic Error:*** The experiment quantified the error in measuring the orientation of a bone embedded with its own coordinate frame. This error represented the minimum error of measuring the orientation of any bone in the MR reference.

**2.2. *Image Processing Bone-on-Bone Angle Error:*** The experiment quantified the error of measuring bone-on-bone angles across registered datasets.

**2.3. *Error: Foot or Wedge Deformation:*** The experiment quantified the change in position of the navicular measured from repeated images (Time 1 vs. Time 2) taken while the subject stood for 6 minutes on a wedge for scanning.

**Appendix 3. *Foot Loading Experiment:*** The experiment measured the forces distributed beneath the foot while the subject stood to simulate the progression of gait (MS, HO, TS) foot postures.

**Appendix 4. *Influence of Body Weight on First Ray Kinematics:*** This additional data analysis explored the relationship between body weight and first ray kinematics.

## APPENDIX 2

### Measurement Error Experiments

#### 2.1. Image Processing Basic Error

The error in measuring an object in the MR reference was quantified, and was considered the minimum error involved in measuring the orientation of any single bone. Thus the result could be thought as the accuracy of the measurement.

**Methods:** The navicular was segmented different times on the same scan. The location of the coordinate frame centroid (Table A.1) and axes orientations were extracted. Navicular 1 was imported as a bone.stl file and superimposed on Navicular 2 by computer registration. The computer output a transformation matrix (Table A.2) that expressed the change in orientation between the bone objects.

**Table A.1.** Navicular Centroid Positions

|                    | Z            | Y             | X             |
|--------------------|--------------|---------------|---------------|
| <b>Navicular 1</b> | 34.79        | 146.42        | 125.39        |
| <b>Navicular 2</b> | <u>34.79</u> | <u>146.38</u> | <u>125.52</u> |
| <b>Difference</b>  | 0.00         | 0.04          | 0.13          |

**Table A.2.** Registration Matrix.

|        |        |       |        |
|--------|--------|-------|--------|
| 1.000  | 0.000  | 0.005 | -0.230 |
| 0.001  | 1.000  | 0.006 | 0.255  |
| -0.005 | -0.006 | 1.000 | 1.400  |
| 0.000  | 0.000  | 0.000 | 1.000  |

**Analysis:** A two step analysis was performed: Step 1. Reconstruction error (plus coordinate frame extraction error) was computed by matrix transformation to determine the difference in angulation of the two navicular coordinate frame axes (Z, Y, X). Step 2. Registration error between the two navicular coordinate frames was decomposed from the 4 X 4 registration matrix (Table 2) using a method of matrix transformation.

**Results:** Step 1. Analysis found difference in angulation Z, Y, X axes of 0.16°, 0.93°, 1.45°, respectively. Step 2. Analysis found difference in the two navicular coordinate frames angulation Z, Y, X axes to be 0.33°, 0.03°, and 0.28°, respectively.

**Conclusion:** Reconstruction error was  $\leq 1.45^\circ$ . Registration error was  $\leq 0.33^\circ$ . The errors could potentially sum together ( $\leq 1.78^\circ$ ) in a worst case when measuring the orientation of any single bone.<sup>1</sup>

## 2.2. Image Processing Bone-on-Bone Angle Error

The error associated with measuring bone-on-bone angles from a sequence of MR scanned time instances was evaluated.<sup>1,2</sup>

**Methods:** The bone datasets (MS, HO, TS) of one subject were reconstructed in advance. From the bone datasets, three trials of first ray-navicular<sup>3</sup> and calcaneus-fibula<sup>4</sup> angles were computed across gait events (Table A.3). Of related importance, MIMICS derived a root mean square (RMS) value to record the difference in the outer-edge fit in the bone.stl files registered within, and between gait events.<sup>1,5,6</sup> A  $\leq 1.00$  mm RMS difference in surface fit was targeted as the acceptable level of precision for registration.

**Results:** The RMS values were the same across trials (Table A.3), whereas the bone angles did compute differently. The largest difference was found in the transverse plane calcaneus-fibula angle ( $2.10^\circ$ ) at HO. This angle measured  $-22.4^\circ$ ,  $-22.7^\circ$ , and  $-24.5^\circ$  across Trials.

**Discussion:** The same RMS (surface fit difference) value indicates the computer auto-registration procedure was highly reliable. The measurement of bone-on-bone angles, however, which involved the operations of extracting the coordinate frame location followed by computer registration, produced different angles between trials. The largest difference in angles was  $\leq 2.10^\circ$ . Therefore, we conservatively estimate the difference in angles to be  $\leq 3^\circ$ . Three degrees is the error amount reported in other Kinematics Imaging studies.<sup>1,6</sup>

**Conclusion:** The overall image data processing error for this study was  $\leq 3^\circ$ .

**Table A.3.** Registration closeness-of-fit rms (mm) and angles (°) computed for the first ray-navicular (FR-Nav) and calcaneus-fibula (Cal-Fib) joint segments.

**Trial 1**

**Registration: A) RMS output of anatomical fit; B) RMS output of auto-registration fit.**

| Midstance (MS) |      |      | Heel Off (HO) |      |      | Terminal Stance (TS) |      |      |
|----------------|------|------|---------------|------|------|----------------------|------|------|
| Bones          | A)   | B)   | Bones         | A)   | B)   | Bones                | A)   | B)   |
| First Ray      | 0.51 | 0.51 | First Ray     | 1.30 | 1.30 | First Ray            | 0.88 | 0.88 |
| Navicular      | 0.46 | 0.46 | Navicular     | 0.95 | 0.95 | Navicular            | 0.95 | 0.95 |
| Calcaneus      | 0.47 | 0.47 | Calcaneus     | 0.67 | 0.67 | Calcaneus            | 1.32 | 1.32 |
| Fibula         | 0.54 | 0.54 | Fibula        | 1.00 | 0.93 | Fibula               | 1.84 | 1.84 |

**Angles (°) computed in body planes at gait events.**

| Transverse (Y Axis) |       |       |       | Sagittal (Z Axis) |      |       |       | Frontal (X Axis) |       |       |      |
|---------------------|-------|-------|-------|-------------------|------|-------|-------|------------------|-------|-------|------|
| Segments            | MS    | HO    | TS    | Segments          | MS   | HO    | TS    | Segments         | MS    | HO    | TS   |
| FR-Nav              | 9.0   | 8.9   | 8.9   | FR-Nav            | -9.2 | -15.3 | -14.3 | FR-Nav           | -9.46 | 21.6  | 18.8 |
| Cal-Fib             | -24.2 | -22.4 | -21.8 | Cal-Fib           | 16.3 | 7.9   | -21.1 | Cal-Fib          | -20.8 | -14.8 | -1.6 |

**Trial 2**

**Reconstruction: A) RMS output of anatomical fit; B) RMS output of auto-registration fit.**

| Midstance (MS) |      |      | Heel Off (HO) |      |      | Terminal Stance (TS) |      |      |
|----------------|------|------|---------------|------|------|----------------------|------|------|
| Bones          | A)   | B)   | Bones         | A)   | B)   | Bones                | A)   | B)   |
| First Ray      | 0.51 | 0.51 | First Ray     | 1.30 | 1.30 | First Ray            | 0.88 | 0.88 |
| Navicular      | 0.46 | 0.46 | Navicular     | 0.95 | 0.95 | Navicular            | 0.95 | 0.95 |
| Calcaneus      | 0.47 | 0.47 | Calcaneus     | 0.67 | 0.67 | Calcaneus            | 1.32 | 1.32 |
| Fibula         | 0.54 | 0.54 | Fibula        | 1.00 | 0.93 | Fibula               | 1.84 | 1.85 |

**Angles (°) computed in body planes at gait events.**

| Transverse (Y Axis) |       |       |       | Sagittal (Z Axis) |      |       |       | Frontal (X Axis) |       |       |      |
|---------------------|-------|-------|-------|-------------------|------|-------|-------|------------------|-------|-------|------|
| Segments            | MS    | HO    | TS    | Segments          | MS   | HO    | TS    | Segments         | MS    | HO    | TS   |
| FR-Nav              | 9.0   | 8.9   | 8.9   | FR-Nav            | -9.2 | -15.3 | -14.3 | FR-Nav           | -9.46 | 21.6  | 18.8 |
| Cal-Fib             | -24.2 | -22.7 | -21.8 | Cal-Fib           | 16.3 | 7.7   | -21.1 | Cal-Fib          | -20.8 | -15.6 | -1.6 |

**Trial 3**

**Reconstruction: A) RMS output of anatomical fit; B) RMS output of auto-registration fit.**

| Midstance (MS) |      |      | Heel Off (HO) |      |      | Terminal Stance (TS) |      |      |
|----------------|------|------|---------------|------|------|----------------------|------|------|
| Bones          | A)   | B)   | Bones         | A)   | B)   | Bones                | A)   | B)   |
| First Ray      | 0.51 | 0.51 | First Ray     | 1.30 | 1.30 | First Ray            | 0.88 | 0.88 |
| Navicular      | 0.46 | 0.46 | Navicular     | 0.95 | 0.95 | Navicular            | 0.95 | 0.95 |
| Calcaneus      | 0.47 | 0.47 | Calcaneus     | 0.67 | 0.67 | Calcaneus            | 1.32 | 1.32 |
| Fibula         | 0.54 | 0.54 | Fibula        | 1.00 | 0.93 | Fibula               | 1.84 | 1.84 |

**Angles (°) computed in body planes at gait events.**

| Transverse (Y Axis) |       |       |       | Sagittal (Z Axis) |      |       |       | Frontal (X Axis) |       |       |      |
|---------------------|-------|-------|-------|-------------------|------|-------|-------|------------------|-------|-------|------|
| Segments            | MS    | HO    | TS    | Segments          | MS   | HO    | TS    | Segments         | MS    | HO    | TS   |
| FR-Nav              | 9.0   | 8.9   | 8.9   | FR-Nav            | -9.2 | -15.3 | -14.3 | FR-Nav           | -9.46 | 21.6  | 18.8 |
| Cal-Fib             | -24.2 | -24.5 | -21.8 | Cal-Fib           | 16.3 | 9.0   | -21.1 | Cal-Fib          | -20.8 | -16.2 | -1.6 |



### 2.3. Error: Foot or Wedge Deformation

Repeated scans of the navicular were acquired to assess whether the subject's foot or the wedge deformed during scanning.

**Methods:** The navicular, located at the center of the arch (making it the bone most likely to move should the foot or wedge deform under load) was imaged two times consecutively on a single subject. The foot was positioned in HO (Time 1 vs. Time 2) using a 3 minute scanning protocol. Only 3 minutes were needed to scan the navicular.

- The difference between the centroid of the navicular coordinate frames was computed as a linear distance with the equation:  

$$\sqrt{\sum [(Z_{T1} - Z_{T2})^2 + (Y_{T1} - Y_{T2})^2 + (X_{T1} - X_{T2})^2]}$$
- The difference in angulation of the coordinate frame was computed using a Matrix transformation.

**Table A.4.** Centroid of Navicular (mm). **Table A.5.** Difference in Axis Angulation (°)

|                   | Z     | Y      | X      |                         | Z     | Y    | X     |
|-------------------|-------|--------|--------|-------------------------|-------|------|-------|
| <b>Time 1</b>     | 34.79 | 146.42 | 125.39 | <b>Time 1</b>           | *     | *    | *     |
| <b>Time 2</b>     | 34.78 | 146.39 | 125.61 | <b>Time 2</b>           | *     | *    | *     |
| <b>Difference</b> | 0.01  | 0.03   | 0.22   | <b>Difference</b>       | -0.16 | 0.79 | -0.25 |
|                   |       |        |        | * Transformation Matrix |       |      |       |

**Results:** Time 1 and Time 2 coordinate frame centroids of the reconstructed bones differed by 0.22 mm. Navicular (Time 1 and Time 2) coordinate frame Z, Y, X axes angulation differed by 0.16°, 0.79°, 0.25°, respectively (Table A.4).

**Discussion:** The difference in navicular position between the Time 1 and Time 2 was ≤ 0.22 mm for translation and ≤ 0.79° for rotation (Tables A.4 and A.5). If the navicular changed its orientation when the foot was scanned for 6 minutes, the amount it moved was less than 1.78°.

**Conclusion** This amount was determined (in a previous experiment) the accuracy of using MIMICS to measure the orientation of any joint angle.

## APPENDIX 3

### Foot Loading Experiment

This experiment measured the loading between the foot and ground while subjects stood in a research laboratory to reproduce the gait event of MS, HO, and TS (Fig. A.1). The aims of the experiment were to quantify the load carried by the first ray, as well as the foot GRF and center-of-pressure (CoP) at each gait event.

**Methods:** Five subjects were tested (Table A.6). All had participated in the larger study. They stood to replicate the gait events. The foot postures were MS, HO, and TS. Figure 1 shows how TS was replicated. The subject stood with her weight distributed equally on both feet. Only the data collected on the right foot was analyzed. Measures were made with the PEDAR system (Novel Inc., St Paul, MN, USA), and with a force plate (Bertec Corp., Columbus, OH, USA). The PEDAR is a capacitive sensor insole that yields the vertical load distribution of plantar pressures. The pressure data was matched to 8 separate masks which are areas of the foot (Fig. A.2).<sup>7</sup> Additional measurements were made with the force plate. These were 3D ground reaction forces (Fig. A.3) and CoP. Because the foot was positioned in a known location on the force plate, the CoP registered on the force plate was inferred to the foot (Fig. A.4). Three seconds of static loading data were collected on each subject at each gait event (MS, HO, TS). Both the PEDAR system and the force plate sampled data at 90 Hz.

**Analysis:** A single instant of the loading measurements was selected from the stream of data for analysis. The data analyzed was observed to best represent a stable measure of static foot loading. A descriptive analysis was performed, with the mean (SD) data reported. Mask M04 (Fig. A.2) captured the plantar pressure borne by the first ray expressed as a percent of load carried by the right foot. Force plate GRFs were reported as N of force (Fig. A.3.A) and as percent body load (Fig. A.3.B). CoP was mapped upon a foot-print scaled to represent the foot of all subjects (Fig A.4).

**Results:** The PEDAR plantar pressure data are presented in Table 6. Pressures were distributed across the foot. The heel (M01) carried most of the load, with the first ray carrying an average 11%, 9%, and 19% of the foot pressures at gait MS, HO, and TS, respectively. The GRF group means ( $n = 5$ ) are displayed in Figure 3. In addition to reporting GRF in Newtons (N), the data was normalized to the subject's weight (Fig. A.3.B). The right foot carried half of total body weight. The direction of loading was mostly vertical, and the pattern of the forces was similar between and across gait events. Foot CoP was located in the midfoot at each gait event (Fig. A.4).

**Discussion:** Plantar pressures were highest beneath the first ray at TS (Table A.6). Greater than 90% of the load was directed vertically. Regardless of the gait event, foot CoP was located near the navicular. Since the navicular itself did not contact the ground,

the location of CoP indicates the arch carried significant load. My method of simulating gait postures while the subject stood in the scanner did not replicate the kinetics of gait. Listed are the primary differences. First, the load carried by the foot was half of body weight (Fig. A.3). Second, the directions of the GRFs stayed nearly constant across gait events with the heel supporting no less than 32% body weight load. Finally, foot CoP remained in the medial midfoot, and it did not track forward during our progression of simulated gait events (Fig. A.4). Though kinematics measured were comparable to the data collected in gait trials,<sup>8-10</sup> the loading forces were unique to this study.

**Table A.6.** Mean (SD) planter pressures collected. Measures were made with the subject standing to replicate the midstance (MS), heel off (HO), and terminal stance (TS) gait events. Data are reported as % load carried at the 8 masks. The location and area of the identified masks are shown in Fig. A.2.

| <b>MIDSTANCE</b> |            |           |          |                          |            |            |          |          |        |
|------------------|------------|-----------|----------|--------------------------|------------|------------|----------|----------|--------|
| ID               | M01        | M02       | M03      | <b>M04</b>               | M05        | M06        | M07      | M08      | % Load |
| C03-MS           | 23         | 19        | 0        | 3                        | 28         | 27         | 0        | 0        | 100    |
| C06-MS           | 32         | 0         | 0        | 4                        | 22         | 39         | 3        | 0        | 100    |
| C07-MS           | 27         | 0         | 0        | 15                       | 17         | 37         | 4        | 0        | 100    |
| C11-MS           | 76         | 0         | 0        | 14                       | 4          | 5          | 0        | 0        | 100    |
| B02-MS           | 21         | 0         | 0        | 18                       | 29         | 18         | 14       | 0        | 100    |
| Mean             | 36<br>(23) | 4<br>(8)  | 0        | <b>11</b><br><b>(7)</b>  | 20<br>(10) | 25<br>(14) | 4<br>(6) | 0        | 100    |
| <b>HEELOFF</b>   |            |           |          |                          |            |            |          |          |        |
| ID               | M01        | M02       | M03      | M04                      | M05        | M06        | M07      | M08      | % Load |
| C03-HO           | 49         | 22        | 4        | 2                        | 11         | 7          | 0        | 4        | 100    |
| C06-HO           | 48         | 15        | 3        | 3                        | 15         | 13         | 3        | 1        | 100    |
| C07-HO           | 46         | 12        | 1        | 4                        | 12         | 20         | 5        | 1        | 100    |
| C11-HO           | 58         | 6         | 0        | 20                       | 10         | 0          | 1        | 4        | 100    |
| B02-HO           | 39         | 10        | 4        | 15                       | 8          | 7          | 17       | 1        | 100    |
| Mean             | 48<br>(7)  | 13<br>(6) | 2<br>(2) | <b>9</b><br><b>(8)</b>   | 11<br>(2)  | 9<br>(7)   | 5<br>(7) | 2<br>(2) | 100    |
| <b>TERMINAL</b>  |            |           |          |                          |            |            |          |          |        |
| ID               | M01        | M02       | M03      | M04                      | M05        | M06        | M07      | M08      | % Load |
| C03-TS           | 50         | 13        | 2        | 6                        | 13         | 7          | 2        | 7        | 100    |
| C06-TS           | 4          | 6         | 0        | 23                       | 28         | 17         | 6        | 16       | 100    |
| C07-TS           | 25         | 10        | 0        | 6                        | 22         | 23         | 11       | 2        | 100    |
| C11-TS           | 30         | 5         | 2        | 35                       | 17         | 4          | 3        | 3        | 100    |
| B02-TS           | 53         | 7         | 8        | 25                       | 0          | 1          | 6        | 2        | 100    |
| Mean             | 32<br>(20) | 8<br>(3)  | 2<br>(3) | <b>19</b><br><b>(13)</b> | 16<br>(11) | 11<br>(9)  | 6<br>(3) | 6<br>(6) | 100    |

MO4 (bolded in middle of graph) gives the percent of load carried by the first metatarsal.

**Figures** (all figures referred to in Appendix 3)

**Fig. A.1** Shows terminal stance (TS) data collection positioning. The subject stood on PEDAR insoles and force plates. Subjects knelt into the examiner's hands to replicate how they leaned against a bolster while standing in the scanner.

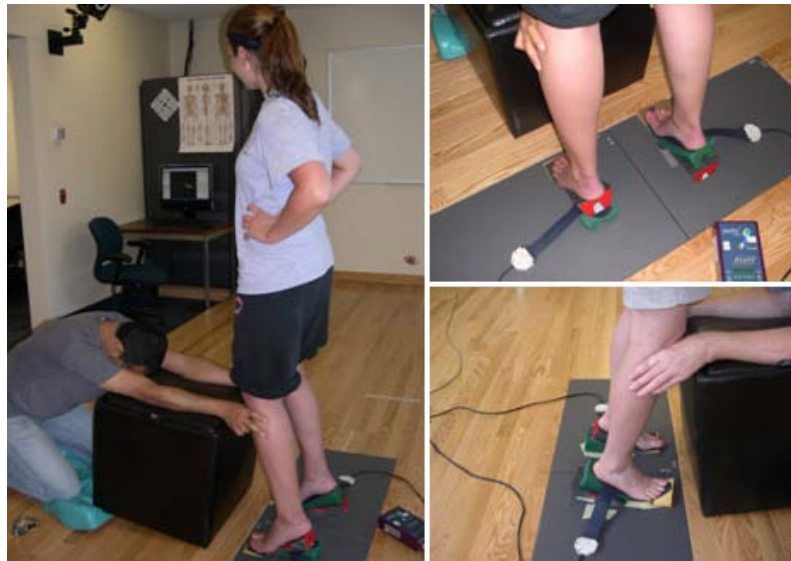


**Fig. A.2** Plantar Pressure Distributions: **A.** Masks (areas) of the foot defined for plantar pressure analysis. **B.** Shows the PEDAR computer screen-shot of pressure data collected on a subject at terminal stance (TS).

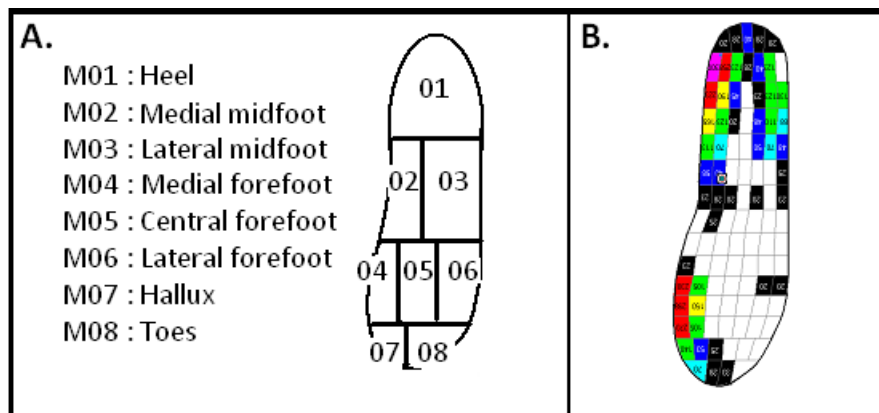


**Fig. A.3** Bar graphs data showing mean (N = 5) ground reaction forces. Data collected on the right foot were analyzed at each gait events. **Graph A.** displays data in units of force. **Graph B.** shows the same data as percent body weight. Error bars are standard deviations.

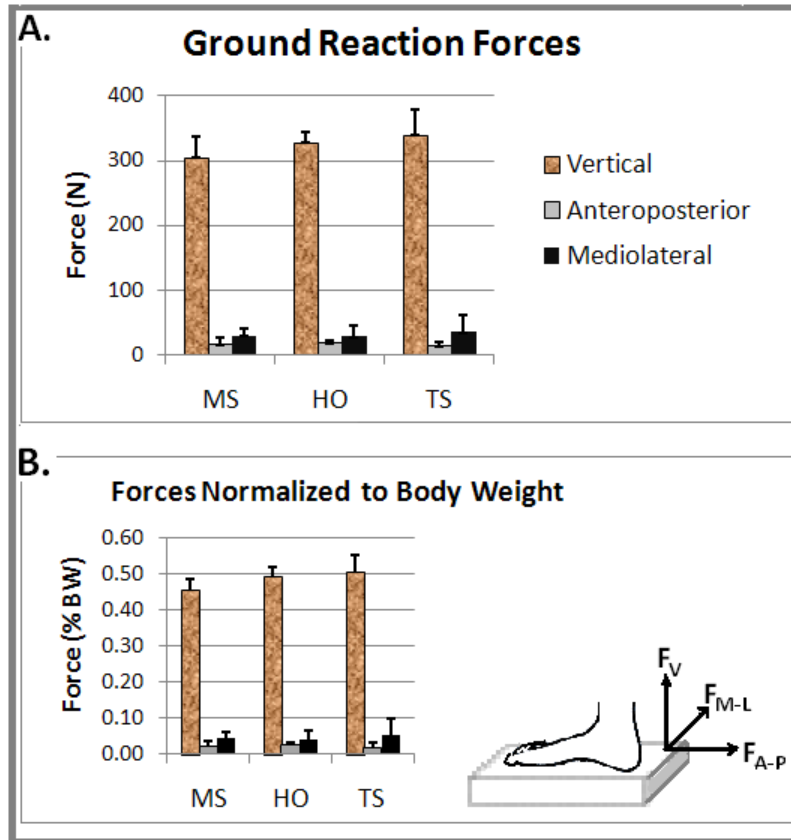
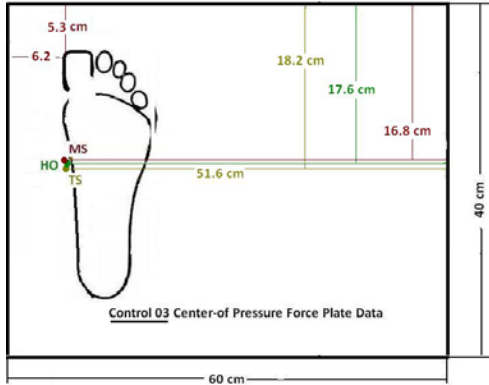
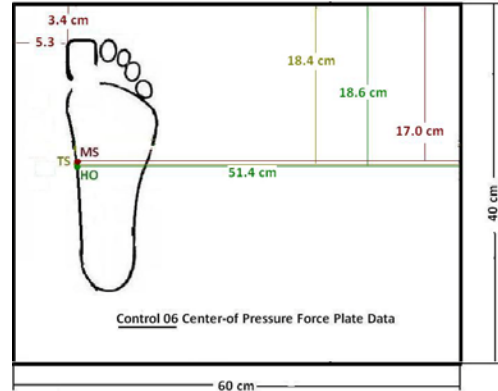


**Fig. A.4** Subject center of pressures (CoP) for the right foot (N = 5) calculated at MS, HO, and TS. CoP measured in reference to the upper right corner of the force plate. Foot location measured in reference upper left corner of the plate. Note: distances shown are not drawn to scale.

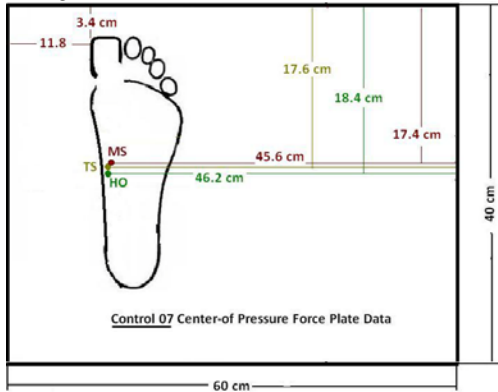
**Subject C04**



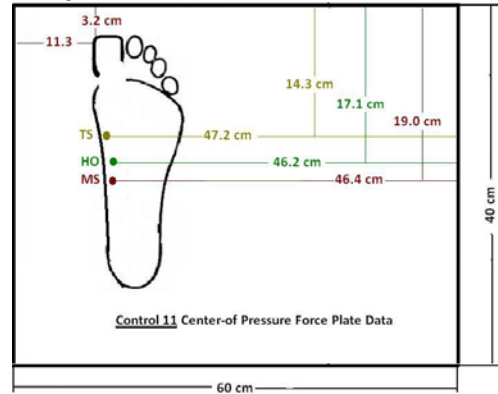
**Subject C06**



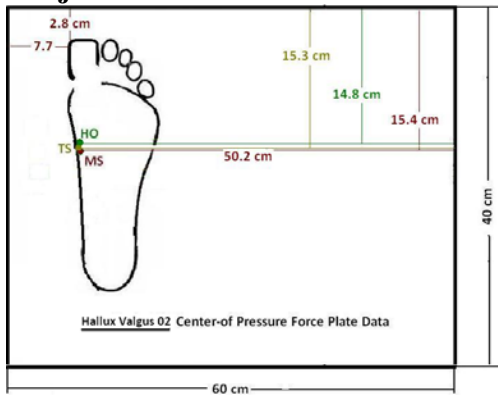
**Subject 07**



**Subject 11**



**Subject HV02**

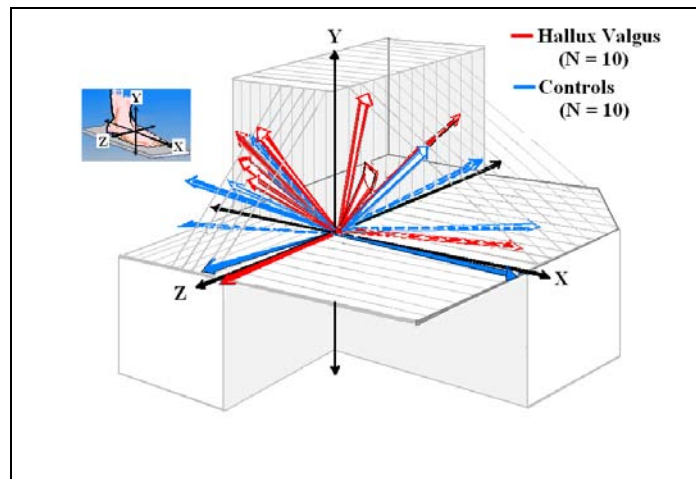


## APPENDIX 4

### Individual subject data: display of helical axis vectors

Group difference in first ray (helical) axis orientation was assessed in Chapter V. Table below shows the helical axis components of each subject (N = 20) computed for the middle stance gait event. This data are displayed as hand-drawn estimates (Figure) of the component vectors. Vectors are drawn in reference to the navicular coordinate frame.

| Hallux Valgus: Helical Axis Components |             |             |              | Control: Helical Axis Components |             |              |              |
|--|-------------|-------------|--------------|----------------------------------|-------------|--------------|--------------|
| ID#                                    | Y(c)        | Z(c)        | X(c)         | ID#                              | Y(c)        | Z(c)         | X(c)         |
| HV02-R                                 | 0.45        | 0.02        | -0.89        | C01-R                            | -0.62       | -0.67        | 0.40         |
| HV03-L                                 | 0.64        | 0.44        | -0.63        | C02-L                            | -0.04       | 0.11         | 0.99         |
| HV04-R                                 | 0.47        | -0.02       | -0.88        | C03-R                            | 0.22        | 0.97         | -0.06        |
| HV05-R                                 | 0.37        | 0.76        | -0.54        | C04-R                            | 0.48        | -0.33        | -0.81        |
| HV06-R                                 | 0.55        | -0.81       | -0.20        | C05-R                            | 0.32        | -0.01        | -0.95        |
| HV07-L                                 | -0.17       | -0.31       | 0.93         | C06-L                            | -0.11       | -0.60        | -0.79        |
| HV08-R                                 | 0.88        | 0.35        | 0.31         | C07-R                            | 0.16        | -0.97        | -0.17        |
| HV09-R                                 | 0.45        | 0.63        | -0.63        | C09-L                            | -0.18       | 0.47         | -0.86        |
| HV10-R                                 | 0.36        | 0.77        | 0.53         | C10-R                            | 0.66        | 0.25         | 0.70         |
| HV11-L                                 | -0.03       | -1.00       | 0.01         | C11-R                            | 0.14        | -0.30        | -0.94        |
| <b>Ave</b>                             | <b>0.40</b> | <b>0.08</b> | <b>-0.20</b> | <b>Ave</b>                       | <b>0.10</b> | <b>-0.11</b> | <b>-0.25</b> |



All subject data and statistical analyses are available for distribution. To request copy, contact Ward Glasoe ([glaso008@umn.edu](mailto:glaso008@umn.edu)), Univ of MN, Program in Physical Therapy.

## APPENDIX 5

### Data analysis: influence of body weight on first ray kinematics

A potential concern was that weight of the individual could influence the kinematics measured. Not on all of dependent variables, but for the primary measures of first ray kinematics a secondary analysis was run assess the relationship between measures made and body weight.

**Methods:** A series of simple correction analysis were run to investigate the relationship between weight and the kinematics measured in this study. If subject weight was shown to have good correlation with the kinematics measured, then it could be considered a covariate (ANCOVA) for analysis.

**Analysis:** A Pearson correlation (r) value of  $\leq 0.50$  is regarded as a weak-to-moderate relationship in the physical sciences. Therefore this value was established *a priori* to making this analysis as the threshold used to indicate a relationship between variables.

**Results:** Table shows the body weight vs. first ray kinematics correlation (r) values determined on the *in vivo* data (N =20).<sup>3, 4</sup> All of the correlation coefficients reported are smaller than  $r = 0.50$ .

|        | Transverse Angles |       |       | Sagittal Angles |      |      | Frontal Angles |      |       |
|--------|-------------------|-------|-------|-----------------|------|------|----------------|------|-------|
|        | MS                | HO    | TS    | MS              | HO   | TS   | MS             | HO   | TS    |
| Weight | -0.29             | -0.37 | -0.38 | 0.26            | 0.13 | 0.04 | -0.06          | 0.07 | -0.12 |

|        | Y Component Axis |             | Z Component Axis |             | X Component Axis |             |
|--------|------------------|-------------|------------------|-------------|------------------|-------------|
|        | Midstance        | Late Stance | Midstance        | Late Stance | Midstance        | Late Stance |
| Weight | -0.44            | -0.03       | -0.04            | -0.06       | 0.24             | -0.21       |

**Conclusion:** Only weak-to-moderate correlation was found between the variables. Thus body weight was not considered as a covariate in the statistical analysis performed in this study of hallux valgus foot kinematics.



## APPENDIX 6

### IRB Approval Document

0709M16823 - PI Glasoe - IRB - APVD Continuing Review

TO : [ludew001@umn.edu](mailto:ludew001@umn.edu), [pena0013@umn.edu](mailto:pena0013@umn.edu), [glaso008@umn.edu](mailto:glaso008@umn.edu),

The IRB: Human Subjects Committee renewed its approval of the referenced study listed below:

Study Number: 0709M16823  
Principal Investigator: Ward Glasoe  
Expiration Date: 08/25/2010  
Approval Date: 08/26/2009

Title(s): Genesis of Bunion and Development of Treatment Strategies

This confirmation is your official University of Minnesota RSPP notification of continuing review approval. You will not receive a hard copy or letter. This secure electronic notification between password protected authentications has been deemed by the University of Minnesota to constitute a legal signature.

You may go to the View Completed section of <http://eresearch.umn.edu/> to view or print your continuing review submission.

For grant certification purposes you will need this date and the Assurance of Compliance number, which is FWA00000312 (Fairview Health Systems Research FWA00000325, Gillette Childrens Specialty Healthcare FWA00004003). Approval will expire one year from that date. You will receive a report form two months before the expiration date.

In the event that you submitted a consent document with the continuing review form, it has also been reviewed and approved. If you provided a summary of subjects' experience to include non-UPIRTSO events, these are hereby acknowledged.

As Principal Investigator of this project, you are required by federal regulations to inform the IRB of any proposed changes in your research that will affect human subjects. Changes should not be initiated until written IRB approval is received. Unanticipated problems and adverse events should be reported to the IRB as they occur. Research projects are subject to continuing review. If you have any questions, please call the IRB office at (612) 626-5654.

The IRB wishes you continuing success with your research.

## APPENDIX 7

### Appendix Citations

1. Mattingly B, Talwalker V, Tylkowski C, Stevens D, Hardy P, Pienkowski D. Three-dimensional in vivo motion of adult hind foot bones. *J Biomech.* 2006;39:726-733.
2. Wolff K, Wicks A, Shaw A, Smith J, Ludewig P, Glasoe W. Clinical measurement correlates of the first metatarsal axis leading to intervention strategies for hallux valgus. *Foot Ankle Int.* 2010:In Review.
3. Glasoe W, et al. First ray kinematics in hallux valgus: a weightbearing imaging study. *TBD.* 2011:Ready for Journal Submission.
4. Glasoe W, et al. Calcaneus and navicular kinematics in hallux valgus: a weightbearing imaging study. *TBD.* 2011:Ready for Journal Submission.
5. Cargill S, Pearcy M, Barry M. Three-dimensional lumbar spine postures measured by magnetic resonance imaging reconstruction. *Spine.* 2007;32:1242-1248.
6. Wolf P, Stacoff A, Liu A, et al. Does a specific MR imaging protocol with a supine-lying subject replicate tarsal kinematics seen during upright standing? *Biomed Tech.* 2007;52:290-294.
7. HO I, Hou Y, Yang C, Wu W, Chen S, Guo L. Comparison of plantar pressure distribution between different speed and incline during treadmill jogging. *J Sport Science Med.* 2010;9:154-160.
8. Allen M, Cuddeford T, Glasoe W, et al. Relationship between static mobility of the first ray and first ray, midfoot, and hindfoot motion during gait. *Foot Ankle Int.* 2004;25:391-396.
9. Leardini A, Benedetti M, Berti L, Bettinelli D, Nativo R, Giannini S. Rear-foot, mid-foot and fore-foot motion during the stance phase of gait. *Gait Posture.* 2006;25:453-462.
10. Nester C, Jones R, Liu A, et al. Foot kinematics during walking measured using bone and surface mounted markers. *J Biomech.* 2007;40:3412-3423.